AN ABSTRACT OF THE THESIS OF

Jeremy M. Mull for the degree of Master of Ocean Engineering in Ocean Engineering presented on December 7, 2010.

Title: Coastal Sand Dunes in the U.S. Pacific Northwest: Regional Variability in Foredune Geomorphology and Associated Physical Vulnerability to Hazards

Abstract approved:

Peter Ruggiero

Coastal foredunes protect lives, infrastructure, and ecosystems during severe winter storms. In the U.S. Pacific Northwest (PNW), coastal foredune geomorphology is determined by both physical and ecological mechanisms. Before the 1900's, the native plant *Elymus mollis* was the dominant dune grass and dune morphology was largely determined by sediment supply and other physical factors. The introduction of two different invasive beach grasses in the first half of the 20th century resulted in significant changes to PNW foredune geomorphology. Recent work has shown that the invasive beach grass *Ammophila arenaria* is associated with taller, narrower foredunes while the grass *Ammophila breviligulata* is associated with shorter, broader foredunes. We hypothesize that this may impact coastal vulnerability as the taller, narrower foredunes may be more resistant to overtopping, but less resistant to erosion, while the shorter, broader foredunes may be more resistant to erosion, but less resistant to overtopping.

The work presented in this thesis is part of a larger, interdisciplinary effort to determine the relative importance of physical and ecological mechanisms in controlling

coastal foredune geomorphology and vulnerability in the PNW. Airborne topographic lidar data is used to characterize the regional variability in foredune geomorphology within several littoral cells, subcells, and beaches of the PNW. We present and discuss techniques to automatically and accurately extract foredune morphometric parameters from a lidar elevation data set of the coasts of Oregon and Washington. If the different grass species do affect foredune geomorphology, it is important to understand how managing them might impact coastal vulnerability. Therefore, we use the geomorphological parameters and measured hydrodynamic parameters during a major winter storm to estimate vulnerability to overtopping and erosion at beaches with distinctly different foredunes. Estimates of overtopping and erosion are normalized by the foredune heights and widths to elucidate how the different foredune types, and possibly the associated beach grasses, affect vulnerability. A series of simple foredune erosion models including a geometric model, an equilibrium profile model, and a wave impact model are evaluated for applicability to the PNW coast.

Coastal Sand Dunes in the U.S. Pacific Northwest: Regional Variability in Foredune Geomorphology and Associated Physical Vulnerability to Hazards

by

Jeremy M. Mull

A THESIS

submitted to

Oregon State University

in partial fulfillment of
the requirements for the
degree of

Master of Ocean Engineering

Presented December 7, 2010
Commencement June 2011

Master of Ocean Engineering thesis of Jeremy M. Mull presented on December 7, 2010.

APPROVED:

Major Professor, representing Ocean Engineering

Head of the School of Civil and Construction Engineering

Dean of the Graduate School

I understand that my thesis will become part of the permanent collection of Oregon State University libraries. My signature below authorizes release of my thesis to any reader upon request.

Jeremy M. Mull, Author

ACKNOWLEDGEMENTS

Funding for this project was provided by the Oregon Sea Grant (NOAA Grant #NA060AR4170010) and the Environmental Protection Agency (EPA/NCER R833836). I would also like to acknowledge and thank my committee members, including Merrick Haller and David Hill. Their advice on specific analyses and reviews of this document were extremely helpful. I particularly wish to thank my advisor, Peter Ruggiero, who acquired funding and developed the direction and scope of this project. His advice and ideas throughout the study were crucial.

I would also like to acknowledge Eric Seabloom and Sally Hacker, who as co-principal investigators worked to develop this project and initiate new directions for research. In addition, Kara Doran and Hilary Stockdon provided data, codes, and guidance for analyses.

Many fellow students and colleagues provided support. They include Erica Harris, Heather Baron, and John Stanley. In particular, I would like to thank Meg Palmsten, Greg Guannel, Greg Wilson, and Phoebe Zarnetske for their advice and help. Finally I would like to acknowledge Kristin for her endless support and helpfulness in completing late-night edits of this text.

TABLE OF CONTENTS

Page

TABLE OF CONTENTS (Continued)

Page

LIST OF FIGURES

LIST OF FIGURES (Continued)

Figure Page

LIST OF FIGURES (Continued)

Figure Page

LIST OF TABLES

LIST OF TABLES (Continued)

Table Page

1. GENERAL INTRODUCTION

The Pacific Northwest (PNW) has some of the largest coastal dune sheets in the continental United States and dune-backed beaches cover approximately 40% of the Oregon and Washington coastlines (Cooper, 1958). These dunes are part of a dynamic system that includes relatively large waves and high seasonal and interannual variability in nearshore and beach geomorphology (Ruggiero et al., 2005).

Foredunes directly serve coastal communities by protecting lives, infrastructure, and ecosystems from inundation and erosion during severe winter storms (Cooper, 1958; Komar et al., 1999; Allan and Priest, 2001). However, the processes which drive foredune evolution in the PNW are not completely understood. In the PNW, coastal foredune geomorphology is determined by both physical and ecological mechanisms, and we ultimately aim to understand the relative importance of each.

In the late 1800's, the dominant beach grass in this region was the native grass *Elymus mollis*, and the backshore consisted of small hummocks with loose sand (Cooper, 1958). There was no distinct foredune at the juncture between the foreshore and backshore regions. In 1868, European Beach Grass, *A. arenaria*, was first introduced to stabilize sand and inhibit wind-blown sand from accumulating on roads and in beach properties (Seabloom and Weidemann, 1994). The introduction of *A. arenaria* coincided with a shift in the backshore topography as relatively large distinct foredunes evolved (Cooper, 1958; Seabloom and Weidemann, 1994). The tall foredunes provided the additional benefit of affording coastal protection to developing communities (Cooper,

1958). By the 1950's, *A. arenaria* had replaced *E. mollis* as the dominant dune grass species in many areas (Seabloom and Weidemann, 1994; Hacker et al., in press).

In 1935, American Beach Grass, *A. breviligulata*, was introduced near the Columbia River in Warrenton, OR. Seabloom and Weidemann (1994) and Hacker et al. (in press) have documented the spread of *A. breviligulata* north into Washington and south to Sand Lake, OR as it has become overtaken *A. arenaria* as the dominant dune grass species in some locations. The spread of this second invasive species has been correlated with successive changes in foredune geomorphology. In 2007, Hacker et al. (in press) re-surveyed 57 profiles in Oregon and Washington that had initially been surveyed 19 years previously by Seabloom and Weidemann (1994) and found a decrease in foredune height on cross-shore profiles where *A. breviligulata* is the dominant grass. They found that *A. breviligulata* had replaced *A. arenaria* as the dominant grass species on profiles north of the Columbia River and that the foredunes dominated by *A. breviligulata* are approximately half as tall as those dominated by *A. arenaria*. Foredunes dominated by *A. breviligulata* tend to be wider and less steep, although these findings are not statistically significant (Hacker et al., in press). This implies that dune grass species may have a complex role in foredune evolution. Coastal communities on the east and Gulf coasts of the US have long planted *Ammophila* grasses to build up foredunes and increase protection from storms (Psuty and Rohr, 1992). However, the two grasses may trap and contain sand differently facilitating the growth of two distinct dune morphologies. Recent unpublished results of wind tunnel experiments demonstrate that *A. arenaria* trapped sand more effectively than *A. breviligulata* under certain conditions (Phoebe Zarnetske, personal communication). This is important to the

geomorphological evolution of dune-backed beaches as the dune grasses may alter the exchange of sediment between beach and dunes and change the coupled beach-dune system (Carter, 1980).

The spread of the second invasive grass, *A. breviligulata*, may also have implications for coastal vulnerability. It is possible that the taller, narrower dunes are more resistant to overtopping during storms but less resistant to erosion as waves do not have to erode as far inland to completely wash away the dune. The shorter, broader dunes may be more resistant to erosion and less resistant to overtopping during storms with elevated water levels. The introductions of the exotic grasses has had ecological impacts as well as they are associated with a decrease in abundance of six plant species that are listed as federally endangered and the decline of the Western snowy plover, which is listed as federally threatened (Hacker at al., in press). This presents a paradox as managing the different exotic species via removal to reduce pressure on native species might have negative ramifications on coastal vulnerability to flooding and erosion.

Foredune geomorphology is also controlled by physical mechanisms, including sediment supply and frequency and extent of scarping (e.g., Short and Hesp, 1982; Psuty, 1992). Short and Hesp (1982) studied beaches along the southeast coast of Australia and concluded that foredune geomorphology along beaches in equilibrium is determined by the morphodynamic beach state, magnitude of aeolian transport, and frequency of scarping and erosion. Psuty (1992) developed a conceptual model for foredune evolution in which foredune size and type is determined by the beach sediment budget (often controlled by hydrodynamics) and the dune sediment budget (often controlled by hydrodynamics and aeolian transport). The model predicts that tall foredunes develop

with a neutral beach sediment budget coupled with a positive dune sediment budget. Shorter foredunes are found on beaches that have a large positive or negative sediment budget as this affects the exchange of sediments to the dunes. On prograding beaches, the foredune is starved of sediment as incipient foredunes develop seaward. On eroding beaches, waves frequently erode the foredune and dune height is limited. This conceptual model implies that foredunes are not static, stable features, but are adjusting to changes in sediment transport on seasonal, annual, and decadal time scales. They are also strongly coupled to the beach system and the mechanisms which drive change in the foreshore and backshore.

In the present study, we use airborne topographic lidar data to characterize the regional variability in foredune geomorphological features and associated vulnerability to overtopping and erosion for dune-backed beaches within the PNW. This helps us begin to examine the role of physical mechanisms in foredune geomorphology and coastal vulnerability. Understanding these processes will be useful in managing the competing interests of natural habitat restoration and coastal protection.

The PNW coast consists of several distinct littoral cells which are typically separated by rocky headlands. The headlands generally block the exchange of sediment so that each littoral cell has unique geomorphological characteristics. The PNW coast is located on an active continental margin with a relatively steep and narrow continental shelf. The beaches within each littoral cell are generally relatively flat and dissipative. Many of the study areas have a distinct seasonal cycle with beach erosion in the winter months when larger waves transport sand offshore and form multiple sand bars. In the summer months, sand is generally transported onshore as accretion occurs on beaches.

The monthly mean offshore significant wave height in the region is 3.9 m for December and 1.6 m for July (Ruggiero et al., 2010). Ruggiero et al. (2010) found that the annual maximum wave height in this region is approximately 10 m as well as evidence of an increase in the annual maximum wave height over the past 30 years. These results suggest that coastal foredunes may be of even greater importance in the future if the coast continued to be subjected to storms with increased intensity and larger waves.

In this study we focus on foredunes, or primary dunes, because they are more active than secondary dunes further in the backshore and because they represent the first line of defense against coastal flooding and erosion for backing properties and ecosystems (Cooper, 1958). They are directly and frequently influenced by changing beach conditions and the presence of dune grass (Psuty, 1992; Psuty and Rohr 2000). Therefore, they present a unique opportunity to examine the relative roles of physical and biological mechanisms in coastal geomorphology. Areas of the PNW coast can experience rapid erosion during the winter months, particularly during El Niño winters when elevated water levels, large waves, and an increase in the wave incident angle (waves approach from the south) maximize erosion (Komar, 1998; Allan and Komar, 2002). At some beaches in the region, particularly Neskowin and Rockaway in Oregon, homes and structures are imminently threatened when the foredune erodes or is overtopped (Komar, 1998; Allan and Priest, 2001).

This study is part of a larger, interdisciplinary effort in which our primary goal is to determine the relative importance of physical and biological mechanisms in controlling coastal foredune geomorphology in the PNW. Our first objective is to develop a methodology to automatically and accurately extract beach and foredune

geomorphological parameters from PNW airborne lidar coastal elevation data. Lidar elevation data has been used to assess coastal geomorphology and coastal vulnerability in several regions (e.g., Brock et al., 1999; Brock and Sallenger, 2001; Elko et al., 2002; Sallenger et al., 2003; Shresta et al., 2005; Stockdon et al., 2009). Stockton et al. (2009) developed methods to extract cross-shore profiles and foredune crest elevations from lidar elevation data of the U.S. east and Gulf coasts. We modify these techniques to be applicable to lidar data sets in the PNW and to automatically extract several additional dune morphological parameters from each cross-shore profile (e.g., dune heel elevation, dune volume, backshore beach width, dune width, and dune slopes). Our techniques are developed using a 2002 lidar data set of the Oregon and Washington coasts (NOAA Coastal Services Center, 2002) but are applicable to any large coastal topographic data set.

The techniques are evaluated by comparing the automatically selected foredune parameters to those visually identified on selected cross-shore profiles. This enables us to calculate the vertical root mean squared error (RMSE) and vertical bias of the automatic selection process. We also compare the automatically selected values to those extracted visually from cross-shore profile data collected in the field with GPS backpack units in August, 2002. This data was collected approximately one month before the lidar data was collected in the Columbia River Littoral Cell (CRLC). The comparisons demonstrate that the vertical errors in the automatic selection process are random and unbiased.

Our second objective is to quantify regional variability in beach and foredune geomorphology. Trends in the automatically selected geomorphological parameters

within each study area are examined and discussed. We look for correlations between beach and foredune characteristics to help determine the relative role of physical mechanisms in foredune evolution. We also look for correlations between the geomorphological parameters and estimates of shoreline change rate (SCR), which can be used as a proxy for beach sediment supply rate. We discuss the results of these analyses within the framework of Psuty's (1992) model.

Finally, we aim to assess the regional variability in coastal vulnerability that results from the regional variability in beach and foredune geomorphology. Sallenger (2000) developed a storm impact scale to classify the effects of storm water levels on beaches and foredunes. The swash, collision, overtopping, and inundation regimes are distinguished by the maximum total water level (TWL) generated by storm conditions relative to the foredune elevations. Hurricanes that strike beaches with relatively low foredunes on the U.S. east and Gulf coasts are often in the overtopping and inundation regimes of the Sallenger (2000) impact scale, when TWL elevations exceed the foredune crest elevations (Stockdon et al., 2009). However, foredunes are relatively tall in the PNW and runup is often in the collision regime of the Sallenger (2000) storm impact scale, when TWL elevations reach the foredune face but are below the foredune crest. This results in some areas being particularly susceptible to erosion while limiting overtopping and inundation (Komar, 1998; Allan and Priest, 2001).

Foredune erosion is dependent upon backshore and foredune geometries, and the automatically selected geomorphological features allow us to estimate potential erosion during a severe winter storm. We apply three simple 1-D foredune erosion models to estimate foredune erosion at each profile. The models include the Komar et al. (1999)

geometric model (K99), the Kriebel and Dean (1993) equilibrium profile model (KD93), and the Larson et al. (2004) wave impact model (L04). The 1-D erosion models can be applied with only a few hydrodynamic variables from any storm and we use conditions from the storm of record for the PNW; a major extratropical cyclone that made landfall in 1999 (Allan and Komar, 2002). To expedite the synthesis of the model results, we develop indices in which the maximum storm TWL values are normalized by the foredune height at each profile to determine the relative vulnerability to overtopping. The predicted foredune retreat distances are normalized by the foredune width at each profile to determine the relative vulnerability to erosion.

We find that each of the erosion models can be easily applied to the PNW, however they have distinctly different environmental dependencies. The K99 model has a negative dependence upon beach slope (erosion decreases with increasing beach slope) and the KD93 and L04 models have a positive dependence upon beach slope (erosion increases with increasing beach slope).

We find distinct differences between the geomorphological features and physical vulnerabilities of the different study areas. However, we are not yet able to attribute these differences exclusively to physical or ecological processes. The results suggest that both dune grasses and physical coastal processes are important in foredune geomorphology. In future work, the automatically extracted geomorphological parameters will be combined with ecological data to determine the relative roles of these processes. In addition, the procedure to extract geomorphological parameters can be applied to other lidar data sets of the PNW to assess coastal evolution.

2. COASTAL SAND DUNES IN THE U.S. PACIFIC NORTHWEST: REGIONAL VARIABILITY IN FOREDUNE GEOMORPHOLOGY AND ASSOCIATED VULNERABILTY TO HAZARDS

2.1 INTRODUCTION

The PNW (Figure 1) has some of the largest coastal dune systems in the continental United States while dune-backed beaches cover approximately 40% of the Oregon and Washington coastlines (Cooper, 1958). They are part of a dynamic geomorphological system that includes relatively large waves and high seasonal and interannual variability in nearshore and beach geomorphology (Ruggiero et al., 2005).

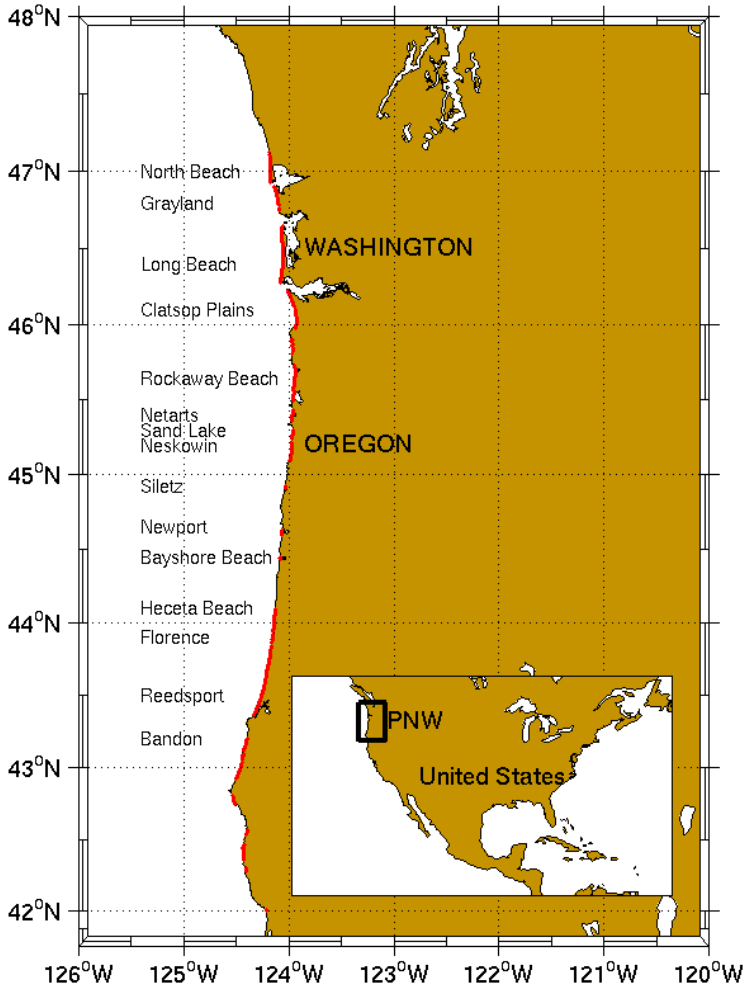

Figure 1. Map of the dune-backed littoral cell, subcells, and beaches in the PNW. All dune-backed beaches along the coasts of Oregon and Washington are shown in red. For this project, we focus on the study areas listed by name.

2.1.1 Motivation

Foredunes directly serve coastal communities by protecting lives, infrastructure, and ecosystems from inundation and erosion during severe winter storms (Cooper, 1958; Komar et al., 1999; Allan and Priest, 2001). However, the processes which drive foredune evolution in the PNW are not completely understood. In the PNW, coastal

foredune geomorphology is determined by both physical and ecological mechanisms, and we ultimately aim to understand the relative importance of each.

In the late 1800's, the dominant beach grass in this region was the native grass *Elymus mollis*, and the backshore consisted of small hummocks with loose sand (Cooper, 1958). There was no distinct foredune at the juncture between the foreshore and backshore regions. In 1868, European Beach Grass, *A. arenaria*, was first introduced to stabilize sand and inhibit wind-blown sand from accumulating on roads and in beach properties (Seabloom and Weidemann, 1994). The introduction of *A. arenaria* coincided with a shift in the backshore topography as relatively large distinct foredunes evolved (Cooper, 1958; Seabloom and Weidemann, 1994). The tall foredunes provided the additional benefit of affording coastal protection to developing communities (Cooper, 1958). By the 1950's, *A. arenaria* had replaced *E. mollis* as the dominant dune grass species in many areas (Seabloom and Weidemann, 1994; Hacker et al., in press).

In 1935, American Beach Grass, *A. breviligulata*, was introduced near the Columbia River in Warrenton, OR. Seabloom and Weidemann (1994) and Hacker et al. (in press) have documented the spread of *A. breviligulata* north into Washington and south to Sand Lake, OR as it has overtaken *A. arenaria* and become the dominant dune grass species in some locations. The spread of this second invasive species has been correlated with successive changes in foredune geomorphology (Figure 2). In 2007, Hacker et al. (in press) re-surveyed 57 profiles in Oregon and Washington that had initially been surveyed 19 years previously by Seabloom and Weidemann (1994) and found a decrease in foredune height on cross-shore profiles where *A. breviligulata* is the dominant grass. They found that *A. breviligulata* had replaced *A. arenaria* as the

dominant grass species on profiles north of the Columbia River and that the foredunes dominated by *A. breviligulata* are approximately half as tall as those dominated by *A. arenaria*. Foredunes dominated by *A. breviligulata* tend to be wider and less steep, although these findings are not statistically significant (Hacker et al., in press). This implies that dune grass species may have a complex role in foredune evolution. Coastal communities on the east and Gulf coasts of the US have long planted *Ammophila* grasses to build up foredunes and increase protection from storms (Psuty and Rohr, 1992). However, the two grasses may trap and contain sand differently facilitating the growth of two distinct dune geomorphologies. Recent unpublished results of wind tunnel experiments demonstrate that *A. arenaria* trapped sand more effectively than *A. breviligulata* under certain conditions (Phoebe Zarnetske, personal communication). This is important to the geomorphological evolution of dune-backed beaches as the dune grasses may alter the exchange of sediment between beach and dunes and change the coupled beach-dune system (Carter, 1980).

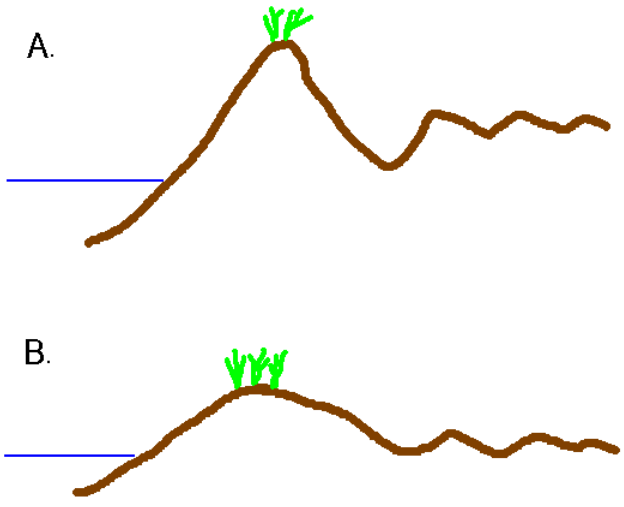

Figure 2. A) A relatively tall, narrow foredune dominated by *A. arenaria* and B) a relatively broad, short foredune dominated by *A. breviligulata*.

The spread of the second invasive grass, *A. breviligulata*, may also have implications for coastal vulnerability. It is possible that the taller, narrower dunes are more resistant to overtopping during storms but less resistant to erosion as waves do not have to erode as far inland to completely wash away the dune. The shorter, broader dunes may be more resistant to erosion and less resistant to overtopping during storms with elevated water levels. It is important to note that foredune erosion can occur as a foredune is overtopped and sand is transported inland in overwash deposits (Sallenger, 2000). In this paper, we do not consider this type of dune erosion, but focus on erosion that occurs when wave runup collides with the foredune face but does not overtop the foredune.

The introductions of the exotic grasses has had ecological impacts as well as they are associated with a decrease in abundance of six plant species that are listed as federally endangered and the decline of the Western snowy plover, which is listed as federally threatened (Hacker at al., in press). This presents a paradox as managing the different exotic species via removal to reduce pressure on native species, might have negative ramifications on coastal vulnerability to flooding and erosion.

Foredune geomorphology is also controlled by physical mechanisms, including sediment supply and frequency and extent of scarping (e.g., Short and Hesp, 1982; Psuty, 1992). Short and Hesp (1982) studied beaches along the southeast coast of Australia and concluded that foredune geomorphology along beaches in equilibrium is determined by the morphodynamic beach state, magnitude of aeolian transport, and frequency of scarping and erosion. Psuty (1992) developed a conceptual model for foredune evolution in which foredune size and type is determined by the beach sediment budget (often

controlled by hydrodynamics) and the dune sediment budget (often controlled by hydrodynamics and aeolian transport). The model predicts that tall foredunes develop on beaches with a neutral sediment budget coupled with dunes that have a positive sediment budget. Shorter foredunes are found on beaches that have a large positive or negative sediment budget as this affects the sediment budget of the dunes. On prograding beaches, the foredune is starved of sediment as incipient foredunes develop seaward. On eroding beaches, waves frequently erode the foredune and dune height is limited. This conceptual model implies that foredunes are not static, stable features, but are adjusting to changes in sediment transport on seasonal, annual, and decadal time scales. They are also strongly coupled to the beach system and the mechanisms which drive change in the foreshore and backshore.

In the present study, we use airborne topographic lidar data to characterize the regional variability in foredune geomorphological features and associated vulnerability to overtopping and erosion for dune-backed beaches within the PNW. This helps us begin to examine the role of physical mechanisms in foredune geomorphology and coastal vulnerability. Understanding these processes will be useful in managing the competing interests of natural habitat restoration and coastal protection.

2.1.2 Study Region

The PNW coast consists of several distinct littoral cells typically separated by rocky headlands. The headlands generally block the exchange of sediment so that each littoral cell has unique geomorphological characteristics. For this study, we focused on dune-backed stretches of beach which range in size from complete littoral cells to

beaches only approximately 2 km long (Figure 1), all of which we refer to as study areas. The coast is located on an active continental margin with a relatively steep and narrow continental shelf. The beaches within each study area are generally relatively flat and dissipative. Many of the beaches in the region have a distinct seasonal cycle with beach erosion in the winter months when larger waves transport sand offshore. In the summer months, sand is generally transported onshore as accretion occurs on beaches. The monthly mean offshore significant wave height in the region is 3.9 m for December and 1.6 m for July (Ruggiero et al., 2010). Ruggiero et al. (2010) found that the annual maximum wave height in this region is approximately 10 m and found evidence of an increase in the annual maximum wave height over the past 30 years at several buoys within the region. This implies that coastal foredunes may be of even greater importance in the future if the coast is subjected to storms with increased intensity and larger waves.

In this paper we focus on foredunes (Figure 3), or primary dunes, because they are more active than secondary dunes further in the backshore and because they represent the first line of defense against coastal flooding and erosion for backing properties (Cooper, 1958).

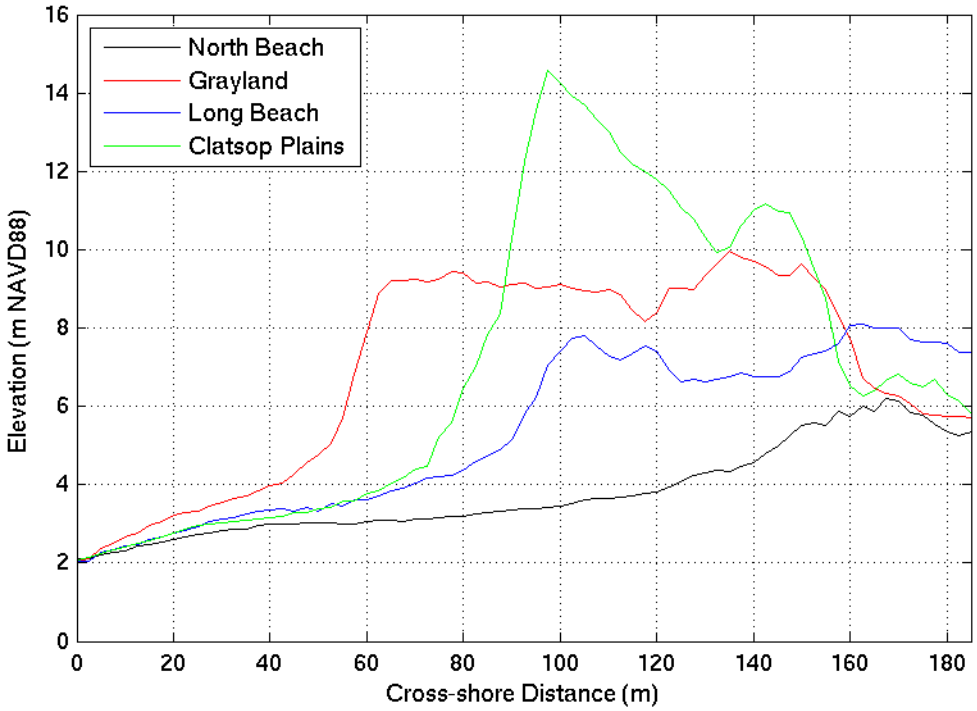

Figure 3. Examples of lidar-derived cross-shore profiles from North Beach, WA (black), Grayland, WA (red), Long Beach, WA (blue), and Clatsop Plains, OR (green). In each profile, the shoreline is located at 0 m and the foredune crest is local maximum closest to the shoreline. Secondary dunes are behind each foredune. There is considerable regional variability in beach and foredune geomorphology.

Foredunes are directly and frequently influenced by changing beach conditions and the presence of dune grass (Psuty, 1992; Psuty and Rohr 2000). Therefore, they present a unique opportunity to examine the relative roles of physical and biological mechanisms in coastal geomorphology.

Foredune geomorphology is important to the physical vulnerability of dune-backed beaches in the PNW. At some beaches in the region, including Neskowin and Rockaway in Oregon, homes and structures are imminently threatened when the foredune erodes or is overtopped (Komar, 1998; Allan and Priest, 2001). Areas of the PNW coast can experience rapid erosion during the winter months, particularly during El Niño

winters when elevated water levels, large waves, and an increase in the wave incident angle (waves approach from the south) maximize erosion (Komar, 1998; Allan and Komar, 2002).

2.1.3 Objectives

This study is part of a larger, interdisciplinary effort in which our primary goal is to determine the relative importance of physical and biological mechanisms in controlling coastal foredune geomorphology in the PNW. Our first objective is to develop a methodology to automatically and accurately extract beach and foredune morphological parameters from PNW airborne lidar coastal elevation data. Lidar elevation data has been used to assess coastal geomorphology and coastal vulnerability in several regions (e.g., Brock et al., 1999; Brock and Sallenger, 2001; Elko et al., 2002; Sallenger et al., 2003; Shresta et al., 2005; Stockdon et al., 2009). Stockton et al. (2009) developed methods to extract cross-shore profiles and foredune crest elevations from lidar elevation data of the U.S. east and Gulf coasts. We modify these techniques to be applicable to lidar data sets in the PNW and to automatically extract several additional dune morphological parameters from each cross-shore profile (e.g., dune heel elevation, dune volume, backshore beach width, dune width, and dune slopes). Our techniques are developed using a 2002 lidar data set of the Oregon and Washington coasts (NOAA Coastal Services Center, 2002) but are applicable to any large coastal topographic data set.

Our second objective is to quantify regional variability in beach and foredune geomorphology. Trends in the automatically selected geomorphological parameters

within each study area (Figure 1) are examined and discussed. We look for correlations between beach and foredune characteristics to help determine the relative role of physical mechanisms in foredune evolution. We also look for correlations between the geomorphological parameters and estimates of shoreline change rate (SCR), which can be used as a proxy for beach sediment supply rate. We discuss the results of these analyses within the framework of Psuty's (1992) model.

Finally, we aim to assess the regional variability in coastal vulnerability that results from the regional variability in beach and foredune geomorphology. Sallenger (2000) developed a storm impact scale to classify the effects of storm water levels on beaches and foredunes. The swash, collision, overtopping, and inundation regimes are distinguished by the maximum total water level (TWL) generated by storm conditions relative to the foredune elevations. Hurricanes that strike beaches with relatively low foredunes on the U.S. east and Gulf coasts are often in the overtopping and inundation regimes of the Sallenger (2000) impact scale, when TWL elevations exceed the foredune crest elevations (Stockdon et al., 2009). However, foredunes are relatively tall in the PNW and runup is often in the collision regime of the Sallenger (2000) storm impact scale, when TWL elevations reach the foredune face but are below the foredune crest. This results in some areas being particularly susceptible to erosion while limiting overtopping and inundation (Komar, 1998; Allan and Priest, 2001).

Foredune erosion is dependent upon backshore and foredune geometries, and the automatically selected geomorphological features allow us to estimate potential erosion during a severe winter storm. We apply three simple 1-D foredune erosion models to estimate foredune erosion rates at each profile. The models include the Komar et al.

(1999) geometric model (K99), the Kriebel and Dean (1993) equilibrium profile model (KD93), and the Larson et al. (2004) wave impact model (L04). We use these models as they are computationally simple and can be applied to many profiles to analyze vulnerability over a regional scale. More complex process-based foredune erosion models, such as XBEACH, can only be applied over relatively small areas and require detailed storm hydrodynamic conditions, sediment characteristics, and bathymetric data (Roelvink et al., 2007). The 1-D erosion models can be applied with only a few hydrodynamic variables from any storm and we use conditions from the storm of record for the PNW; a major extratropical cyclone that made landfall in March 1999 (Allan and Komar, 2002). In addition, the models do not require bathymetric data and can be applied with lidar-derived cross-shore profiles. To expedite the synthesis of the model results, we develop indices in which the maximum storm TWL values are normalized by the foredune height at each profile to determine the relative vulnerability to overtopping. The predicted foredune retreat distances are normalized by the foredune width at each profile to determine the relative vulnerability to erosion.

To assess how dune grasses may impact foredune geomorphology and physical vulnerability, we compare variability in geomorphology and vulnerability between three distinct study areas. We compare foredunes in Long Beach, WA, which are dominated by *A. breviligulata*, with foredunes in Clatsop Plains, OR, which have approximately 50% *A. breviligulata* and 50% *A. arenaria* (Seabloom and Weidemann, 1994; Hacker et al., in press). In addition, we examine foredunes in Rockaway, OR, which have a similar dune grass composition to that in Clatsop Plains but different foredune characteristics (Seabloom and Weidemann, 1994; Hacker et al., in press). Ultimately, differences in

geomorphology and erosion and flooding responses of different dune profiles may indicate how managing for the different grass species and dune morphologies might impact coastal vulnerability.

2.2 METHODS

All dune-backed beaches along the coasts of Washington and Oregon have been catalogued (Figure 1, Appendix A). Dune backed-beaches were identified by visiting several sites during field surveys within the Columbia River, Rockaway, Newport, and Reedsport littoral cells. We also examined aerial photographs and incorporated the PNW coastal maps of Byrne (1964) and Peterson et al. (2007). For this study we focus on the study areas listed in Figure 1.

2.2.1 Automated Foredune Morphological Parameter Selection

We have developed automated techniques for extracting beach and foredune features from high resolution lidar elevation data along the PNW coast. We focus on lidar data collected in September 2002, when the coasts of northern California, Oregon, and Washington were surveyed during the National Aeronautics and Space Administration (NASA)/United States Geological Survey (USGS) Airborne Lidar Assessment of Coastal Erosion (ALACE) Project (USGS St. Petersburg Coastal and Marine Science Center, 2002; NOAA Coastal Services Center, 2002). Airborne topographic lidar surveys have been conducted in many regions to analyze coastal

geomorphological change and vulnerability (Brock et al., 1999; Brock and Sallenger, 2001; Elko et al., 2002; Sallenger et al., 2003; Shresta et al., 2005; Stockdon et al., 2009).

Plant et al. (2002) and Stockdon et al. (2009) developed techniques for gridding, interpolating, and filtering lidar data to enable foredune feature extraction. Here we modify these existing approaches to optimize foredune feature extraction from PNW lidar data. Lidar point cloud data is first rotated such that individual gridded surfaces are oriented in the alongshore and cross-shore direction for each stretch of beach since we extract foredune features from cross-shore profiles derived from the gridded surfaces. Individual grids consist of approximately 2 km long sections of data in which the average shoreline orientation is used to rotate the raw data. Gridded surfaces with 2.5 m spacing in the cross-shore direction and 5 m spacing in the alongshore direction minimize vertical interpolation errors, particularly at dune crests. A quadratic loess filter , with smoothing window sizes of 5 m in the cross-shore direction and 10 m in the alongshore direction, further minimizes vertical interpolation error while preserving the required cross-shore resolution in each profile extracted from the gridded surfaces.

The geomorphological parameters extracted from each profile include the backshore slope, defined as the average slope between the horizontal location of mean high water (MHW) and the dune toe, the dune toe elevation (*dtoe*), dune face slope, dune crest elevation (*dhigh*), dune back slope, dune heel elevation (*dheel*), dune width (length from toe to heel), beach width (length from MHW to toe), and two separate estimates of dune volume per unit length of dune (Figure 4). The first estimate of dune volume (*V1*) consists of the integrated area beneath each cross- shore profile from the dune toe to the dune heel. The integrated area extends from the dune crest to the toe or heel, whichever

is the lowest elevation. Because our estimates of *dheel* have relatively high errors compared to the estimates of *dhigh*, we compute a second estimate of dune volume (*V2*), which consists of the integrated area beneath each cross-shore profile between the dune toe and dune heel. The integrated area extends from the dune crest to the dune toe.

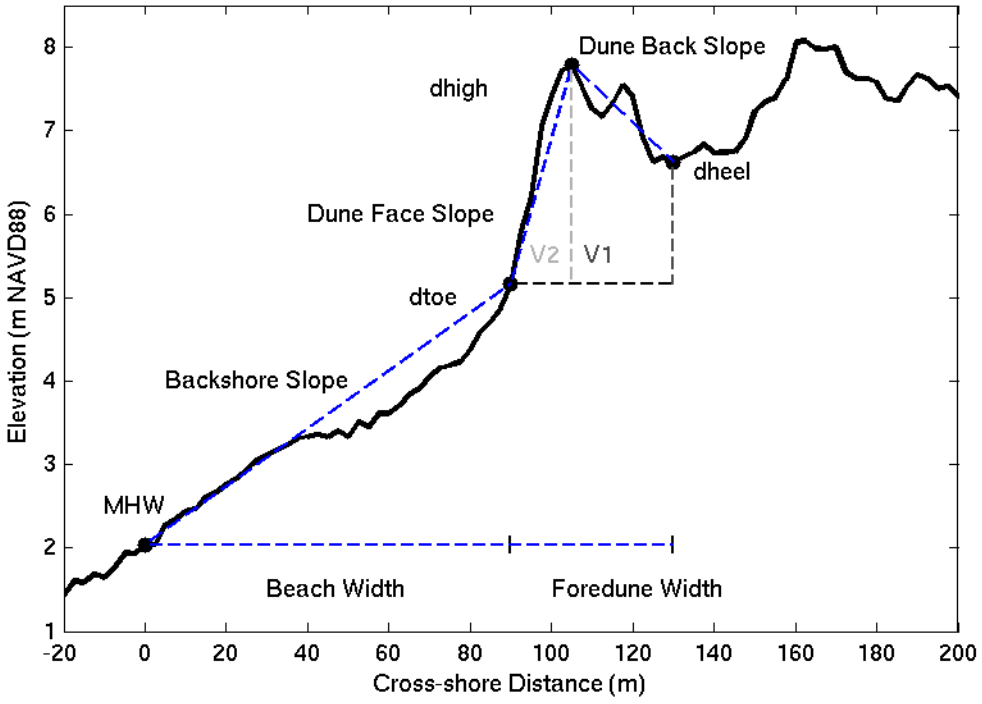

Figure 4. An example of a lidar-derived cross-shore profile and the beach and foredune geomorphological parameters extracted from the profile. The data have been smoothed and interpolated onto a 2.5 m spaced grid in the cross-shore direction. The *dhigh* elevation indicates the foredune crest and is the most shoreward dune crest with a minimum backshore drop of 0.60 m. The dune heel (*dheel*) is the lowest swale between *dhigh* and a subsequent dune crest. The dune toe (*dtoe*) is the maximum difference between the profile and the profile detrended with a cubic function. The dune volume is the numerically integrated area between the profile and the horizontal line at the *dtoe* elevation. The area can be integrated from the *dtoe* location to the *dheel* location for a large estimate of dune volume (*V1*) or from the *dtoe* location to the *dtoe* location for a small estimate of volume (*V2*).

The 'shoreline' is designated as the horizontal location on each profile of the MHW elevation for this region (2.1 m NAVD88) (Weber et al., 2005). Stockdon et al.

(2009) identify the highest elevation within a specified cross-shore distance from the shoreline as *dhigh*. For most beaches, a cross-shore distance of 400 m landward of the MHW is sufficient to capture the complete foredune. However, we find that the highest elevation within a cross-shore profile is often not the foredune crest, particularly at prograding beaches in the PNW with multiple dune ridges. On prograding beaches, new foredunes develop which can be shorter than historically or geologically older dunes (Psuty, 1992). To define the characteristics of foredunes in the PNW we rely on Cooper's (1958) observation that foredunes in the PNW have an elevation drop of at least 0.60 m from the crest to the heel. Visual inspection of several cross-shore profiles from each study area confirmed that most foredunes indeed have this elevation drop. Therefore for each cross-shore profile, we select the most shoreward dune with this characteristic. Care must be taken to avoid selecting beach berms as dunes so we select a minimum elevation above MHW under which we prescribe that *dhigh must be above* (typically an elevation of 2-3 m above MHW). To find *dhigh* on each cross-shore profile, we first identify all local maxima as potential dune crests. We identify relative maxima and minima by comparing each interpolated points' elevation relative to the elevation of neighboring interpolated points.

The foredune toe (*dtoe*) is the junction between the beachface and foredune (Figure 4) and it can often be visually identified as a significant inflection point on a cross-shore profile. Elko et al. (2002) developed a semi-automated technique to extract *dtoe* elevations in from airborne topographic lidar data. The data for a select beach is viewed as a grayscale image in GIS and the *dtoe* scarp line is visually identified, selected, and digitized. Elko et al. (2002) demonstrated that this technique is subjective but

repeatable between different operators. While it could be applicable to select beaches within the PNW, it would be difficult to apply this technique over all of the study areas within the PNW. We therefore explored several techniques, which could easily be applied over an entire region, to automatically extract the location and elevation of the foredune toe from each lidar-derived cross-shore profile. We tried calculating the changes in slope over cross-shore distances (the first derivative of the slope) and looking for points at which the slope rapidly increased (maxima in slope accelerations). This technique generally selects points that are too low in elevation and shoreward of the dune toe, particularly on profiles in which the backshore slope increased shoreward of the dune toe. Many cross-shore profiles in the 2002 PNW lidar data have relatively noisy backshores and the resulting multiple inflection points make it difficult to identify the inflection point corresponding to the dune toe. We also attempted to detrend each cross-shore profile with a linear function. This technique entails fitting a linear regression to the interpolated points between the MHW and the foredune crest and subtracting the trend from the profile. The absolute minimum on the detrended profile corresponds to a major inflection point on the cross-shore profile. This technique often selects points that again were too low and shoreward of the foredune toe. This is particularly true for profiles with a relatively wide beach and slight concave shape.

Via trial and error we found that the most accurate and repeatable method for automatically extracting *dtoe* from cross-shore profiles consists of detrending the section of beach profile between the crest and shoreline with a cubic function. The cubic takes the form of

$$\hat{y}_j = \beta_0 + \beta_1 x_j + \beta_2 x_j^2 + \beta_3 x_j^3; \quad (1)$$

where $\hat{y}_j$ is the predicted elevation at each cross-shore grid location, β is each coefficient determined by a least squares fit, and x_j is each cross-shore grid location. The cubic trend is then subtracted from the profile to obtain a detrended profile. Minimum and maximum points in the detrended profile indicate inflection points in the original profile. The absolute minimum on the detrended profile generally corresponds to *dtoe* (Figure 5) and vertical errors in the technique were found to be random and unbiased.

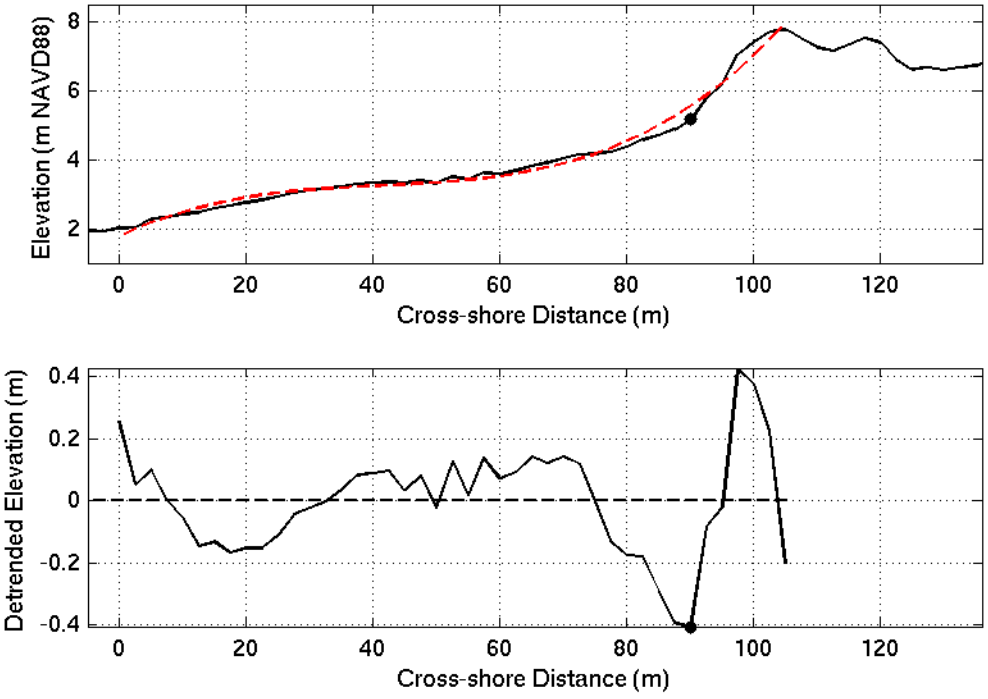

Figure 5. The dune toe on each cross-shore profile can be identified by fitting a cubic function to the segment of beach profile between the shoreline (MHW) and *dhigh*. In the top panel, the gridded and smoothed cross-shore profile is shown in back, and the fitted cubic function is shown by the red dashed line. The cubic trend is subtracted from the profile to obtain a detrended profile. The minimum point on the detrended profile corresponds to *dtoe*. This is shown in the bottom panel where the detrended profile is shown as the black line.

On approximately 20% of the profiles examined this technique selects an incorrect dune toe that is landward of the correct dune toe. This occurs on profiles on

which an incipient foredune is forming shoreward of the foredune (noisy backshore) and the absolute minimum on the detrended profile is the low point behind the incipient dune. To avoid this problem, the cubic detrending function is instead fit between the incipient foredune crest and the shoreline. To find the incipient foredune crest, we select an appropriate vertical elevation which is subtracted from *dhigh*. All local maxima higher than this elevation are identified and we then select the most shoreward of these maxima to fit the cubic function. We found few selection errors of this type when using an elevation of 1 m within *dhigh* on most beaches.

The dune heel is selected as the minimum elevation on a cross-shore profile between the foredune crest and the next landward local maxima in the beach profile. To identify additional dune crests behind the foredune, we use the same criteria used to distinguish the foredune crest and look for all local maxima with a minimum landward elevation drop of 0.60 m. Visual inspection of several profiles from each study area confirmed that this criterion identified all significant dune crests. For profiles on which there are no dune crests behind the foredune we identify the minimum elevation behind the foredune crest. We also identify minimum elevations on the profile which are followed by a landward elevation increase of 0.60 m. This elevation change was chosen after visually inspecting several profiles from each study area. The most shoreward minimum point with this criterion is compared with the absolute minimum point behind the foredune, and the point closest to the foredune is selected as the dune heel. Once the dune toe, dune crest, and dune heel are selected, the dune slopes, width, and volumes are easily calculated (Figure 4).

To visually check the automatic methods for extracting foredune morphological parameters the locations of *dtoe* and *dhigh* are overlaid on aerial photographs (2005-2010) using GoogleEarth or GIS. This process reveals that structures or significant vegetation (e.g. trees) are occasionally selected as foredune crests by the automatic techniques. After identifying the spurious points, we either re-select the features by hand from each cross-shore profile or remove them entirely from future analyses. Foredune toe locations that appear too close to shore, sometimes located in a low point behind a berm, or too close to *dhigh* are re-selected by hand from each cross-shore profile or removed from the data. Finally, the vertical elevations of the *dtoe* and *dhigh* are plotted in plan view for each study area and spurious values that are clearly indentified as outliers are excluded from further analysis.

To assess the accuracy of the automated techniques to extract geomorphological parameters we estimate the vertical error and bias for the foredune crest, toe, and heel elevations. The vertical root mean squared error (RMSE) between each interpolated and smoothed point and surrounding raw lidar data points is calculated during the gridding routine using the formula given in Plant et al. (2002)

$$\hat{q}_i^2 = \frac{1}{\hat{\varepsilon}_i^2} \sum_j \left(\hat{z}_i - z_j \right)^2 \hat{a}_{ij}^2 \qquad (2)$$

where *i* is each interpolation index, *j* is each observation index, $\hat{q}_i^2$ is the vertical mean square residual error for each interpolated point, $\hat{\varepsilon}_i^2$ is the sampling error for each interpolation, $\hat{z}_i$ is each interpolated point, z_j is each observed data point, and a_{ij} are a set of quadratic loess interpolation weights between the interpolated points and the observed values. We calculate the square root of the vertical mean square residual error to obtain

the vertical RMSE and set an error threshold of 1 m. Profiles for which the RMSE exceeded 1 m at *dhigh* or *dtoe* are excluded from further analysis (Stockdon et al., 2009).

The total vertical error, $\hat{q}_t$, in each automatically chosen dune parameter is composed of two components combined in quadrature via

$$\hat{q}_t = \sqrt{\hat{q}_i^2 + \hat{q}_s^2} \tag{3}$$

in which $\hat{q}_i^2$ is the vertical interpolation error (Equation 2) and $\hat{q}_s^2$ is the vertical uncertainty of the automatic selection techniques. The first component incorporates the instrument measurement RMSE of approximately 0.20 m (NOAA Coastal Services Center, 2002; Plant et al., 2002). To estimate the second component of the total error term, we randomly chose 30 cross-shore profiles from each study region. Elevation values for *dtoe*, *dhigh*, and *dheel* were manually estimated based on visual cues in the data at each profile. The vertical RMSE between these manually estimated values and the elevations picked automatically are taken to be the selection uncertainty, $\hat{q}_s$. We also estimate the vertical bias of the automatic selection methodology by computing the mean vertical difference between the automatically-selected parameters and the parameters selected by hand. It is important to note that we estimate the vertical error and bias before outlier points are identified and removed by hand for each study area as these contribute to the inaccuracies in the automatic selection process.

To further assess the vertical accuracy of the automatic selection process, we compare the automatically selected parameters to those selected manually from cross-shore profiles collected in situ in the Columbia River Littoral Cell (CRLC). These data were collected with GPS in August 2002 as part of the Southwest Washington Coastal Erosion Study (SWCES (Ruggiero et al., 2005)). Each cross-shore profile is filtered and

interpolated using a quadratic loess filter with an interpolation grid distance of 2.5 m and a smoothing distance of 5 m (Plant et al., 2002). This is identical to the methods used to filter and interpolate the lidar data. The gridded and smoothed cross-shore profiles are plotted and the dune parameters are chosen by visual inspection of each plot. The vertical RMSE and bias between the *dhigh*, *dtoe*, and *dheel* elevations on each SWCES profile and the closest lidar profile are then computed.

2.2.2 Foredune Geomorphology

We quantify alongshore trends and variability in beach and foredune geomorphology within each study area. We focus on backshore slopes, foredune crest, and foredune toe elevations as these are critical to calculations of the TWL and foredune retreat distances in analysis of vulnerability to overtopping and erosion. We quantify regional trends and variability in beach and foredune geomorphology by calculating the means and standard deviations of foredune crest and toe elevations, foredune width, beach width, beach slopes, foredune volumes, and SCR.

We look for correlations between the beach and foredune characteristics within each study area. Correlation coefficients are calculated between the alongshore series of foreshore slopes, backshore slopes, dune face slopes, dune toe elevations, dune crest elevations, dune heel elevations, beach widths, dune widths, dune volumes, and SCR. The SCR are averages and were estimated by the USGS from aerial photographs of the Washington and Oregon shorelines taken approximately 40 years apart (Peter Ruggiero, personal communication). The geomorphological parameters are linearly interpolated onto the SCR locations for direct comparison. Positive values of SCR indicate a

prograding beach while negative values of SCR indicate an eroding beach. The magnitude of the SCR is often important as strongly negative and positive values of SCR indicate that a beach is rapidly changing and this could impact foredune geomorphology. Therefore, we look for correlations between the beach and foredune characteristics and the absolute value of SCR as well.

To begin to examine the relative importance of physical processes in foredune geomorphology and physical vulnerability, we focus on variability in geomorphology and physical vulnerability within three distinct study areas. We compare foredunes in Long Beach, WA, which are dominated by *A. breviligulata*, with foredunes in Clatsop Plains, OR, which have approximately 50% *A. breviligulata* and 50% *A. arenaria* (Seabloom and Weidemann, 1994; Hacker et al., in press). In addition, we examine foredunes in Rockaway, OR, which has a similar dune grass composition to Clatsop Plains but different foredune characteristics (Seabloom and Weidemann, 1994; Hacker et al., in press).

2.2.3 Estimating Physical Vulnerability to Erosion and Flooding

The physical vulnerability of PNW foredunes to overtopping and erosion during the storm event 'of record'is estimated using the lidar-derived morphological data and three simple 1-D foredune erosion models. The erosion models and storm conditions are applied to each cross-shore profile within each study area. The predicted instances of overtopping and estimated dune retreat distances are compared for Long Beach, WA and Clatsop Plains and Rockaway, OR.

2.2.3.1 Example Storm Conditions and Total Water Level Model

The foredune erosion models can be applied with hydrodynamic conditions from any storm. Utilizing an event selection approach we examine flooding and erosion during a single major winter storm, with an approximately 30-year return period, that struck the PNW between March 2–4, 1999 (Allan and Komar, 2002). During the storm, significant wave heights (H_s) measured at the National Data Buoy Center (NDBC) Columbia River Buoy (Station # 46029) exceeded 12 m (Allan and Komar, 2002). Tidal residuals of approximately 1.0 m were measured at the National Oceanic and Atmospheric Administration (NOAA) Toke Point, WA Tide Gage (Station # 9440910). The highest high tide observed during the storm was approximately 0.4 m above MHW (Figure 6). These storm conditions are similar to those used to determine coastal erosion hazard zones by the Oregon Department of Geology and Mineral Industries (DOGAMI) (Allan and Priest, 2001) for the state of Oregon. Similar offshore wave conditions were observed at the Newport, OR buoy (# 46050) but the peak storm surge measured at the Newport Tide Gauge (# 9435385) was approximately half of that measured at Toke Point (Allan and Komar, 2002).

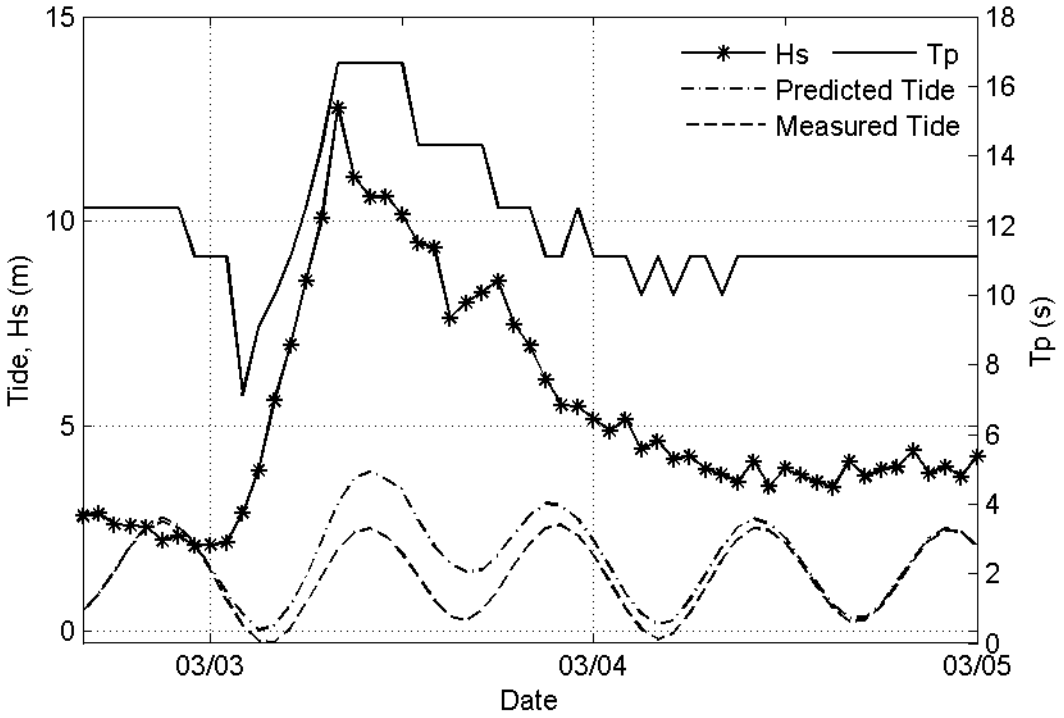

Figure 6. Storm conditions from the PNW storm of record on March 2–4, 1999. The black line with asterisks is the significant wave height observed at the NDBC Columbia River Buoy (Station # 46029). The solid black line is the peak spectral period measured at the buoy. The black line with dots is the measured tide at the NOAA Toke Point, WA Tide Gage (Station # 9440910). The black dashed line is the predicted tide for this station. The difference between the predicted and measured tides is the non-tidal residual, most of which is attributed to storm surge (Allan and Komar, 2002).

The measured tides and tidal residuals from Station 9440910 are combined to obtain the TWL values for each hour of the storm at each profile:

$$\text{TWL} = \text{astronomical tide} + \text{non-tidal residual} + \text{runup} \quad (4)$$

where the astronomical tide is the predicted water elevation due to tides and the non-tidal residual (measured minus predicted tides) is assumed to be dominated by storm surge. The offshore significant wave heights and offshore wave lengths are combined with the backshore slope at each profile to determine the runup at each profile:

$$R_2 = 1.1\left(0.35\tan\beta_b \left(H_0 L_0\right)^{1/2} + \frac{\left[H_0 L_0 \left(0.563\tan^2\beta_b + 0.004\right)^{1/2}\right]}{2} \right) \quad (5)$$

where R_2 is the 2% exceedence runup height, or the elevation that 2% of the runup events will exceed given specific offshore wave conditions, *tan* β_b is the backshore beach slope (used in all calculations of runup), and H_0 and L_0 are the deep water significant wave height and deep water wave length derived from the peak spectral period respectively (Stockdon et al., 2006). The Columbia River buoy is located in approximately 135 m of water and is therefore in intermediate water for many of the storm waves. We use the peak spectral periods (T_p) measured at the buoy and linear theory to obtain the deep water significant wave heights and wavelengths. If the TWL exceeds the foredune crest elevation at any point during the storm, the profile is in the overtopping regime of the Sallenger (2000) storm impact scale.

2.2.3.2 Erosion Models

The K99 model is a simple conservative geometric foredune erosion model which assumes that the inland erosion distance is a function of the maximum TWL during a storm. Retreat distance of the dune toe occurs along the backshore slope as

$$E\_K99 = \frac{\left(TWL - dtoe\right)}{\tan\beta_b} \quad (6)$$

where *E_K99* is the maximum potential dune toe retreat distance during a storm (Komar et al., 1999). While simple, this model is recommended by the Federal Emergency Management Agency (FEMA (FEMA, 2004) as one approach for estimating erosion during storms for Pacific coast beaches. This approach is also currently used by the State of Oregon in determining coastal hazard zones (Allan and Priest, 2001).

The KD93 equilibrium profile foredune erosion model is more complex than K99 and assumes that the volume of sediment eroded from the foredune during storms is deposited in the nearshore as a new equilibrium profile is established. The model initially predicts a potential erosion response (time-independent) for a particular storm based upon equilibrium profile theory. Kriebel and Dean (1993) extend the time-independent approach by assuming that the time scale for an erosion response would often be greater than a typical storm duration. Therefore, they develop an empirical method to estimate the time scale of the erosion response. The potential erosion is then adjusted by the ratio of the two time scales.

The potential foredune retreat distance, E_KD93_{∞}, is predicted by the following equation:

$$E\_KD93_{\infty} = \frac{TWL\left(x_b - \frac{h_b}{\tan\beta_f}\right)}{D + h_b - TWL/2} \tag{7}$$

where x_b is the surf zone width determined from an equilibrium profile, h_b is the breaking wave depth, $tan\ \beta_f$ is the foreshore beach slope, and D is the vertical elevation of the dune crest above the dune toe (Kriebel and Dean, 1993). *TWL* is the maximum TWL achieved during the storm at each profile. It is important to note that FEMA (2004) apply the equation in this way but Kriebel and Dean (1993) estimate erosion with storm surge elevations rather than TWL elevations. Kriebel and Dean (1993) developed the model to be applicable to east coast hurricanes and north-eastern storms where storm surge can dominate TWL elevations.

The breaking wave water depth, h_b, is found by linear theory assuming no refraction with

$$h_b = \frac{1}{g^{1/5}\gamma^{4/5}}\left(\frac{H_0^2 C_0}{2}\right)^{2/5} \tag{8}$$

where g is the acceleration due to gravity (9.81 m/s^2), γ is the ratio of breaking wave height to breaking wave depth (assumed to be 0.78), H_0 is the deep water significant wave height, and C_0 is the deep water celerity (Dean and Dalrymple, 1994).

To apply the KD93 equilibrium profile model it is necessary to estimate the shape parameter *A*, which describes the concavity of an equilibrium beach profile

$$h = Ax^{2/3} \tag{9}$$

where *h* is the water depth, and *x* is the offshore distance from MHW. The shape parameter is related to the median grain size (D_{50}) by Moore's (1982) equation:

$$A = 10^{\left(\frac{\log D_{50} - .237}{.924}\right)} \text{ if } D_{50} < .262 \text{ or}$$

$$A = 10^{\left(\frac{\log D_{50} - .2.264}{3.30}\right)} \text{ if } D_{50} \geq .262. \tag{10}$$

Since lidar provides no information about sediment grain size we need an approach for computing the alongshore variability of *A*. As beach slope is roughly correlated with sediment grain size (Komar, 1998a), we utilize coincident measurements of foreshore slope (from profile data) and D_{50} that were collected at 44 locations during the summers of 1997, 1998, and 1999 as part of the SWCES (Figure 7). We use the least-squares method to fit an equilibrium profile (9) to each of these profiles below MHW and determine the shape parameter. We next fit a linear regression between the foreshore slope ($tan\ \beta_f$) and shape parameter at each profile and find the following relationship (solid line Figure 8, middle panel)

$$A = 0.036 + 2.26(\tan \beta_f). \tag{11}$$

This enables us to estimate values of *A* with foreshore slopes only. The RMSE between the values of *A* predicted by the linear regression (11) and Moore's (1982) equation is 0.016 (Figure 8, right panel).

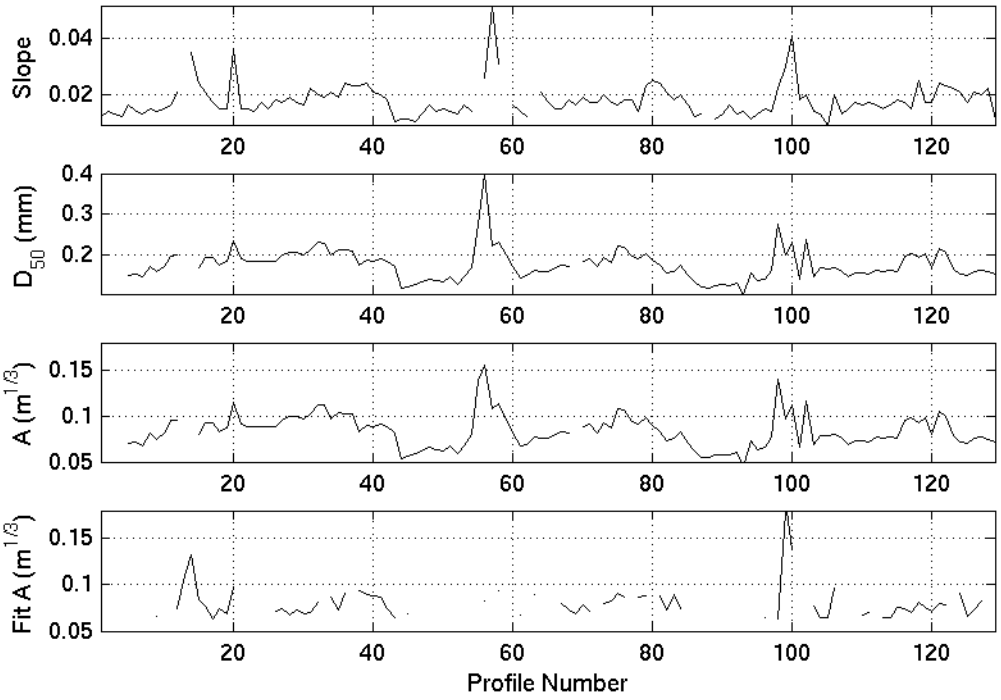

Figure 7. Coincident measurements of foreshore slope (top panel), D_{50} (second panel), *A* values determined from Moore's (1982) Equation (third panel), and best-fit *A* values for profiles within the CRLC. Slope is correlated with D_{50} and *A* values determined from Moore's (1982) Equation.

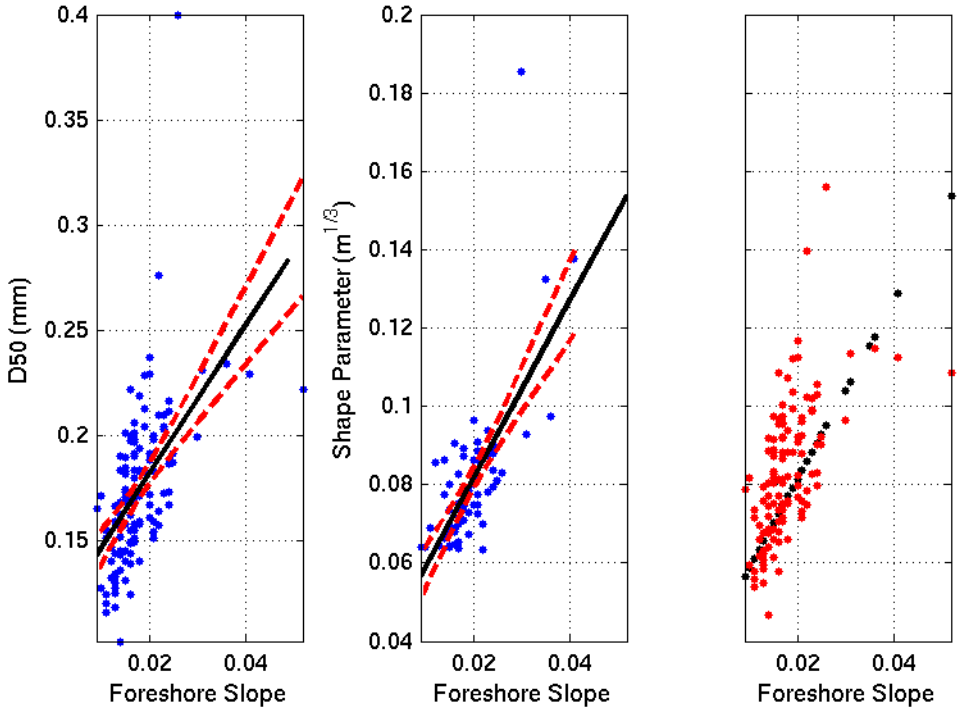

Figure 8. The left panel shows a linear regression (black line) between the foreshore slope and D_{50} values for summer profiles within the CRLC. The regression, with a correlation coefficient of 0.55, is significant at the 95% confidence level. The middle panel shows a linear regression (black line) between the foreshore slope and estimated shape parameter for summer profiles within the CRLC. The regression, with a correlation coefficient of 0.69, is significant at the 95% confidence level. Confidence bands are shown as red-dashed lines. The right panel shows the values of A predicted by the linear regression with foreshore slope (11) as black dots. The red dots are the values of A predicted by Moore (1982)'s equation with D_{50} from each profile, plotted against the foreshore slopes at each profile. The RMSE between the A values is 0.016.

The time-dependent erosion is determined by the ratio of erosion response time scale (T_S) to the storm duration (T_D). Kriebel and Dean (1993) assumed that a storm hydrograph typically has a sinusoidal shape. They ran numerous numerical simulations and determined the erosion response time scale empirically as

$$T_S = 320 \frac{H_b^{3/2}}{g^{1/2} A^3} \left(\frac{1}{1 + h_b / B + x_b \left(\tan \beta_f \right) / h_b} \right) \tag{12}$$

where H_b is the breaking wave height (equivalent to γh_b) and B is the vertical elevation of the foredune toe above MHW (*dtoe* – MHW). T_D was assumed to be the total number hours that the TWL exceeded MHW plus a local bias due to mean elevations of wave setup at each profile (Ruggiero and List, 2009). The ratio of time scales is then $\beta = 2\pi T_S / T_D$, which is used in the transcendental equation

$$\exp\left(-\frac{2X}{\beta}\right) - \cos(2X) + \frac{1}{\beta}\sin(2X) = 0 \tag{13}$$

where X is the root of the equation. The first root of this equation (between 0 and $\pi/2$) was substituted into (14) to determine the ratio of time-dependent erosion to potential erosion as follows

$$\alpha = \frac{1}{2}[1 - \cos(2X)]. \tag{14}$$

Finally, the time-dependent erosion is computed by multiplying the potential erosion by this fraction:

$$E\_KD93 = (\alpha) \text{ x } (E\_KD93_{\infty}) \tag{15}$$

Larson et al. (2004) developed an analytical wave impact model, L04, to predict the volume eroded from foredunes during a storm. This model is an extension of Overton et al.'s (1994) model which assumes that the weight of eroded sand is a linear function of the wave impact force

$$W = C_E F\ ; \tag{16}$$

where C_E is an empirical coefficient and F is the wave impact force. The L04 model ignores friction between swash and the beach and assumes that the velocity of a bore traveling up the beach is constant. In its simplest version (L04_1), the model ignores

temporal variations in tide, storm surge, wave period, and runup such that the volume of eroded sediment is given as:

$$V\_L04_1 = 4C_s(R - z_0)^2 \frac{t}{T}; \quad (17)$$

where C_s is an empirical coefficient (includes C_E and other parameters), R is the runup height, t is time, and T is the wave period. In our application of this model to each cross-shore profile, we assume that R can be represented by the maximum R_2 elevation during the storm, and t is the length of time that the TWL exceeded *dtoe* (similar to our application of KD93). The model relies upon changes in runup and does not account for changes in TWL so we further assume that z_0 is the elevation of the dune toe above the measured tide (predicted tide + non-tidal residual) at the time when the TWL first exceeds the foredune crest elevation. This enables us to account for the elevated water levels due to tides and surge during the storm. We calculate the mean wave period during the time that the TWL exceeded the dune toe elevation and use the R_2 elevation at the time of the maximum TWL of the storm. This model does not account for the change in dune toe elevation as the foredune is eroded (Larson et al., 2004).

The empirical coefficient, Cs, includes various physical properties of the water and sand and is represented as:

$$C_s = \frac{1}{2}\frac{C_E}{C_u^2}\frac{\rho}{\rho_s}\frac{1}{(1-p)} \quad (18)$$

where ρ is the density of the water, ρ_s is the density of the sand, p is the porosity of the sand, and C_u is a coefficient that accounts for the difference between the speed of a shallow water wave and a broken bore. Combining these various parameters into a single parameter that can be calibrated significantly reduces the complexity of applying this

model. To calibrate the model and estimate C_s, Larson et al. (2004) linearly regress measurements of eroded foredune volume on calculations of the impact parameter (all terms on the right hand side of Equation 17 excluding C_s) from several lab and field experiments. We use data from a large-scale dune erosion experiment conducted at the O.H. Hinsdale Wave Research Laboratory at Oregon State University in 2006. We perform a linear regression between the observed eroded volumes and the impact parameters at all time steps during the experiment to yield a coefficient of 0.00117 (Figure 9).

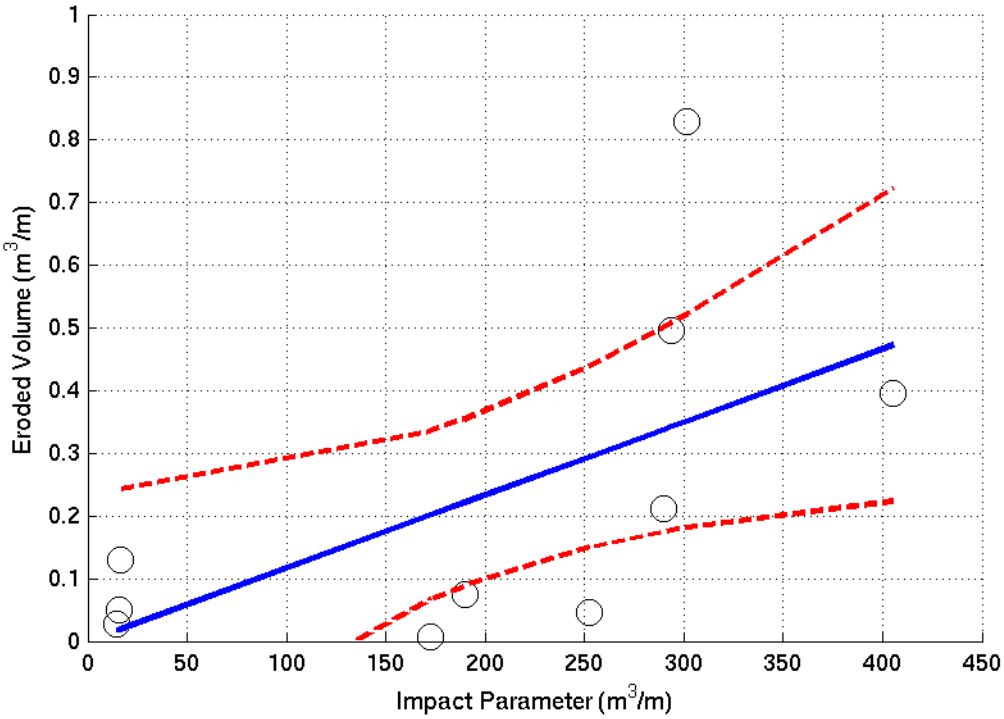

Figure 9. Linear regression between the calculated Larson et al. (2004) impact parameters (17) and observed eroded volumes at each hour of the wave tank experiment. The regression is shown by the blue line and the confidence bands are indicated by the red dashed lines.

Larson et al. (2004) also present an empirical equation to calculate the coefficient C_s with the root mean square wave height (H_{rms}) and sediment grain size

$$C_s = 0.00134e^{\left(-0.000319\frac{H_{rms}}{D_{50}}\right)}. \quad (19)$$

We found this equation to be relatively insensitive to D_{50} as it yielded a value of 0.00134 for a large range of D_{50} values from the summer SWCES data and the H_{rms} of the design storm. This differs from the value of C_s determined previously by linear regression by 14.5%. As estimates of dune erosion are scaled by this coefficient in Equation 17, use of either of these coefficients will change estimates of dune erosion by only 14.5%. As Equation 19 is valid for a range of D_{50} values that includes many beaches in the PNW, we hereafter use 0.00134 as the empirical coefficient.

A slightly more complicated (realistic) version of the L04 model (L04_2) accounts for the change in the hydrograph as a storm progresses. It assumes that storm surge increases linearly in time and represents the eroded volume as:

$$V\_L04_2 = 4\frac{C_s}{T}\left((R-z_i)^2 t + a(R-z_i)^2 t^2 + \frac{1}{3}a^2 t^3\right) \quad (20)$$

where a is the rate of increase in surge. This model accounts for the rise in water level due to storm surge so we assume that z_i is the initial dune toe height above MHW. During our storm of record, the peak storm surge was approximately 1.56 m and the time that the surge increased from 0.1 m to the peak was approximately 11 hours, so a is 3.9 x 10^{-5} m/s. We assume that R is the estimated peak runup value for each profile during the storm.

The final version of the L04 model (L04_3) that we apply to the PNW accounts for temporal variations in both surge and runup. It assumes that both the surge and runup increases and decreases throughout the storm approximate a sine curve. Eroded volume is then

$$V\_L04_3 = 8\frac{C_s}{T}\left(\left(\frac{T_D}{2} - t_L\right)\left(\frac{1}{2}R_T^2 + z_D^2\right) + R_T^2\frac{T_D}{4\pi}\sin\left(2\frac{\pi t_L}{T_D}\right) - 2R_T z_D\frac{T_D}{\pi}\cos\left(\frac{\pi t_L}{T_D}\right)\right) \quad (21)$$

where R_T is the combined amplitudes of the surge and runup, and z_D is the initial height of the dune toe above the surge and runup. T_D is the storm duration which we assume to be the same as that used in the KD93 model. Plots of the predicted hydrograph at several profiles confirmed that the storm duration was approximately the same as that determined by Kriebel and Dean (1993). t_L is the time when bores begin to strike the dune face and is determined by

$$t_L = \frac{T_D}{\pi}\arcsin\left(\frac{z_D}{R_T}\right). \quad (22)$$

Since L04 only reports the volume of eroded foredune material and both K99 and KD93 report erosion distances we develop an approach to directly compare all three models. Kriebel and Dean (1993) use beach geometry and estimated dune retreat distance to derive an equation for eroded volume on a particular profile as a function of the eroded distance

$$V\_KD93_\infty = EKD93_\infty(dhigh - MHW) + \frac{TWL^2}{2\tan\beta_b} - \frac{2}{5}\frac{TWL^{5/2}}{A^{3/2}} \quad (23)$$

where V_KD93_∞ is the maximum time-independent eroded volume in the KD93 model. This approach assumes that there is no foredune heel and that the foredune extends inland at the foredune crest elevation. To compare the erosion estimates of the L04 models to those of the other models, we re-arrange (23) to yield an erosion distance

$$E\_L04_{1,2,3} = \frac{V\_L04_{1,2,3} - \frac{TWL^2}{2\tan\beta_b} + \frac{2}{5}\frac{TWL^{5/2}}{A^{3/2}}}{dhigh - MHW} \quad (24)$$

where the equilibrium parameters are the same as those used in the KD93 model for each profile.

Table 1 summarizes the input parameters required by each model. The TWL calculations are used by both the K99 model and the KD93 model. The L04 models depend on variations in runup and surge but do not incorporate TWL elevations. This distinction could be important as the variations in tide are greater than the variations in the non-tidal residual for this storm which implies that erosion could most likely depend on all components of the TWL rather than just storm surge and runup.

Table 1: The parameters required for the TWL, K99, KD93, and L04 models.

Model	**Parameters**
TWL	H_0, T_P, *tan* β_b, astronomical tide, non-tidal residual
K99	TWL, *dtoe*, *tan* β_b
KD93	TWL, *A*, *tan* β_b, *tan* β_f, *dhigh*, *dtoe* H_0, T_P
L04	R_2, *surge*, *dtoe*, *t*, *T*

2.3 RESULTS

Foredune geomorphological parameters were successfully extracted from cross-shore profiles within each study area. For most study areas, we extracted parameters from every other profile in the alongshore direction (approximately 10 m spacing). In

areas where gridded lidar sections overlap the alongshore resolution of extracted parameters increases to approximately 5 – 10 m.

2.3.1 Automated Dune Morphological Parameter Selection

Out of 16,536 gridded cross-shore profiles for Long Beach, WA, foredune crest elevations were successfully extracted from 15,113 profiles. Foredune toe elevations were successfully extracted from 15,036 profiles and foredune heel elevations were successfully extracted from 14,859 profiles. The high resolution of the extracted parameters reveal variability in geomorphology on both small and large scales (Figure 10).

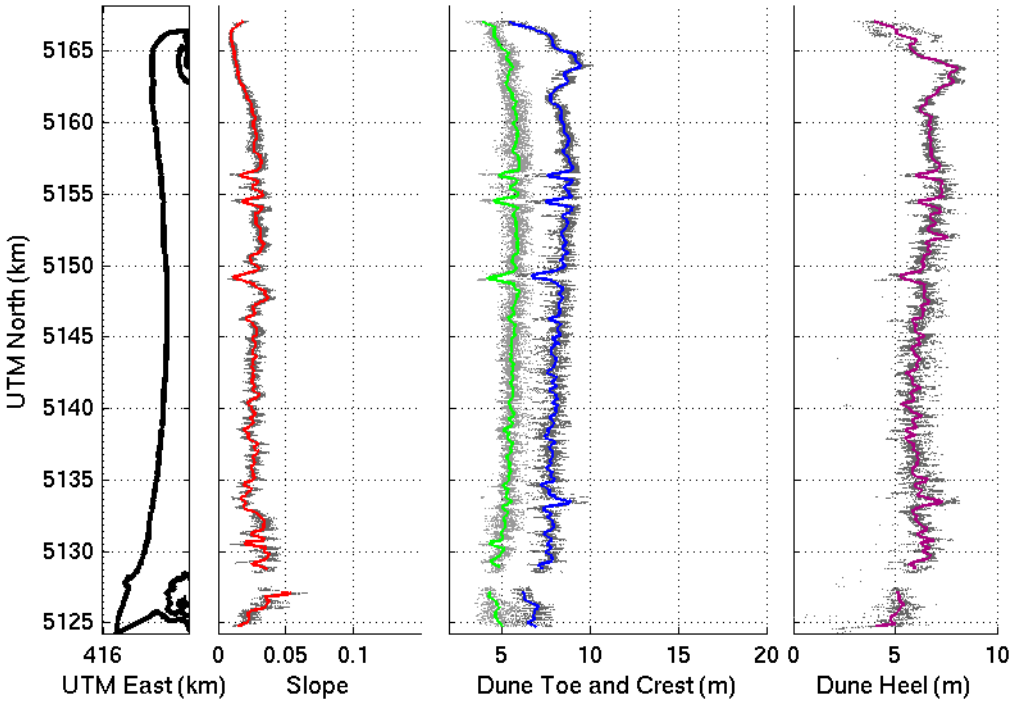

Figure 10. Foredune parameters for Long Beach, WA. The left panel indicates the alongshore position of each profile. The next panel shows backshore slopes in dark grey. The red dots represent slopes that have been smoothed in the alongshore direction with a linear loess filter with a window size of 250 m. The next panel shows foredune toe and crest elevations. The toe elevations are shown in light grey and the crest elevations are shown in dark grey. The green dots and blue dots represent smoothed toe and crest elevations, respectively. The right panel shows the dune heel elevations at each profile in grey. The purple dots are smoothed dune heel elevations.

The comparisons between the foredune toes, crests, and heels selected automatically and those estimated by visually inspecting 30 random profiles from each study area are shown in Table 2. The total vertical errors (Equation 3) for the dune toe are greater than those for the other parameters, although they are generally less than 1 m. The mean selection RMSE for the foredune toe is 0.60 m. This is reasonably similar to Elko et al.'s (2002) technique, which resulted in RMSE values of 0.50 m and 0.23 m for the extraction of the foredune toe at two beaches. The mean selection RMSE for the foredune crest is 0.04 m. This also compares well with Elko et al.'s (2002) technique

which resulted in RMSE values of 0.05 m and 0.60 m for the foredune crest. The mean selection RMSE for the foredune heel is 0.40 m.

The mean vertical biases for the foredune toe and crest are 0.03 m and 0.00 m, much less than the vertical measurement RMSE for the lidar scanner (0.20 m). This indicates that the automatic selection methodology is not biased high or low for these parameters. However, the mean vertical bias for the foredune heel is 0.27 m which indicates that the foredune heel elevations could be biased high. This could be due to the difficulty in subjectively choosing a dune heel, or trough behind the dune crest. On several profiles, especially those with multiple dune crests, there was no obvious dune heel and no way to determine if the methodology or researcher visually estimating the dune heel was correct. Because of this uncertainty, we chose to estimate foredune volume by two methods. The area of the dune from the foredune toe to the foredune crest (*V2*) excludes uncertainties in the foredune heel elevation and location.

Table 2: Vertical RMSE and bias, in meters, between visually selected lidar foredune parameters and automatically selected foredune parameters.

	Dune Toe				Dune Crest				Dune Heel			
Study Area	Selection	Interpolation	Total	Bias	Selection	Interpolation	Total	Bias	Selection	Interpolation	Total	Bias
North Beach	0.57	0.17	0.59	-0.01	0.02	0.27	0.27	0.00	0.26	0.17	0.31	0.07
Grayland	0.63	0.20	0.66	-0.07	0.02	0.24	0.24	0.02	0.15	0.21	0.26	0.02
Long Beach	0.47	0.19	0.51	0.19	0.02	0.25	0.25	0.00	0.01	0.19	0.19	0.00
Clatsop Plains	0.92	0.21	0.94	-0.05	0.03	0.20	0.20	0.00	0.46	0.23	0.51	0.21
Rockaway	0.80	0.27	0.84	0.06	0.04	0.40	0.40	0.00	0.24	0.63	0.67	0.06
Netarts Spit	0.45	0.43	0.62	0.03	0.04	0.56	0.56	0.00	0.33	0.70	0.77	0.11
Sand Lake	0.51	0.30	0.59	0.12	0.03	0.04	0.05	0.00	1.30	0.52	1.40	1.70
Neskowin	0.80	0.24	0.84	-0.08	0.07	0.39	0.40	0.01	0.71	0.43	0.83	0.50
Siletz	0.71	0.19	0.73	0.10	0.07	0.27	0.28	0.00	0.36	0.31	0.13	0.21
Newport	0.59	0.31	0.67	-0.20	0.07	0.30	0.31	0.00	0.45	0.39	0.60	0.20
Bayshore Beach	0.37	0.21	0.43	0.02	0.05	0.36	0.36	0.00	0.53	0.30	0.61	0.28
Heceta Beach	0.43	0.27	0.51	-0.07	0.03	0.45	0.45	0.00	0.12	0.35	0.37	0.01
Florence	0.53	0.25	0.59	0.19	0.04	0.34	0.34	0.00	0.04	0.30	0.30	0.00
Reedsport	0.57	0.25	0.62	0.22	0.02	0.32	0.32	0.00	0.26	0.23	0.35	0.07
Bandon	0.66	0.22	0.70	0.00	0.02	0.36	0.36	0.00	0.77	0.24	0.81	0.60
Mean	**0.60**	**0.25**	**0.66**	**0.03**	**0.04**	**0.32**	**0.32**	**0.00**	**0.40**	**0.35**	**0.54**	**0.27**

The vertical RMSE and bias between the automatically chosen lidar parameters and the CRLC parameters estimated visually from the SWCES profiles are shown in Table 3. The mean vertical RMSE for the dune toe is 0.58 m which compares with Elko et. al's (2002) values and suggests that the cubic-detrending technique is a reliable method to extract dune toes from remotely sensed elevation data. The mean vertical RMSE for the dune crests is 0.75 m and larger than that calculated between the automatically-chosen crests and the hand-selected crests from the lidar data. In addition, there is a positive bias in the lidar dune crests. This is most likely due to the presence of vegetation, which is accounted for by definition in the SWCES profiles (surveyors walk on the sand, not the top of the grass) but may cause a bias in the first-return lidar elevation data. The mean bias of the automatically selected lidar dune crests approximately corresponds to the mean tiller length of the three dominant PNW dune grass species in moderately windy conditions (Zarnetske, personal communication). We discuss how these biases, and the presence of vegetation, likely do not strongly impact estimates of vulnerability in the Discussion section. The mean vertical RMSE value for the dune heels is 0.50 m with a positive vertical bias of 0.27 m, also most likely due to vegetation. No values for the dune heel elevations in Clatsop Plains, OR were available in the SWCES profile data.

Table 3: RMSE and bias between automatically-selected dune parameters and hand-picked dune parameters from SWCES profiles and parameters

	Dune Toe		**Dune Crest**		**Dune Heel**	
Beach	RMSE	Bias	RMSE	Bias	RMSE	Bias
North Beach	0.35	0.12	0.44	0.19	0.69	0.48
Grayland	0.64	0.40	0.79	0.62	0.32	0.11
Long Beach	0.78	0.61	1.08	1.16	0.48	0.23
Clatsop Plains	0.56	0.32	0.67	0.46	xx	xx
Mean	**0.58**	**0.36**	**0.75**	**0.61**	**0.50**	**0.27**

2.3.2 Foredune Geomorphology

Beach and foredune features extracted from the lidar data along Long Beach, WA, Clatsop Plains, OR, and Rockaway, OR are shown in Figures 10 - 12. The automatically chosen morphometric parameters (with spurious points removed by hand) are shown with values smoothed in the alongshore direction over a length scale of 250 m to reduce noise and small-scale variability. We focus on the backshore slopes, foredune crest, and foredune toe elevations as these parameters are used in the simple estimates of vulnerability to overtopping and erosion discussed later. In the plot of the Long Beach, WA geomorphological features (Figure 10), the variability of the slopes, crest, and toe elevations decrease near the northern tip of the peninsula. The beach is flatter here and the crest and toe elevations are lower. This is an area where the beach is prograding rapidly and the tip of the peninsula is building out. As the beach builds out, new foredune ridges form successively to the west (Psuty and Rohr, 2000). Sand is accreting along most of the peninsula and the foredune crests are relatively low here compared with other study areas (Ruggiero et al., 2005).

Along the Clatsop Plains study area (Figure 11) the backshore slope values and dune crest elevations both decrease near the southern end of the littoral sub-cell while the

dune toe elevations are relatively constant throughout. The tall foredunes in the northern part of the subcell are some of the tallest along the PNW coast. An incipient dune ridge is forming between 5111 and 5096 km (UTM) which is indicated by the smaller dune crests within this area. This can be found on most profiles although many are not indicated in Figure 11 as the incipient dunes have not grown enough to develop the minimum dune heel elevation drop of 0.60 m to be classified as a foredune (Cooper, 1958).

The double foredune ridge has implications when predicting vulnerability to flooding and erosion. Estimating vulnerability to flooding with a shorter incipient foredune instead of a taller dune implies that a particular profile may be more vulnerable to overtopping. In addition, using an incipient foredune instead of a geologically older dune, located landward of the incipient dune on a particular profile, implies less vulnerability to erosion as estimated dune retreat distances do not extend as far inland. When estimating vulnerability at Clatsop Plains, we reason that development is unlikely between the incipient foredune ridge and the older foredune ridge in the near future. We exclude the profiles with incipient dune ridges from the vulnerability calculations.

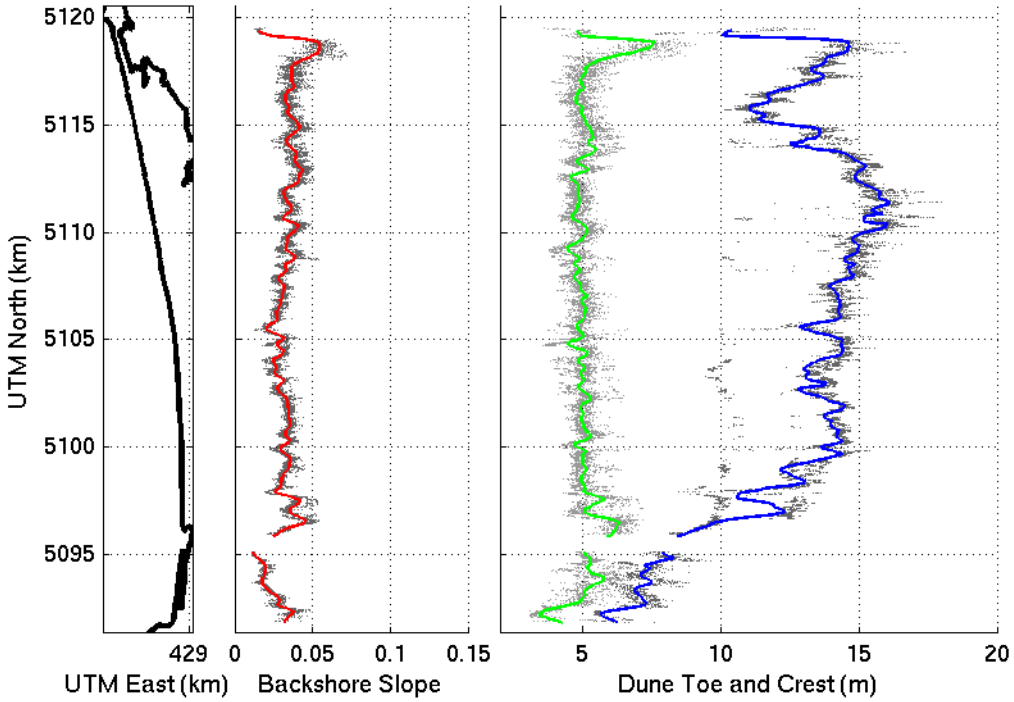

Figure 11. Dune parameters for Clatsop Plains, OR. The left panel indicates the alongshore position of each profile. The middle panel shows backshore slope values at each profile in grey. The red dots are backshore slope values that have been smoothed in the alongshore direction with a linear loess filter with a window size of 250 m. The right panel shows foredune toe and crest elevations. The toe elevations are shown in light grey and the crest elevations are shown in dark grey. The green dots and blue dots represent smoothed toe and crest elevations, respectively.

Figure 12 shows relatively high variability in the backshore slopes, foredune toe, and foredune crest elevations in Rockaway, OR. Foredune crests are relatively low along the middle section of the littoral cell. This has important implications for vulnerability to overtopping as this area is relatively developed with man-made structures built directly behind the foredunes. Some foredunes in the study area have been reinforced with beach armoring. Geomorphological features for the remaining study areas are presented and discussed in Appendix B.

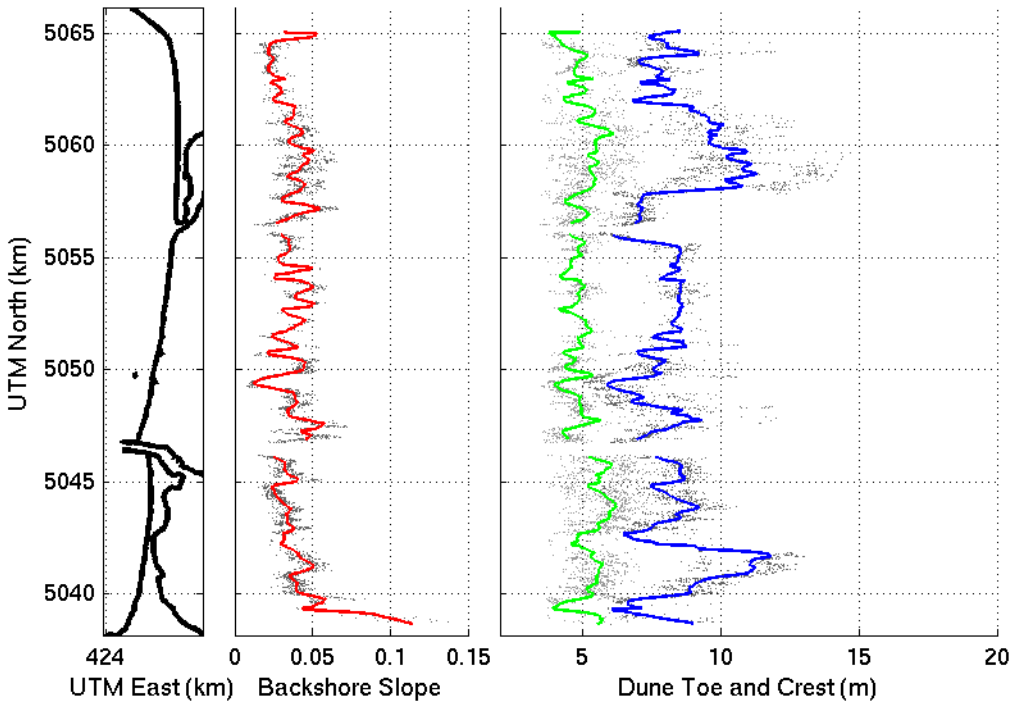

Figure 12. Dune and beach parameters for Rockaway, OR. The left panel indicates the alongshore position of each profile. The middle panel shows backshore slope values at each profile in grey. The red dots are backshore slope values that have been smoothed in the alongshore direction with a linear loess filter with a window size of 250 m. The right panel shows foredune toe and crest elevations. The toe elevations are shown in light grey and the crest elevations are shown in dark grey. The green dots and blue dots represent smoothed toe and crest elevations, respectively.

The extracted foredune parameters can be used to characterize geomorphology over the entire PNW. The means and standard deviations of SCR, backshore slope, foredune toe elevation, and foredune crest elevation are show in Figure 13. SCR are relatively large and variable within the CRLC (North Beach, WA – Clatsop Plains, OR). South of Clatsop Plains the magnitude and variability in the rates decrease. Beaches are relatively flat in the CRLC. Beaches are steeper from Sand Lake, OR to Siletz, OR. Foredune toe elevations are relatively similar throughout the PNW and there are no strong alongshore trends. Foredune crest heights are relatively small along the

Washington Beaches and tall in Clatsop Plains, Netarts, Sand Lake, and Neskowin, OR. Foredune crest elevations are relatively variable in Heceta Beach and Florence.

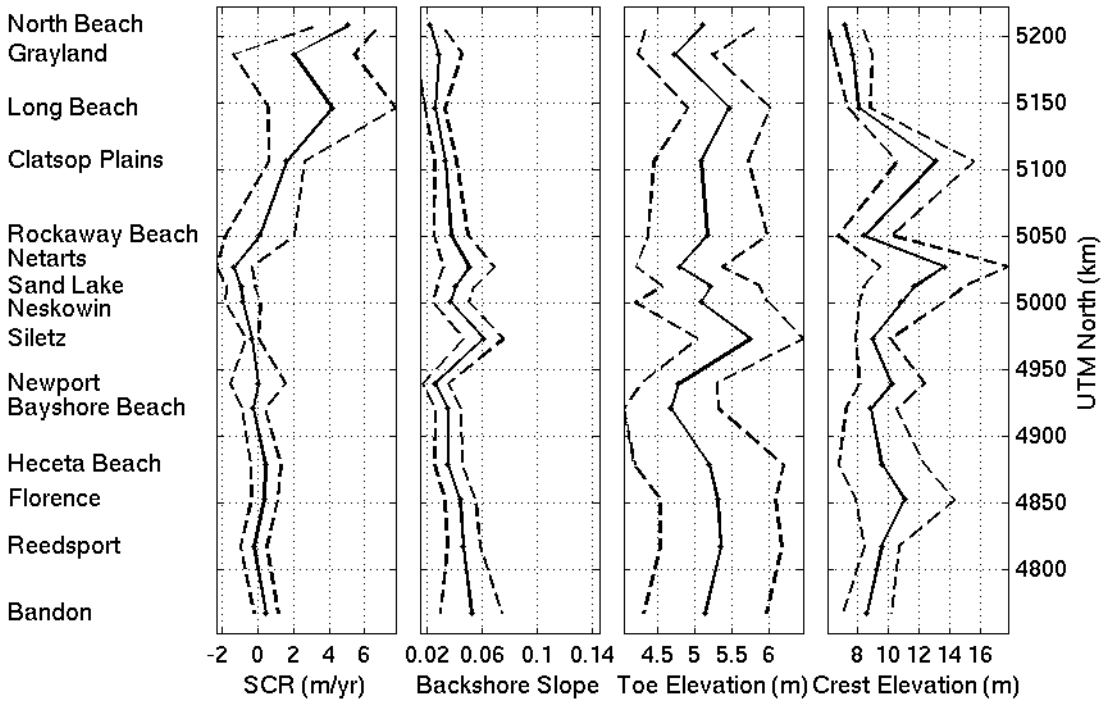

Figure 13. The means and the means plus and minus one standard deviation of SCR, backshore slope, and foredune toe elevations, and foredune crest elevations. The means are indicated by black solid lines while the means with a range of one standard deviation unit are indicated by black dashed lines.

Correlations between the geomorphological parameters are generally weak to moderate and not consistent between study areas. We include correlations between the geomorphological characteristics and both the SCR and absolute value of the SCR. The correlation coefficients between the geomorphological parameters in Long Beach, WA, Clatsop Plains, OR, and Rockaway, OR are presented in Tables 4 – 6. The foredune volumes, *V1* and *V2*, are moderately correlated with SCR and the absolute value of SCR at Clatsop Plains, OR (*R* ranges from 0.61 to 0.63). Foredune width is moderately correlated with SCR and the absolute value of SCR at this beach as well ($R = 0.64$).

Beach width is weakly correlated with SCR and the absolute value of SCR in Long Beach, WA (R = 0.52). Tables of correlation coefficients for the remaining study areas are presented and discussed in Appendix C.

Table 4: Cross-correlation coefficients between foredune and beach geomorphological parameters in Long Beach, WA. Statistically significant correlations are italicized and followed by an asterisk.

	SCR	**abs (SCR)**	**dtoe**	**dhigh**	**dheel**	**Fore-shore Slope**	**Back-shore Slope**	**Dune Face Slope**	**V1**	**V2**	**Dune Width**	**Beach Width**
SCR	*1.00*											
abs(SCR)	*1.00**	*1.00*										
dtoe	*-0.23**	*-0.23**	*1.00*									
dhigh	*-0.15**	*-0.15**	*0.44**	*1.00*								
dheel	-0.03	-0.03	0.02	-0.03	*1.00*							
Foreshore Slope	-0.03	-0.03	0.00	*-0.20**	0.04	*1.00*						
Backshore Slope	*-0.45**	*-0.45**	*0.51**	*0.16**	0.04	*0.25**	*1.00*					
Dune Face Slope	*-0.36**	*-0.36**	*0.35**	*0.51**	*-0.09**	*-0.08**	*0.41**	*1.00*				
V1	*0.33**	*0.33**	*-0.47**	*0.14**	0.04	-0.04	*-0.30**	*-0.31**	*1.00*			
V2	*0.29**	*0.29**	*-0.47**	0.05	*0.09**	-0.07	*-0.37**	*-0.53**	*0.82**	*1.00*		
Dune Width	*0.47**	*0.47**	*-0.40**	*-0.13**	0.01	*0.08**	*-0.29**	*-0.50**	*0.84**	*0.67**	*1.00*	
Beach Width	*0.52**	*0.52**	*-0.14**	*0.09**	-0.05	*-0.33**	*-0.85**	*-0.26**	*0.21**	*0.26**	*0.21**	*1.00*

Table 5: Cross-correlation coefficients between foredune and beach geomorphological parameters in Clatsop Plains, OR. Statistically significant correlations are italicized and followed by an asterisk.

	SCR	abs (SCR)	dtoe	dhigh	dheel	Fore-shore Slope	Back-shore Slope	Dune Face Slope	V1	V2	Dune Width	Beach Width
SCR	*1.00*											
abs(SCR)	*1.00**	*1.00*										
dtoe	*-0.13**	*-0.13**	*1.00*									
dhigh	*0.16**	*0.16**	*0.09**	*1.00*								
dheel	*-0.28**	*-0.27**	*0.16**	0.07	*1.00*							
Foreshore Slope	*-0.29**	*-0.29**	*0.23**	0.06	0.08	*1.00*						
Backshore Slope	*-0.35**	*-0.35**	*0.57**	*0.32**	*0.11**	*0.53**	*1.00*					
Dune Face Slope	*-0.63**	*-0.63**	*0.55**	0.03	*0.29**	*0.42**	*0.64**	*1.00*				
V1	*0.61**	*0.61**	*-0.22**	*0.58**	*-0.15**	*-0.12**	*-0.14**	*-0.59**	*1.00*			
V2	*0.63**	*0.63**	*-0.32**	*0.59**	*-0.17**	*-0.19**	*-0.22**	*-0.68**	*0.89**	*1.00*		
Dune Width	*0.64**	*0.64**	*-0.20**	*0.43**	*-0.17**	*-0.15**	*-0.19**	*-0.61**	*0.95**	*0.81**	*1.00*	
Beach Width	*0.13**	*0.13**	*0.29**	*-0.35**	0.06	*-0.34**	*-0.56**	*-0.13**	*-0.16**	*-0.16**	*-0.10**	*1.00*

Table 6: Cross-correlation coefficients between foredune and beach geomorphological parameters in Rockaway, OR. Statistically significant correlations are italicized and followed by an asterisk.

	SCR	**abs (SCR)**	**dtoe**	**dhigh**	**dheel**	**Fore-shore Slope**	**Back-shore Slope**	**Dune Face Slope**	**V1**	**V2**	**Dune Width**	**Beach Width**
SCR	*1.00*											
abs(SCR)	*0.27**	*1.00*										
dtoe	*0.47**	0.03	*1.00*									
dhigh	0.14	*-0.21**	*0.42**	*1.00*								
dheel	-0.13	0.13	0.02	*0.23**	*1.00*							
Foreshore Slope	-0.09	-0.04	*-0.18**	-0.14	0.01	*1.00*						
Backshore Slope	*-0.35**	*-0.28**	*0.29**	0.06	-0.03	*0.18**	*1.00*					
Dune Face Slope	*-0.37**	*-0.27**	0.06	*0.29**	0.07	-0.09	0.07	*1.00*				
V1	-0.02	*-0.30**	-0.02	*0.66**	-0.08	-0.15	0.00	0.08	*1.00*			
V2	0.06	-0.12	-0.02	*0.76**	*0.19**	-0.01	-0.02	-0.13	*0.75**	*1.00*		
Dune Width	0.03	*-0.22**	-0.03	*0.22**	*-0.23**	-0.15	0.04	-0.05	*0.78**	*0.29**	*1.00*	
Beach Width	-0.14	-0.02	*-0.38**	*-0.24**	0.16	*0.36**	*-0.24**	-0.12	*-0.278*	-0.06	*-0.33**	*1.00*

2.3.3 Estimating Physical Vulnerability to Erosion and Flooding

The extracted morphological parameters enable us to analyze vulnerability to overtopping at most profiles within each study area. Maximum TWL elevations in Long Beach, WA from the March 1999 storm conditions (Figure 14) exceed the dune toe elevations at all of the profile locations, which indicates that 100% of the profiles were at least in the Collision Regime of the Sallenger (2000) Storm Impact Scale. Maximum TWL values exceed the dune crest elevations (Overtopping Regime) at approximately 10.5% of the cross-shore profiles. This is predicted at both the north end of the peninsula

and in the south where dune crest elevations are low. This implies that these areas may be vulnerable to flooding during an event of this magnitude.

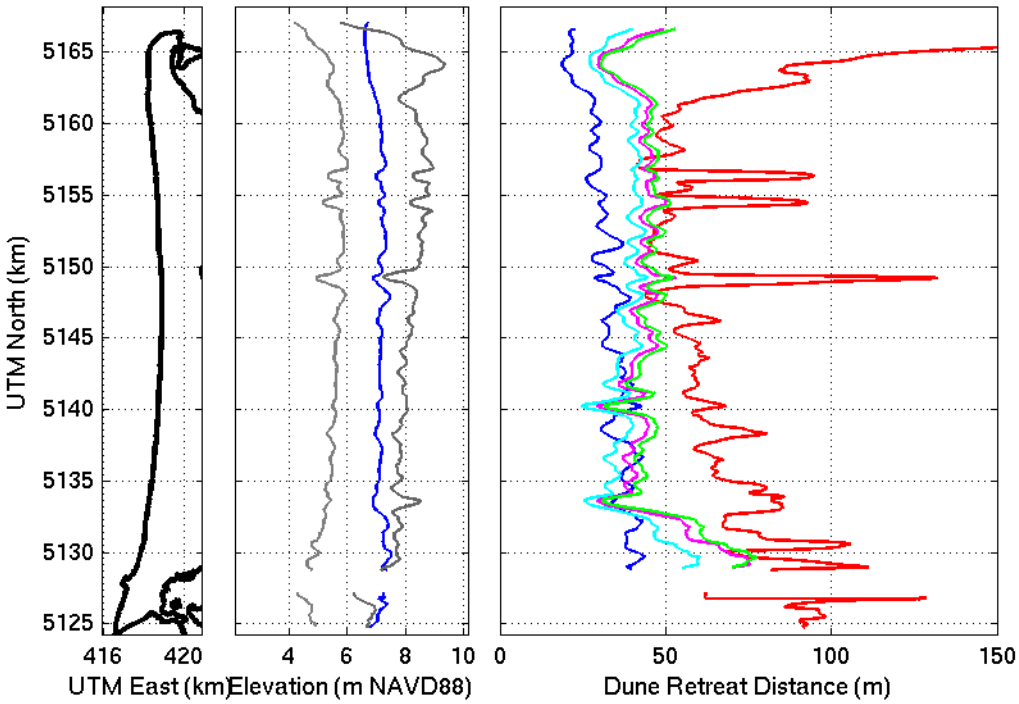

Figure 14. Estimated dune overtopping and retreat distance due to erosion during a severe winter storm at Long Beach, WA. The left panel indicates the alongshore position of each profile. The middle panel shows alongshore-smoothed dune toe elevations in light grey and smoothed dune crest elevations in dark grey. The alongshore-smoothed maximum TWL during the modeled storm is shown in blue. The right panel shows the dune retreat distances predicted by the K99 model (red) and the KD93 model (blue). The other lines are retreat distances predicted by the L04_1 model (purple), L04_2 model (turquoise), and L04_3 model Equation 20 (green). All parameters are smoothed with a linear loess filter and a window size of 500 m.

The vulnerability to overtopping is slightly different for foredunes in Clatsop Plains, OR (Figure 15). Maximum TWL values exceed the foredune toe elevations at all of the profiles so that they are in the Collision regime of the Sallenger (2000) impact scale. However, only approximately 4.7% of the profiles are predicted to be overtopped. All of the overtopped profiles are in the south of the study area, near Seaside, OR.

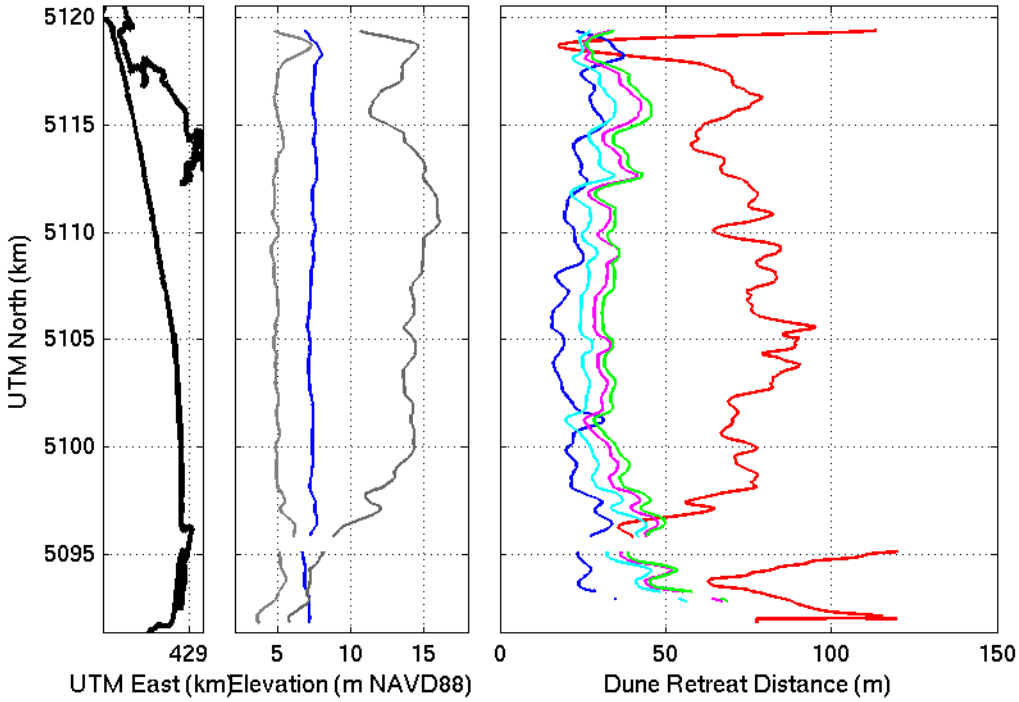

Figure 15. Estimated dune overtopping and retreat distance due to erosion during a severe winter storm at Clatsop Plains, OR. The left panel indicates the alongshore position of each profile. The middle panel shows alongshore-smoothed dune toe elevations in light grey and smoothed dune crest elevations in dark grey. The alongshore-smoothed maximum TWL during the modeled storm is shown in blue. The right panel shows the dune retreat distances predicted by the K99 model (red) and the KD93 model (blue). The other lines are retreat distances predicted by the L04_1 model (purple), L04_2 model (turquoise), and L04_3 model Equation 20 (green). All parameters are with smoothed with a linear loess filter and a window size of 500 m.

Maximum TWL elevations are in the Collision Regime of the Sallenger (2000) Impact Scale for all of the profiles in Rockaway, OR (Figure 16). Dune overtopping is predicted for approximately 23.5% of the profiles; at the southern end of Nehalem Spit, at three areas along Rockaway Beach, and at two sites on the Bayocean Peninsula.

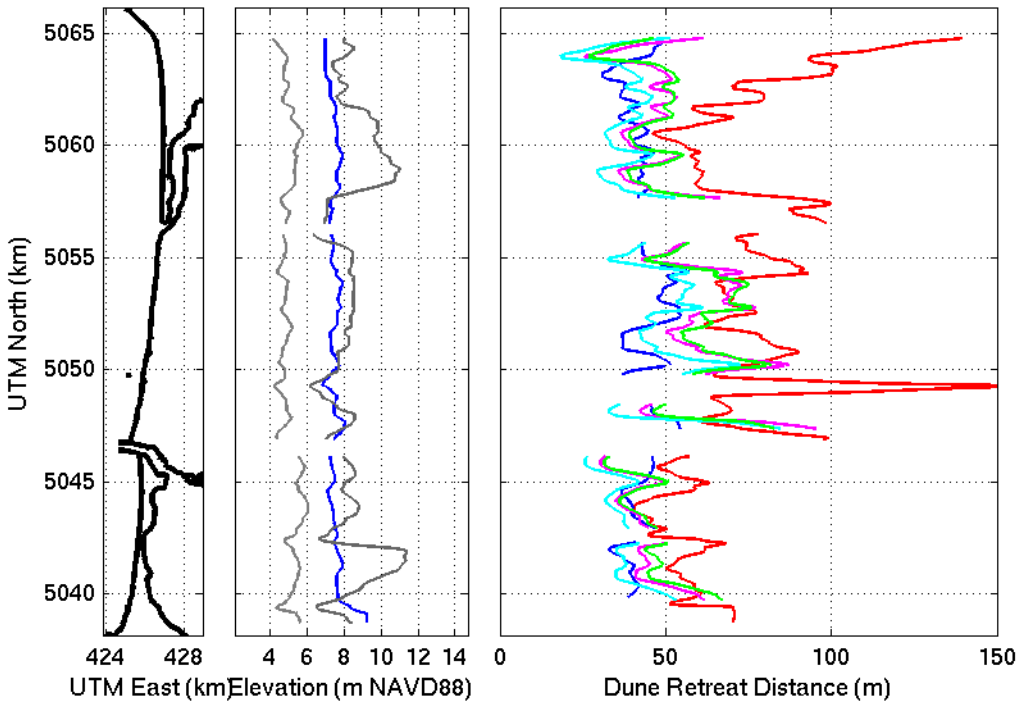

Figure 16. Estimated dune overtopping and retreat distance due to erosion during a severe winter storm at Rockaway, OR. The left panel indicates the alongshore position of each profile. The middle panel shows alongshore-smoothed dune toe elevations in light grey and smoothed dune crest elevations in dark grey. The alongshore-smoothed maximum TWL during the modeled storm is shown in blue. The right panel shows the dune retreat distances predicted by the K99 model (red) and the KD93 model (blue). The other lines are retreat distances predicted by the L04_1 model (purple), L04_2 model (turquoise), and L04_3 model Equation 20 (green). All parameters are with smoothed with a linear loess filter and a window size of 500 m.

As expected, the K99 model is the most conservative dune erosion model and predicts the largest dune retreat distances at the three study areas (Table 7). The KD93 model is generally the least conservative model at the three study areas. Of the L04 models, the L04_2 model is the least conservative and the L04_3 model is the most conservative. Had we used the same initial dune toe elevation in all versions of the L04 models, the L04_1 equation would have predicted the least amount of erosion. For the L04_1 model, we use the elevation of the dune toe above the TWL (excluding runup).

This elevation difference is relatively small and the model predicts a moderate dune retreat distance relative to the other versions of the model. For the L04_2 model, which includes a temporal increase in runup, we use the initial dune toe elevation above MHW. This elevation difference is relatively large the model predicts the least amount of erosion relative to the other versions of the model.

Profiles with relatively low dune toes, including areas with paths and beach access roads, coincide with spikes in the erosion distance as the beach slopes are low and the dune toe elevations are low (Figures 14 – 16). These areas are clearly susceptible to erosion. At profiles with relatively low foredune toe elevations and backshore slopes the K99 model predicts large erosion distances that are unrealistic for a single storm event. Erosion distances at these profiles have been excluded from analyses. The three versions of the L04 model all predict a similar alongshore pattern of erosion at slightly different scales. The KD93 and L04 models are not valid for profiles in which the TWL exceeds the dune crest elevation and so overtopped profiles are excluded for these models.

Table 7: Mean Predicted Foredune Retreat Distances for Long Beach, WA, Clatsop Plains OR, and Rockaway, OR.

	Long Beach (m)	**Clatsop Plains (m)**	**Rockaway (m)**
K99	70	72	64
KD93	33	24	43
L04_1	44	35	48
L04_2	39	29	40
L04_3	46	37	49
Mean	**46**	**39**	**49**

2.4 DISCUSSION

The lidar derived foredune morphometric data enable us to examine regional variability in geomorphology and the associated physical vulnerabilities to storm induced overtopping and erosion. However, it is important to consider that analysis of one lidar data set does not resolve temporal variability. Successive collections of airborne lidar topographic data are necessary to resolve coastal geomorphological change. Although not considered in this paper, unresolved temporal variability adds uncertainty to the geomorphological parameters and the estimates of physical vulnerability.

2.4.1 Automatic Dune Parameter Selection

Comparisons between the automatically selected dune morphological parameters and those selected by hand for specific profiles suggest that these techniques are an unbiased method to extract parameters at a high alongshore resolution. The selection RMSE values for the dune toes are all less than 1 m (Table 2), and the mean vertical bias is less than the vertical RMSE for the lidar scanner (20 cm). The selection RMSE values for the dune crests are low with almost no biases. The vertical RMSE values for the foredune toe and crest elevations compare well with those reported by Elko et al. (2002).

Comparisons between the automatically chosen lidar dune parameters and those extracted manually from the SWCES CRLC profiles also indicate that the automatic-selection methodology extracts reasonable values for dune parameters. Errors for the dune crests and heels are most likely due to vegetation as the lidar parameters have positive biases on the order of dune grass height. The mean vertical bias for the foredune

crest elevation in the CRLC is 0.61 m (Table 3). This is approximately equivalent to the height of the three dominant dune grass species under average wind conditions (Zarnetske, personal communication). In Long Beach, WA the mean difference between the maximum storm TWL and foredune crest elevation at each profile is -1.11 m. Decreasing the dune crest elevations by 0.61 m changes this mean difference to -0.55 m. The percentage of profiles that are predicted to overtop increases from 10.5% to 24.6%. The inclusion of vegetation in the lidar data is less important in regions with taller foredunes and does not impact estimates of vulnerability to erosion with the K99 and L04 models. Although the KD93 model is sensitive to changes in foredune crest elevation, it will be shown later that changes on the order of 0.61 m do not impact estimates of foredune erosion by much.

Buildings can be incorrectly selected as the dune crest on profiles in which houses are built behind the foredune. Stockdon et al. (2009) exclude structures by identifying sections of a profile which exceed a maximum slope threshold and eliminating the entire portion of profile behind the most shoreward location that is too steep. There are relatively steep dunes in the PNW and it is difficult to set a maximum slope threshold that excludes buildings and not some foredunes. This problem is exacerbated with foredunes that have been scraped to remove the crest in front of houses so that there is no discernable maximum on the cross-shore profile. In developed areas, the cross-shore *dhigh* locations must be plotted and compared with aerial photographs. *dhigh* points that fall over buildings or other structures are typically re-selected by hand from each profile or eliminated from the data set.

It is difficult to accurately extract the dune toe on profiles with beach berms, particularly those with relatively deep troughs behind the berms. These low points are often the minima on detrended profiles and one can avoid selecting them as the dune toe by specifying a vertical window, relative to MHW and the dune crest, within which to look for the beach-dune junction. However, if a trough is too high in elevation it cannot be excluded because a vertical window that filters it out also removes relatively low dune toes at other locations. We examine profiles with berms closely, and select the maximum vertical elevation that excludes most beach troughs but includes all correct dune toes. Beach berm troughs that are incorrectly selected as dune toes are immediately identified by plotting the cross-shore dune toe locations and noting those that are too close to the shoreline. For these profiles, one must select the dune toes by hand or exclude them from further analysis.

2.4.2 Foredune Geomorphology

Although there are moderate vertical errors, our methodology reveals beach and dune morphological variability on both small and large length scales that can not be resolved with data collected by any other method. For example, the parameters extracted for each study area may help us begin to understand which processes drive foredune evolution.

Psuty (1992) predicted that tall foredunes can be found on relatively stable beaches. Short foredunes can be found on prograding beaches, where incipient foredunes continually build seaward, or eroding beaches, where foredunes are frequently eroded. North Beach, Grayland, and Long Beach, WA each have relatively high mean SCR and

large SCR variability (Figure 13). The mean foredune crest elevations at these beaches are relatively low with relatively small variability as suggested by Psuty's (1992) model. However, these are also the study areas where *A. breviligulata*, the grass associated with small foredunes, is the dominant dune grass (Seabloom and Weidemann (1994); Hacker et al.; in press). Therefore, there is evidence to suggest that both ecological and physical factors are important in foredune evolution within these study areas and more analyses are required to determine the importance of each.

The SCR at Clatsop Plains, OR are lower and have less variability than the subcells to the north implying that the beach sediment supply is closer to equilibrium. The foredunes in Clatsop are also relatively tall, again as suggested by Psuty's (1992) model. However, the dune grasses in Clatsop Plains consist of approximately 50% *A. breviligulata* and 50% *A. arenaria* (Seabloom and Weidemann (1994); Hacker et al.; in press). This implies that the dune grasses could be important as well as *A. arenaria* is the grass associated with taller foredunes (Hacker et al., in press).

It is interesting to compare the general features of Clatsop Plains with those in Rockaway, OR. Dune grasses in Rockaway mostly consist of *A. arenaria* (Seabloom and Weidemann (1994); Hacker et al.; in press) yet the foredunes there are relatively short. If dune grasses are more important than physical processes in foredune geomorphology, one might expect the foredunes to be taller in Rockaway than Clatsop Plains. However, this is not the case. The mean SCR for Rockaway is approximately 0.10 m/yr. This is relatively small and indicates that the beach sediment supply is near equilibrium. Psuty's (1992) model might predict relatively tall foredunes within this study area, assuming that the dune sediment supply rate is positive. It is important to note that the SCR is not a

proxy for foredune sediment supply rate. A different foredune sediment supply rate could account for the different foredune characteristics between Clatsop Plains and Rockaway but this cannot be determined without more information.

Calculating the means and standard deviations of the foredune parameters for each study area can ignore important variability within each study area. Figures 10 – 12 reveal considerable alongshore variability within Long Beach, Clatsop Plains, and Rockaway. For example, there is a strong north-south gradient in foredune height in Clatsop Plains. If the dune grass composition is consistent along the entire study area, the alongshore trends in geomorphology imply that physical mechanisms are important to foredune evolution. Future work will attempt to resolve the relative importance of physical and ecological mechanisms in controlling foredune geomorphology.

2.4.3 Estimating Physical Vulnerability to Erosion and Flooding

Since our goal is to analyze regional variability in vulnerability due to variability in foredune geomorphology and not variability in hydrodynamics we applied the same March 1999 storm conditions as measured in southern Washington and northwestern Oregon to the entire PNW coast

There are few recorded observations of overtopping and foredune erosion from the March 2-4 1999 storm (Jon Allan, personal communication). However, Allan and Komar (2002) and Allan and Priest (2001) qualitatively report foredune toe retreat distances on the order of tens of meters in Rockaway during the storm. Some foredunes in southwest Washington were observed to have experienced overtopping during the event (Peter Ruggiero, personal communication). Unfortunately these qualitative

observations give us little opportunity to compare the estimates of overtopping and erosion from each model to observations from the region.

To synthesize the relative vulnerability to overtopping of each profile, and compare relative vulnerability between study areas, we normalize the amount of overtopping by the dune face height to create a flooding index as follows

$$I_F = \frac{(TWL - dhigh)}{dhigh - dtoe} \ . \tag{24}$$

Positive values indicate overtopping and negative values indicate no overtopping. A value of one indicates that the water elevation exceeds the dune crest by approximately one dune height. Flooding indices for the March 1999 storm are plotted for Long Beach, WA and Rockaway, OR in Figure 17.

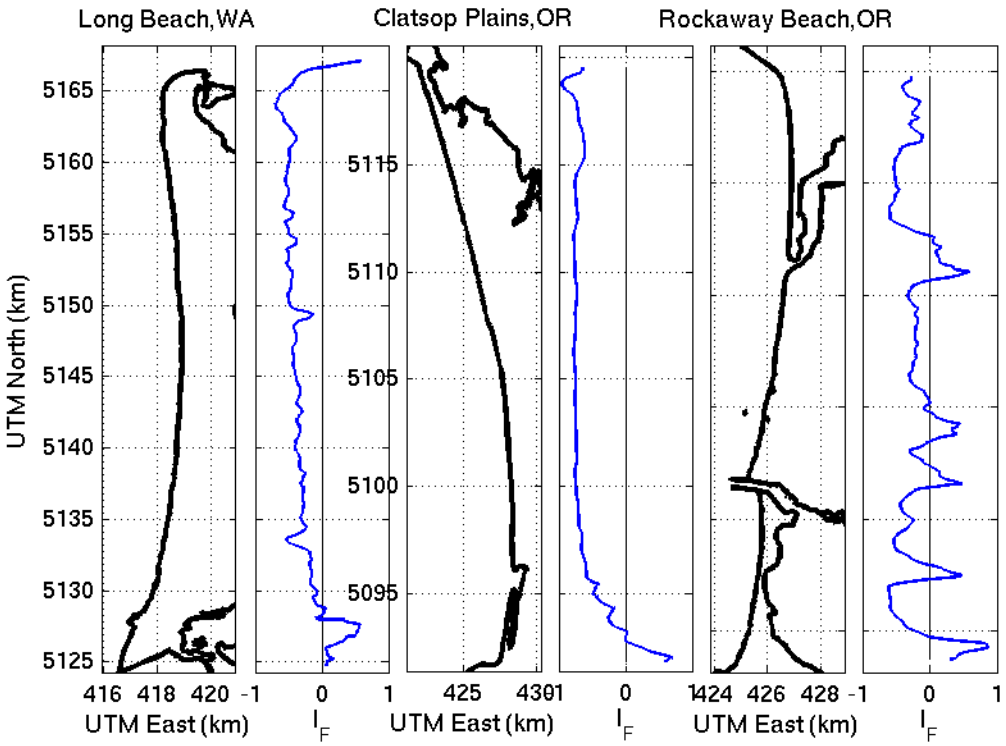

Figure 17. Flooding indices for Long Beach, WA and Rockaway, OR. The flooding index normalizes the amount of overtopping by the height of the foredune to give relative vulnerability of overtopping.

The relatively vulnerability to overtopping between study areas is compared with the mean flooding indices (Table 8). The mean flooding indices are more informative than the percent of overtopped profiles as they provide information about *how much* the TWL values exceed the dune crest elevations. A more positive mean index indicates an increased vulnerability to overtopping. The mean flooding indices indicate that Rockaway is the most vulnerable beach to overtopping and imply that foredunes dominated by *A. breviligulata* are not necessarily more susceptible to overtopping. Clatsop Plains is the least vulnerable to overtopping.

Table 8: Percentage of Overtopped Foredunes and Mean Flooding Indices for Long Beach, WA, Clatsop Plains, OR, and Rockaway, OR.

	Long Beach	**Clatsop Plains**	**Rockaway**
Percentage of Overtopped Foredunes	10.3 %	4.7%	23.5%
Mean I_F	-0.3	-0.6	-0.2

To estimate the relative vulnerability to erosion between study areas, we normalize the amount of erosion predicted by each of the dune erosion models by the dune width to create an erosion index for each profile

$$I_E = 1 + \frac{(E_{\max} - W)}{W} \tag{25}$$

where E_{max} is the maximum dune retreat distance predicted by each model and W is the foredune width. A value of zero indicates no erosion, while a value of 1 indicates that a particular foredune is predicted to be completely eroded. A value greater than one indicates erosion distances in equivalent dune widths. Erosion indices are plotted for Long Beach, WA, Clatsop Plains, OR, and Rockaway, OR in Figure 18. The uncertainties in the foredune heel location discussed earlier can add to inaccuracy in the foredune width estimates and the erosion indices.

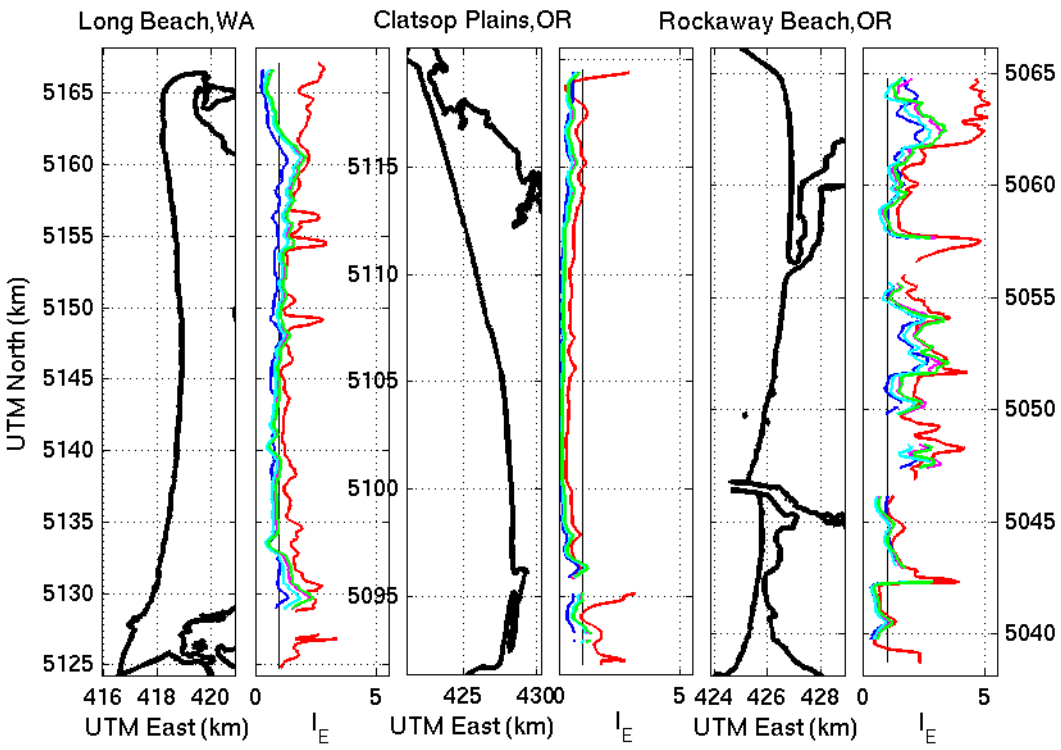

Figure 18. Erosion indices for Long Beach, WA, Clatsop Plains, OR, and Rockaway, OR. The erosion index normalizes the amount of erosion by the width of the foredune to give relative vulnerability of erosion. Indices are plotted for predictions by the K99 model (red), KD93 model (blue), L04_1 model (purple), L04_2 model (turquoise), and L04_3 model (green).

The mean erosion indices determined by each model enable us to quickly compare the relative vulnerabilities to erosion for each study area (Table 9). The overall mean indices imply that Rockaway is the most vulnerable to erosion. This is important as Rockaway Beach is a highly developed area with houses and buildings directly behind the foredune ridge. Clatsop Plains is the least vulnerable to erosion which implies that dunes with *A. arenaria* are not necessarily more susceptible to erosion. The percent of profiles with completely eroded foredunes (Table 9) enable us to compare vulnerability to erosion between littoral cells. However, the mean erosion indices provide more

information than the percentage of completely eroded foredunes and the mean predicted erosion distances (Table 7) as they convey *how much* of each foredune is eroded.

Table 9: Percentage of Completely Eroded Foredunes and Mean Erosion Indices for Long Beach, WA, Clatsop Plains, OR, and Rockaway, OR.

	Long Beach		**Clatsop Plains**		**Rockaway**	
	% Eroded Foredunes	**Mean I_E**	**% Eroded Foredunes**	**Mean I_E**	**% Eroded Foredunes**	**Mean I_E**
K99	100	1.7	20	0.8	91	2.4
KD93	16	1.7	0	0.3	80	1.4
L04_1	55	0.8	8	0.4	82	1.9
L04_2	44	1.1	5	0.4	69	1.7
L04_3	61	1.0	9	0.4	83	1.8
Overall Mean	**55**	**1.3**	**8.4**	**0.5**	**81**	**1.8**

There is no direct quantitative way to compare the erosion observed during the March 1999 storm with erosion predicted from these storm conditions and the 2002 beach and lidar morphology. However, Allan and Komar (2002) and Allan and Priest (2001) report dune retreat distances in Rockaway, OR on the order of tens of meters which is at least moderately consistent with the estimated distances by all three models.

We test the sensitivities of the TWL calculation and each foredune erosion model to the morphological parameters that are input into each model. The K99 model is the most conservative model and it is sensitive to inaccuracies in the automatically selected dune toe elevations and backshore slopes. The horizontal RMSE in the automatically selected dune toes and the errors in the calculated backshore slopes are not presented or discussed in this paper. However, the horizontal RMSE between the automatically selected dune toe locations and those selected by visual inspection of random profiles is 5.3 m for Long Beach, WA. The mean dune toe elevation and beach width for this beach

are 5.5 m and 140 m respectively. Combining this with the total vertical RMSE for automatically selected dune toes from Table 2 (0.51 m) the uncertainty in the backshore slope can then be estimated for this beach as $q_b = (5.5 \pm 0.51)/(140 \pm 5.3)$; which yields a range of approximately 0.013. Figure 19 shows how the TWL values change with backshore beach slope for the maximum wave height, period, and surge observed during the storm. TWL values vary by approximately 0.50 m per 0.01 units of slope which implies that small inaccuracies in the lidar slopes could impact TWL estimates. As discussed previously, the vertical bias in the dune crest elevations at this beach yielded a mean difference of -0.55 m between the predicted maximum TWL and dune crest elevations. This implies that the uncertainties in backshore slope, combined with the bias in dune crest elevations, could lead to a high degree of variability in the estimate of the number of profiles overtopped. In addition, the 2002 lidar data does not capture temporal variability in any of the geomorphological parameters. As the foredune crests change throughout time, the estimated number of overtopped profiles will change accordingly. Uncertainty in the cross-shore location of MHW will also add to uncertainty in the backshore slope and TWL estimates.

The K99 model is sensitive to changes in backshore slope and dune toe elevation (Figure 19). In general the predicted erosion distance decreases with increasing backshore slope. The model is relatively sensitive to changes in slope and dune toe elevation on flat beaches and relatively insensitive to changes in slope and dune toe elevation on steep beaches. The mean backshore slope and dune toe elevation of Long Beach are 0.026 and 5.5 m respectively, which yield a retreat distance of approximately 75 m. The range of total RMSE for the dune toe (~0.50 m) at this slope yields erosion

distance estimates between 60–100 m. For a given dune toe elevation, a range of backshore slope of 0.01 can yield an erosion distance range of approximately 75 m for beaches with gentle slopes and a range of approximately 15 m for steep beaches.

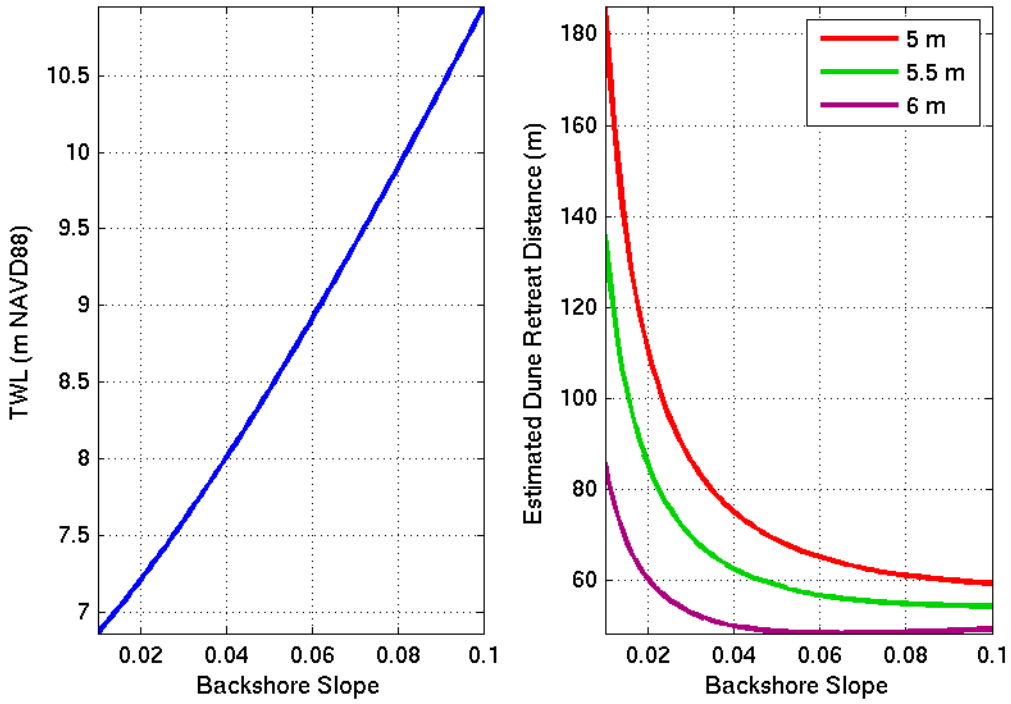

Figure 19. Dependence of the K99 model on backshore beach slope and dune toe elevation. The left panel shows the TWL values for different slopes with the maximum wave height, period, and surge from the storm of record. The right panel shows dune retreat distances predicted by the K99 model with a range of slopes and three dune toe elevations: the mean dune toe elevation for Long Beach, WA (~5.5 m) and the mean with a range of the total dune toe RMSE for Long Beach (~0.5 m).

The K99 model is attractive because it is straightforward to apply and conservative. Foredune erosion in the PNW is difficult to predict and often increases during El Niño events when monthly mean water levels are increased and the mean wave incident angle shifts to the north to maximize erosion (Ruggiero et al., 1996; Komar, 1998b; Allan and Komar, 2002). Rip current embayments, which are also difficult to

predict, can accelerate erosion in a particular area (Komar, 1998b; Komar et al., 1999). The models do not account for this but the K99 model is the most conservative model and may provide a margin of safety if applied to a potential development site in an area that suffers from chronic, or sporadic but intense erosion.

The KD93 model is slightly more complex than the K99 model. We tested the sensitivity of the model to the foredune crest elevation, storm duration, shape parameter, and backshore slope. It should be noted that dune toe elevation is only used in the calculation of the erosion response time scale (12) and tests confirmed that the model is not sensitive to changes in dune toe elevation. In all of these tests we make the simplifying assumption that the backshore slope and foreshore slope are equal. Figure 20 shows the sensitivity of the potential erosion (E_KD93_{∞}), fraction of potential erosion (α), and maximum time-dependent erosion (E_KD93) to the shape parameter (A) and the foredune crest elevation.

When determining the sensitivity of the KD93 model to the shape parameter, the A values were varied while the slope was held constant. This is not a realistic scenario as A values are positively correlated with slope (Figure 8) but it enables us to determine if uncertainties in our calculation of A lead to significant variability in predicted dune retreat distances. The erosion estimates are sensitive to the shape parameter. In general increasing the shape parameter decreases the surf zone width and this decreases E_KD93_{∞} (Figure 20a). Increasing A also decreases the erosion response time scale (T_S) and the estimated fraction of time-independent erosion that occurs during the storm (α) as a smaller value of A indicates a smaller profile that needs to come into equilibrium. The RMSE between the shape parameter predicted by Moore's (1982) equation and the linear

regression (11) is 0.016. This range in the shape parameter leads to a difference of a few meters in the maximum time-dependent erosion distance (*E_KD93*) for a given foredune crest height (Figure 18c). Figure 18d shows that the maximum time-dependent erosion is sensitive to the time duration of the storm. Choosing a storm duration can be subjective, but calculating the time that the water exceeds MHW (plus a local bias due to mean wave setup elevations (Ruggiero and List, 2009)) is intuitive as this is the period when beach and foredune erosion would occur. The mean shape parameter for Long Beach, determined by linear regression, is 0.10 $m^{1/3}$. For this shape parameter, changes in storm duration of one hour lead to differences in the maximum time-dependent erosion distance of approximately 1 m.

The mean dune crest elevation for Long Beach with a range of 1 m (approximately the total RMSE for Long Beach dune crests) is shown. The model is sensitive to changes in crest elevation. A difference of 1 m in crest elevation yields a difference in maximum time-dependent erosion of only a few meters for a range of *A* values. This implies that bias in the foredune crest elevations due to vegetation do not lead to large variability in the dune retreat distances predicted by the KD93 model.

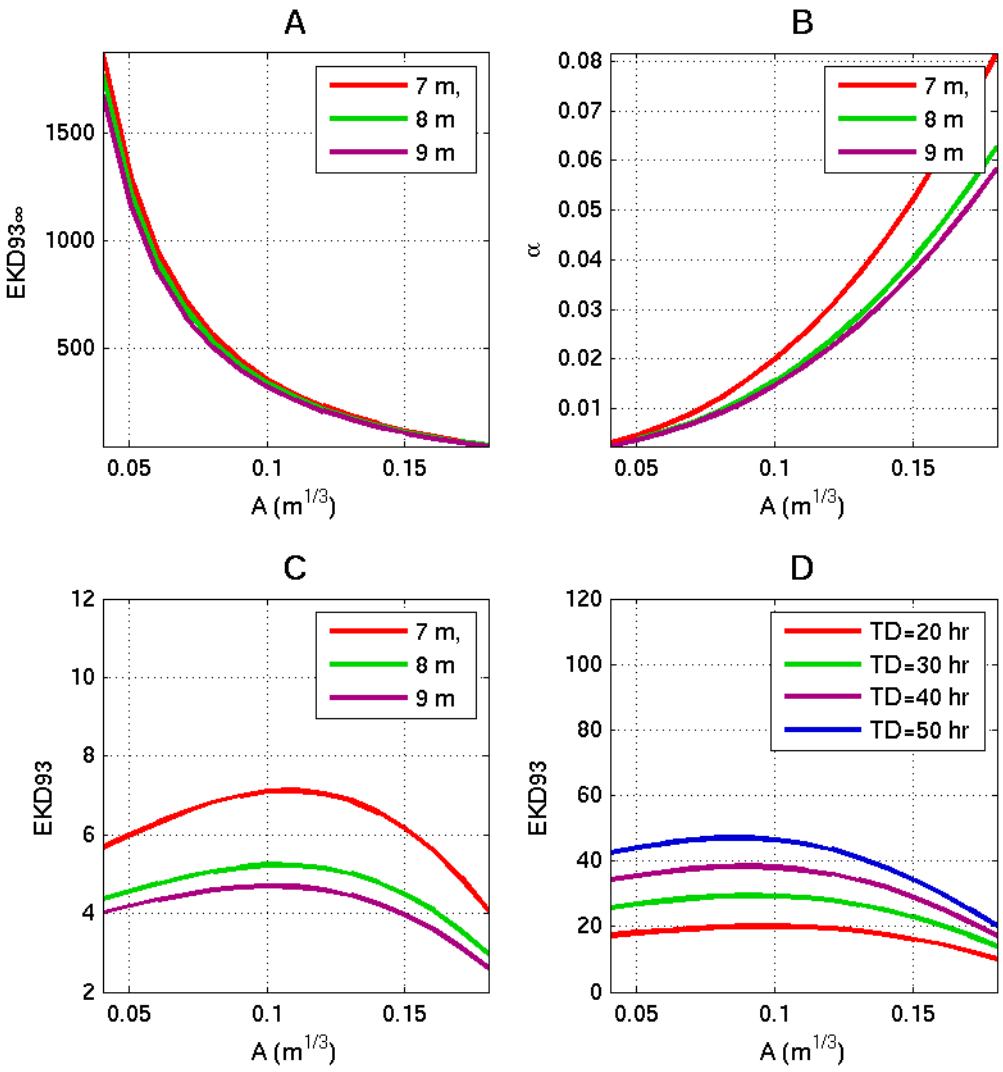

Figure 20. Dependence of A) the potential erosion (*E_KD93*$_\infty$) on the shape parameter and foredune crest elevation; B) fraction of potential erosion (α) on the shape parameter and foredune crest elevation; C) maximum time-independent erosion (*E_KD93*) on the shape parameter and foredune crest elevation; and D) maximum time-dependent erosion (*E_KD93*) on the shape parameter and total storm duration (T_D).

We also test the sensitivity of the KD93 model to changes in backshore slope and foredune crest elevation. For these calculations, slope is varied and *A* values are calculated from the linear regression between slope and *A* (11). Figure 21 shows the sensitivity of the potential erosion (*E_KD93*$_\infty$), fraction of maximum time-dependent

erosion (α), and maximum time-dependent erosion (*E_KD93*) to the backshore slope and the foredune crest elevation. In general, if slopes increase, TWL values increase, *A* values increase, and surf zone width decreases. All of these changes lead to a decrease in E_KD93_{∞} and Figure 21a confirms this. They also lead to a decrease in the erosion response time scale (T_S) and an increase in α, which Figure 21b confirms. In general as foreshore slope, *A*, and surf zone width decrease, there is a relatively shorter profile that has to come into equilibrium during the storm and thus T_S decreases (Kriebel and Dean, 1993). Figure 21c shows that E_KD93_{∞} has a positive dependence on backshore slope, which is the opposite of the K99 model. The predicted *E_KD93* retreat distances are more sensitive to changes in foredune crest elevation on steeper beaches. A slope difference of 0.01 yields a difference in retreat distance of approximately 10-20 m.

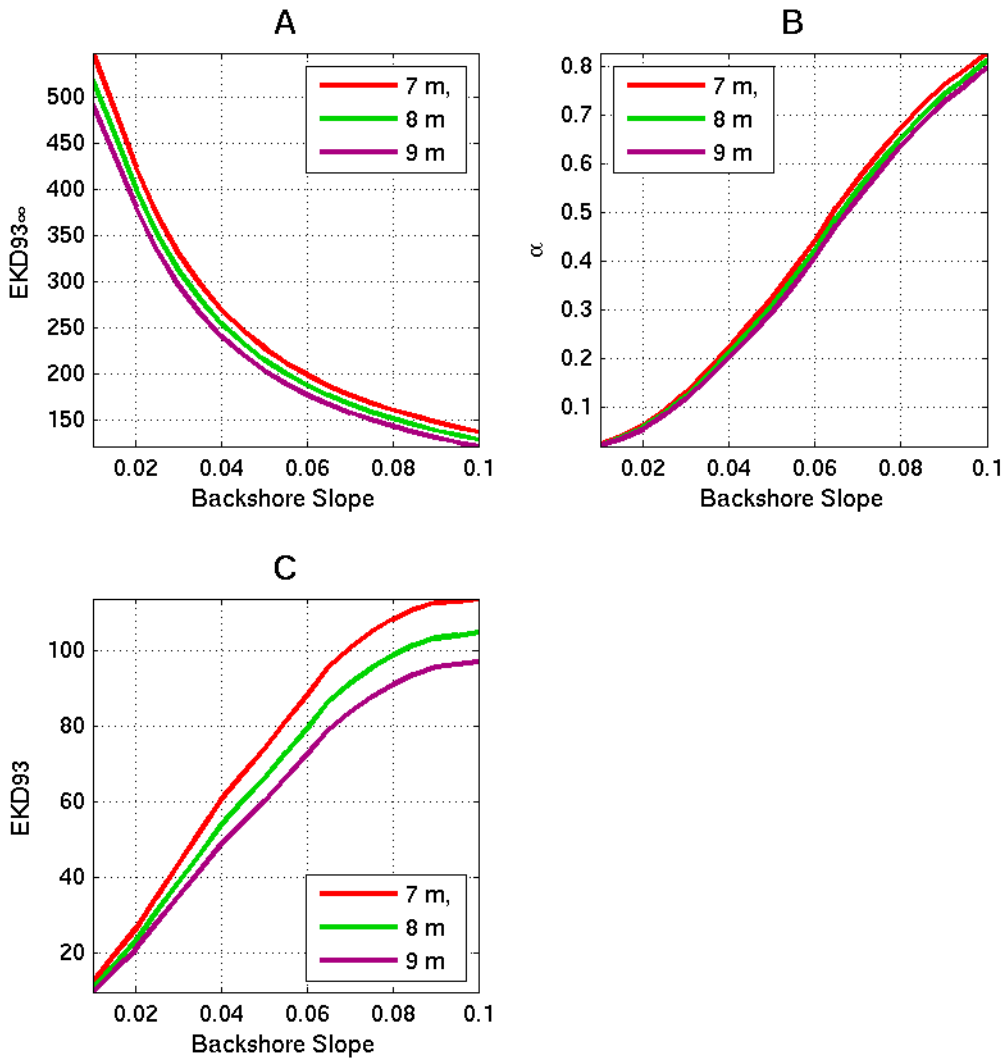

Figure 21. Dependence of A) the potential erosion (*E_KD93*$_\infty$) on the backshore slope and foredune crest elevation; B) fraction of maximum time-independent erosion (α) on the backshore slope and foredune crest elevation; and C) maximum time-dependent erosion (*E_KD93*) on the backshore slope and foredune crest elevation.

Foredune retreat distances were predicted with a version of the KD93 equation that includes beach width (results not shown) (Kriebel and Dean, 1993). Beach widths for each cross-shore profile in Long Beach, WA were used and the alongshore pattern of

erosion was very similar to that calculated without beach width although the retreat distances were approximately 40% smaller.

All of the L04 models predict the same alongshore pattern of erosion at different scales. The L04_3 model predicts the greatest erosion, followed by the L04_1 model and the L04_2 model. We estimate the sensitivity of the simplest model (L04_1) to changes in backshore beach slope and foredune toe elevation (Figure 22). The dune retreat distance cannot be calculated directly from (24) without associated changes in the other variables as negative erosion distances can be calculated. Instead a linear regression between the estimated eroded volumes and dune retreat distances for Long Beach, WA using L04_1 is enables us to convert eroded volume to eroded distance (Figure 22, left panel). The L04_1 model does not explicitly depend upon beach slope, but it is dependent upon R_2 which is a function of beach slope (5). The plots indicate that the model is generally positively dependent upon beach slope which is similar to the KD93 model and opposite to the relationship in the K99 model. The model is less sensitive to changes in slope and toe elevation on flatter beaches and more sensitive to changes in these parameters on steep beaches. This is also similar to the KD93 model. For steep beaches, changes in dune toe elevation on the order of 0.50 m are roughly equivalent to differences in erosion distance of approximately 50 m. For flat beaches, changes in dune toe elevation on the order of 0.50 m are roughly equivalent to differences in erosion distance of approximately 10-20 m. It is important to note that the L04 models do not account for tides or TWL. At many cross-shore profiles, the vertical tide variations from the March 1999 conditions are greater in magnitude than the storm surge.

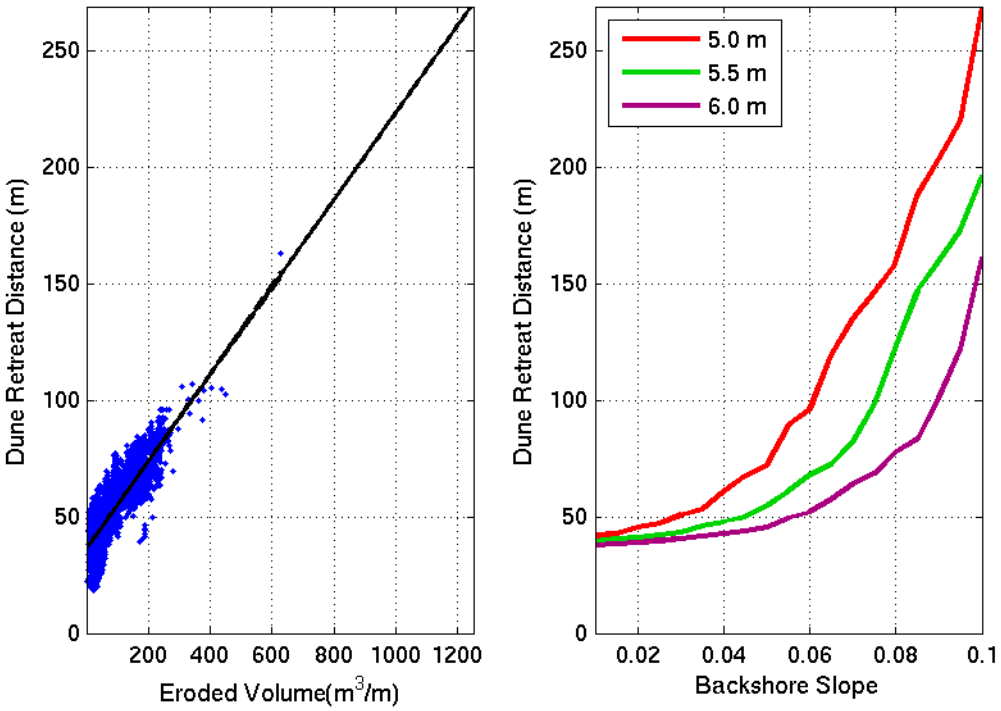

Figure 22. Dependence of the L04 model on dune toe elevation and backshore slope. The left panel is a plot of the eroded volumes for Long Beach, WA, estimated by the L04_1 model (17), and the corresponding dune retreat distances, calculated by (24). The black line shows the linear regression fit to the data, significant at the 95% confidence level. The left panel shows the predicted dune retreat distances estimated by L04_1 with different dune toe elevations and backshore slopes. The eroded volumes calculated by L04_1 have been converted to dune retreat distances by the linear regression in the right panel.

We directly compare the sensitivities of the models to beach slope in Figure 23. The K99 model is negatively dependent upon beach slope while the KD93 and L04_1 models are positively dependent upon beach slope. For relatively dissipative beaches ($tan\ \beta_b$ ranges from 0.01 to 0.03), the K99 model is the most conservative, followed by the L04 models and the KD93 model. The KD93 and L04 models also are less sensitive to changes in foredune crest and toe elevations respectively on dissipative beaches. For steeper beaches, the L04 models are the most conservative followed by the KD93 model and the K99 model. The L04 model is relatively sensitive to changes in foredune toe

elevations at steeper beaches while the K99 model is relatively insensitive to changes in toe elevation at steeper beaches and the KD93 is relatively insensitive to changes in crest elevation at steeper beaches. Currently, there is no reliable storm erosion data for the PNW to determine if foredune erosion is dependent upon beach slope. It is important to note that the K99 and KD93 models seem to reach asymptotes for steeper beaches and are relatively insensitive to changes in beach slope for relatively steep beaches ($tan\ \beta_b >$ 0.07). In contrast, the L04_1 model curves have a positive slope for steeper beaches implying that the model is relatively sensitive to changes in slope for steeper beaches.

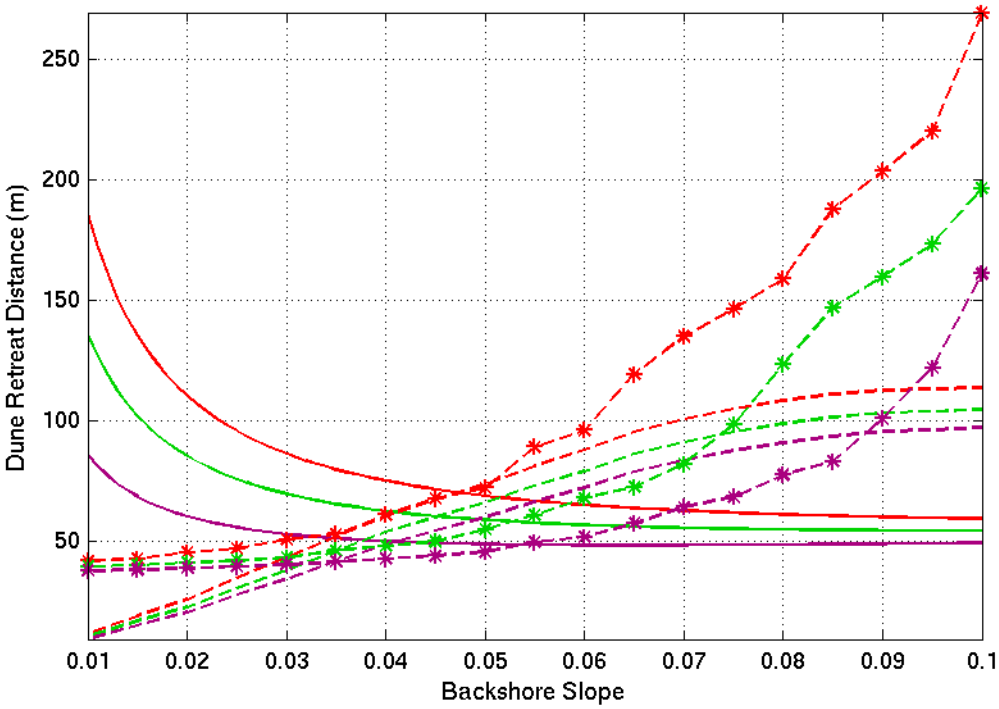

Figure 23. Dependence of the K99 (solid lines), KD_93 (dashed lines), and L04_1 (dashed lines with asterisk) models on beach slope. For the K99 and L04_1 models, foredune toe elevations of 5 m, 5.5 m, and 6 m are shown in red, green, and purple respectively. For the KD93 model, foredune crest elevations of 7 m, 8 m, and 9 m are shown in red, green, and purple respectively

2.5 CONCLUSIONS

The techniques described in this paper enable us to extract morphometric parameters of coastal foredunes and analyze patterns of variability on both small and large length scales. The vertical RMSE and bias estimates for the techniques indicate reasonable, unbiased estimates of the parameters. The vertical RMSE values for the techniques are comparable to subjective techniques which can only be applied to smaller stretches of beach.

The extracted morphometric data reveal significant variability in coastal geomorphology at high resolution within each study area and along the entire PNW coast. In particular, within each study area there is alongshore variability in foredune crest elevation. In Clatsop Plains, OR there is a north-south gradient in foredune crest elevation with relatively tall foredunes to the north and relatively short foredunes to the south. In contrast, the foredunes in Rockaway, OR are smaller than those in Clatsop but demonstrate more alongshore variability. The fact that Rockaway has similar dune grass composition to that of Clatsop (mix of *A. arenaria* and *A. breviligulata*) but different foredune geomorphology suggests that physical mechanisms must be relatively more important that ecological mechanisms to foredune geomorphological evolution at these locations.

In the future, the extracted geomorphological parameters can be combined with ecological data (Hacker et al., in press) for more robust analyses to determine the relative roles of ecological and physical mechanisms in foredune geomorphology. Dune grass species composition from several transects within each study area might the importance of ecological factors. SCR data should be combined with dune sediment supply rate data

to completely analyze physical factors. For example, it is possible that the differences in foredune height between Clatsop Plains and Rockaway are due to differences in dune sediment supply rate.

The TWL and erosion models discussed herein can all be applied to coastal lidar elevation data of the PNW. Specifically, the relationship between foreshore slope and the equilibrium profile shape parameter, *A*, allow the application of the KD93 model without additional information. The K99 model has a negative dependence on beach slope while the other models have a positive dependence on beach slope. On flatter beaches, the K99 model is the most conservative while the KD93 model is the least conservative. On steeper beaches, the L04_1 model is the most conservative while the K99 model is the least conservative. Observations of storm induced dune erosion in the PNW are necessary to confirm that dune retreat distance is dependent upon beach slope.

Calculating non-dimensional overtopping and erosion indices captures the relative vulnerability to overtopping and erosion within littoral cells, highlighting particularly vulnerable areas. The indices also enable us compare vulnerabilities between littoral cells. For example, comparisons between the indices between the three focus areas demonstrate that Rockaway, OR is the most vulnerable to overtopping and erosion. This result implies that foredunes dominated by *A. breviligulata* are not necessarily more vulnerable to overtopping than systems with significant presence of *A. arenaria*.

3. GENERAL CONCLUSIONS

The techniques described in this paper enable us to extract morphometric parameters of coastal foredunes and analyze patterns of variability on both small and large length scales. The vertical RMSE and bias estimates for the techniques indicate reasonable, unbiased estimates of the parameters. The vertical RMSE values for the techniques are comparable to subjective techniques which can only be applied to smaller stretches of beach.

The extracted morphometric data reveal significant variability in coastal geomorphology at high resolution within each study area and along the entire PNW coast. In particular, within each study area there is alongshore variability in foredune crest elevation. In Clatsop Plains, OR there is a north-south gradient in foredune crest elevation with relatively tall foredunes to the north and relatively short foredunes to the south. In contrast, the foredunes in Rockaway, OR are smaller than those in Clatsop but demonstrate more alongshore variability. The fact that Rockaway has similar dune grass composition to that of Clatsop (mix of *A. arenaria* and *A. breviligulata*) but different foredune geomorphology suggests that physical mechanisms must be relatively more important that ecological mechanisms to foredune geomorphological evolution at these locations.

In the future, the extracted geomorphological parameters can be combined with ecological data (Hacker et al., in press) for more robust analyses to determine the relative roles of ecological and physical mechanisms in foredune geomorphology. Dune grass species composition from several transects within each study area might the importance of ecological factors. SCR data should be combined with dune sediment supply rate data

to completely analyze physical factors. For example, it is possible that the differences in foredune height between Clatsop Plains and Rockaway are due to differences in dune sediment supply rate.

The TWL and erosion models discussed herein can all be applied to coastal lidar elevation data of the PNW. Specifically, the relationship between foreshore slope and the equilibrium profile shape parameter, *A*, allow the application of the KD93 model without additional information. The K99 model has a negative dependence on beach slope while the other models have a positive dependence on beach slope. On flatter beaches, the K99 model is the most conservative while the KD93 model is the least conservative. On steeper beaches, the L04_1 model is the most conservative while the K99 model is the least conservative. Observations of storm induced dune erosion in the PNW are necessary to confirm that dune retreat distance is dependent upon beach slope. Calculating non-dimensional overtopping and erosion indices captures the relative vulnerability to overtopping and erosion within littoral cells, highlighting particularly vulnerable areas. The indices also enable us compare vulnerabilities between littoral cells. For example, comparisons between the indices between the three focus areas demonstrate that Rockaway, OR is the most vulnerable to overtopping and erosion. This result implies that foredunes dominated by *A. breviligulata* are not necessarily more vulnerable to overtopping than systems with significant presence of *A. arenaria*.

4. BIBLIOGRAPHY

Allan, J.C. and P.D. Komar, 2002: Extreme storms on the Pacific Northwest coast during the 1997-98 El Niño and 1998 La Niña, Journal of Coastal Research, 18, 175-193.

Allan, J.C. and G.R. Priest, 2001: Open-File Report O-01-03: Evaluation of Coastal Erosion Hazard Zones Along Dune and Bluff Backed Shorelines in Tillamook County Oregon: Cascade Head to Cape Falcon, State of Oregon Department of Geology and Mineral Industries, Preliminary Technical Report to Tillamook County, 56 pp.

Brock, J., A. Sallenger, W. Krabill, R. Swift, S. Manizade, A. Meredith, M. Jansen, and D. Eslinger, 1999: Aircraft laser altimetry for coastal processes studies. In N.C. Kraus (editors), 4th International Symposium on Coastal Engineering and Science of Coastal Sediment Processes, ASCE, 2414-2428.

Brock, J.and A. Sallenger, 2001: Airborne Topographic Lidar Mapping for coastal science and resource management, USGS Open File Report 01-46.

Byrne, J.V., 1964: An erosional classification for the Northern Oregon Coast, Annals of the Association of American Geographers, 54, 329-335.

Carter, R.W., 1982: Vegetation stabilization and slope failure of eroding sand dunes, Biological Conservation, 18, 117-122.

Cooper, W.S., 1958: Coastal Sand Dunes of Oregon and Washington, Memoirs of the Geological Society of America, 72, 169 pp.

Dean, R.G. and R.A. Dalrymple, 1994: Water Wave Mechanics for Scientists and Engineers, World Scientific, 353pp.

Elko, N., A. Sallenger, K. Guy, H. Stockdon, and K. Morgan, 2002: Barrier island elevations relevant to potential storm impacts: 1. Techniques, U.S. Geological Survey Open File Report 02-287, 4pp.

FEMA, 2004:Guidelines and Specifications for Flood Hazard Mapping Partners, Section D.4 – Coastal Flooding Analyses and Mapping: Pacific Coast, D.4.6-1 – D.4.6-48.

Hacker, S.D., P. Zarnetske, E. Seabloom, P. Ruggiero, J. Mull, S. Gerrity, and C. Jones, 2010: Subtle differences in two non-native congeneric beach grasses significantly affect their colonization, spread, and impact, submitted to Journal of Ecology.

Hesp, P.A., 2008: Coastal dunes in the tropics and temperate regions: location, formation, morphology, and vegetation processes. In: M.L. Martinez and N.P. Psuty (editors), Ecological Studies: Coastal Dunes, Ecology, and Conservation, 71, Springer-Verlag Berlin Heidelberg.

Komar, P., 1998a: Beach Processes and Sedimentation, Prentice Hall Inc., 544 pp.

Komar, P., 1998b: The Pacific Northwest Coast: Living with the shores of Oregon and Washington, Duke University Press, 195 pp.

Komar, P., W.G. McDougal, J.J. Marra, and P. Ruggiero, 1999: The rational analysis of setback distances: Applications to the Oregon Coast, Shore and Beach, 67, 41-49.

Kriebel, D.L. and R.G. Dean, 1993: Convolution method for time-dependent beach-profile response, Journal of Waterway, Port, and Coastal Engineering, 119, 204-226.

Larson, M., L. Erikson, and H. Hanson, 2004: An analytical model to predict dune erosion due to wave impact, Coastal Engineering, 51, 675-696.

Masselink, G. and M.G. Hughes, 2002: Introduction to Coastal Processes and Geomorphology, Hoddar Arnold Publishing, 354 pp.

Moore, B.D., 1982: Beach profile evolution in response to changes in water level and wave height, Masters Thesis, University of Deleware, Newark, DE.

NOAA Coastal Services Center, 2002: 2002 NASA/USGS Airborne LiDAR Assessment of Coastal Erosion (ALACE) Project for California, Oregon, and Washington Coastlines, NOAA's Ocean Service, Coastal Service Center, available online at: http://ww.csc.noaa.gov/ldart.

Overton, M.F., J.F. Fisher, and K.N. Hwang, 1994: Development of a dune erosion model using SUPERTANK data, In: B.L. Edge (Editor), Proceedings of the Twenty-Fourth International Conference on Coastal Engineering, ASCE, Kobe Japan, 2488-2502.

Peterson, C.D., E. Stock, D.M. Price, R. Hart, F. Reckendorf, J.M. Erlandson, and S.W. Hosteler, 2007: Ages, distributions, and origins of upland dune sheets in Oregon, USA, Geomophology, 91, 80-102.

Plant, N.G., K.T. Holland, and J.A. Puelo, 2002: Analysis of the scale of errors in nearshore bathymetric data, Marine Geology, 191, 71-86.

Psuty, N.P., 1992: Spatial variation in coastal foredune development. In: R.W.G. Carter, T.G.F. Curtis, and M.J. Sheehy-Skeffington (editors), Coastal Dunes, Proceedings of the 3rd European Dune Congress, Balkema, Rotterdam, 3-13.

Psuty, N.P. and E. Rohr, 2000: Coastal Dunes: A Primer for Dune Management with Models of Dune Response to Strom Frequencies, Institute of Marine and Coastal Sciences, Rutgers – The State University of New Jersey, 40 pp.

Psuty, N.P., 2008: The coastal foredune: A morphological basis for regional coastal dune development. In: M.L. Martinez and N.P. Psuty (editors), Ecological Studies: Coastal Dunes, Ecology, and Conservation, 71, Springer-Verlag Berlin Heidelberg.

Revell, D.L., P.D. Komar, and A.H. Sallenger, 2002: An application of lidar to analyses of El Niño Erosion in the Netarts Littoral Cell, Oregon, Journal of Coastal Research, 18, 792-801.

Roelvink, D., A. Reniers, A. van Dongeren, J. van Thiel de Vries, J. Lescinski, D.J. Walstra, 2007: XBeach Annual Report and Model Description, Delft Hydraulics, Delft University of Technology.

Ruggiero, P., P.D. Komar, W.G. McDougal, W.G. and R.A. Beach, 1996: Extreme water levels, wave runup, and coastal erosion, Proceedings of the 25th Coastal Engineering Conference, ASCE, 2793-2805.

Ruggiero, P., P.D. Komar, W.G. McDougal, J.J. Marra, and R.A. Beach, 2001: Wave runup, extreme water levels, and the erosion of properties backing beaches, Journal of Coastal Research, 17, 407-419.

Ruggiero, P., G.M. Kaminsky, G. Gelfenbaum, and B. Voight, 2005: Seasonal to interannual morphodynamics along a high-energy dissipative littoral cell, Journal of Coastal Research, 21, 553-578.

Ruggiero, P. and J.H. List, 2009: Improving accuracy and statistical reliability of shoreline position and change rate estimates, Journal of Coastal Research, 25, 1069-1081.

Ruggiero, P., P.D. Komar, and J.C. Allan, 2010: Increasing wave heights and extreme-value projections: the wave climate of the Pacific Northwest, Coastal Engineering, 57, 539-552.

Sallenger, A.H., 2000: Storm impact scale for barrier islands, Journal of Coastal Research, 16, 890-895.

Sallenger, A.H., W.B. Krabill, R.N. Swift, J.C. Brock, J. List, M. Hansen, R.A. Holman, S.S. Manizade, J.G. Sonntag, A. Merideth, K. Morgan, J.K. Yunkel, E.B. Frederick, and H. Stockdon, 2003: Evaluation of airborne topographic lidar for quantifying beach change, Journal of Coastal Research, 19, 125-133.

Seabloom, E.W. and A.M. Weidemann, 1994: Distribution and effects of Ammophila breviligulata Fern. (American Beach Grass) on the foredunes of the Washington Coast, Journal of Coastal Research, 10, 178-188.

Short, A.D. and P.A. Hesp, 1982: Wave, beach, and dune interactions in southeastern Australia, Marine Geology, 48, 259-284.

Shresta, R.L., W.E. Carter, M. Sartori, B.J. Luzman, and K.C. Slatton, 2005: Airborne laser swath mapping: Quantifying changes in sandy beaches over time scales of weeks to years, Journal of Photogrammetry & Remote Sensing, 59, 222-232.

Stockdon, H.F., R.A. Holman, P.A. Howd, and A.H. Sallenger Jr., 2006: Empirical parameterization of setup, swash, and runup, Coastal Engineering, 53, 573-588.

Stockdon, H.F., K.S. Doran, and A.H. Sallenger Jr., 2009: Extraction of Lidar-based dune crest elevations for use in examining the vulnerability to beaches during inundation during hurricanes, Journal of Coastal Research, 53, 59-65.

USGS St. Petersburg Coastal and Marine Science Center, 2002: Hurricane and Extreme Storm Impact Studies, Coastal and Nearshore Mapping with Scanning Airborne Laser (Lidar), available online at: http://coastal.er.usgs.gov/lidar

Weber, K.M., J.H. List, and K.L.M. Morgan, 2005: An operational mean high water datum for determination of shoreline position from topographic lidar data, USGS Open-File Report 2005-1027.

APPENDIX A

Table A.1: Catalogue of Dune-Backed Beaches in the Pacific Northwest

State	Littoral Cell	Beach	Northern Boundary (UTM N)	Southern Boundary (UTM N)
Washington	CRLC	North Beach	5220330.95	5197793.30
		Grayland Plains	5195211.92	5177356.49
		Long Beach - Benson Beach	5167121.22	5124606.15
Oregon	CRLC	Clatsop Plains	5119530.98	5091814.39
	Cannon Beach	Cannon Beach	5084348.58	5072630.70
	Rockaway	Rockaway	5065048.99	5038403.61
	Netarts	Netarts Spit	5031348.67	5022915.30
	Sand Lake	Sand Lake	5016473.13	5009902.39
	Neskowin	Pacific City	5007564.84	5001285.76
		Neskowin	5000872.47	4993826.29
	Lincoln	Lincoln City - Siletz	4975671.71	4973047.39
	Newport	North Jetty - South Beach	4941786.26	4938444.43
		Bayshore Beach	4922386.60	4919708.17
	Coos	Heceta Beach	4882448.07	4874608.36
		Florence	4874292.08	4836140.78
		Reedsport	4835176.46	4801361.56
	Bandon	Bandon Beach	4784951.52	4775610.36
		Bandon Beach	4775409.19	4774878.87
		Bandon Beach	4773087.89	4752309.56
	Port Orford	Cape Blanco South	4740252.74	4734024.86
	Nesika	Nesika Beach	4713716.02	4709519.57
	Gold Beach	Gold Beach North	4701776.69	4697699.81
		Gold Beach South	4697251.85	4690073.39
	Pistol	Pistol River North	4683826.64	4680596.74
		Pistol River South	4650909.74	4650328.87

APPENDIX B – Beach and Foredune Geomorphological Parameters for Littoral Cells, Subcells, and Beaches within the PNW.

Plots of the backshore slope values, foredune toe elevations, and foredune crest elevations for each beach a shown in Figures B.1 – B.12. Figure B.1 shows the backshore slopes, dune toe elevations, and foredune crest elevations all increasing towards the south in the North Beach, WA subcell. The maximum dune crest elevations and backshore slope values are near the north jetty at Gray's Harbor. In the middle of the subcell backshore slope values are relatively small. This is one of the wider beaches within the CRLC (Ruggiero et al., 2005).

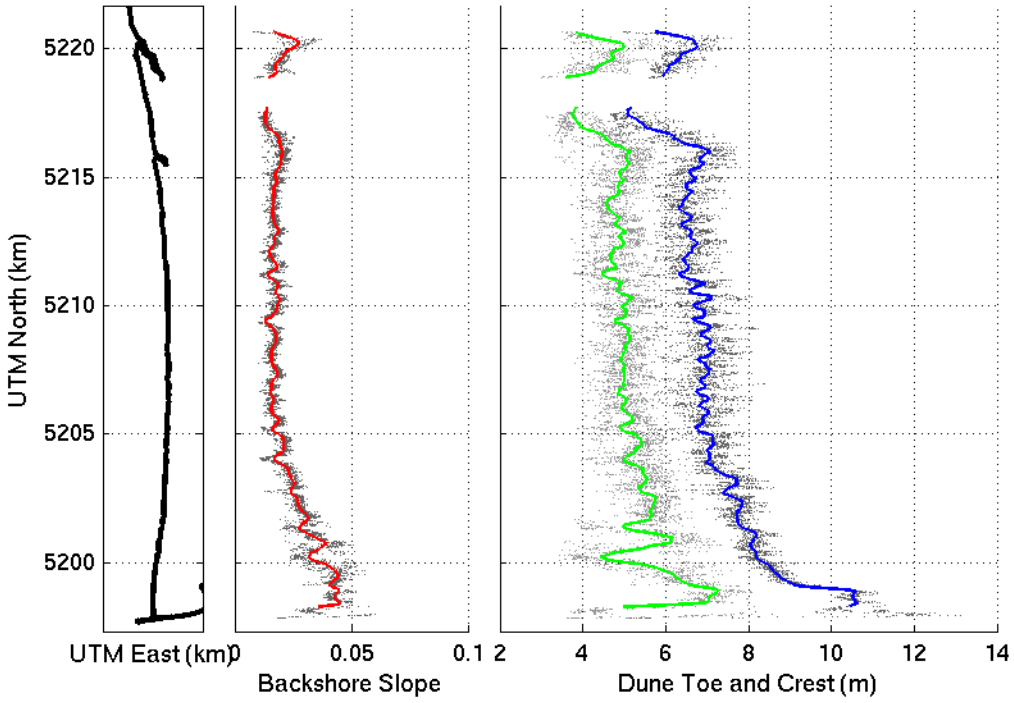

Figure B.1. Foredune parameters for North Beach, WA. The left panel indicates the alongshore position of each profile. The middle panel shows backshore slope values at each profile in grey. The red dots are backshore slope values that have been smoothed in the alongshore direction with a linear loess filter with a window size of 250 m. The right panel shows foredune toe and crest elevations. The toe elevations are shown in light grey and the crest elevations are shown in dark grey. The green dots and blue dots represent smoothed toe and crest elevations, respectively.

The smoothed data reveal that the slopes become steeper and the crest elevations increase near the entrance of Grays Harbor implying a coarser sediment grain size near the jetty (Figure B.2). Between 5190 and 5195 km north (UTM) is an area of relatively high backshore slope. This also corresponds to a region of increased grain size (Ruggiero et al., 2005). Immediately south of this, the dune crests and toes are higher and the backshore slope is lower. There is also a section of relatively low backshore slope between 5182 and 5178 km north. Sand from the shallow ebb-tidal delta at Willapa Bay is rapidly accreting and creating a wide beach here. There are two foredune ridges near 5190 km north (UTM) that can be seen in both the cross-shore positions of the crests (not shown) and the heights of the dune crests. This is most likely an area of accretion in which the beach is building out and new foredunes are growing. At some profiles, the incipient dune has not grown enough to be classified as a foredune because the elevation drop from crest to heel does not exceed 0.60 m.

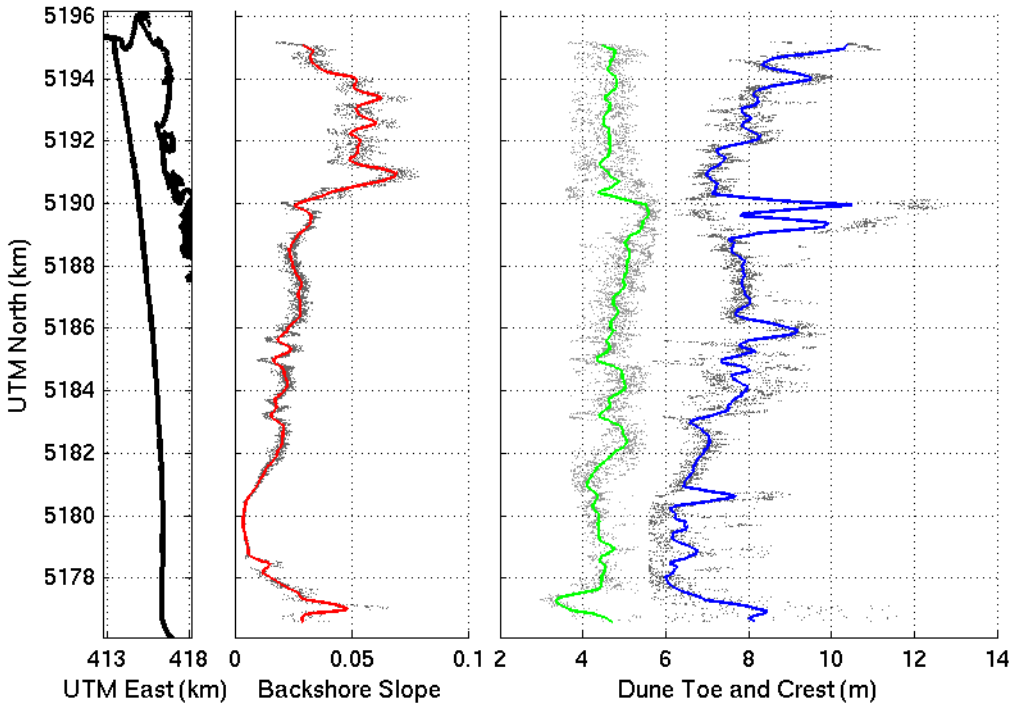

Figure B.2. Foredune parameters for Grayland, WA. The left panel indicates the alongshore position of each profile. The middle panel shows backshore slope values at each profile in grey. The red dots are backshore slope values that have been smoothed in the alongshore direction with a linear loess filter with a window size of 250 m. The right panel shows foredune toe and crest elevations. The toe elevations are shown in light grey and the crest elevations are shown in dark grey. The green dots and blue dots represent smoothed toe and crest elevations, respectively.

Figure B.3 shows relatively high variability in the backshore slopes and foredune crest elevations along the Netarts Spit in Oregon. The three geomorphological parameters do not appear correlated. The foredunes are relatively tall in the middle of the spit. The northern tip of the spit may shift as sediment flows from the estuary change. This area of shifting beach could inhibit tall foredunes from building.

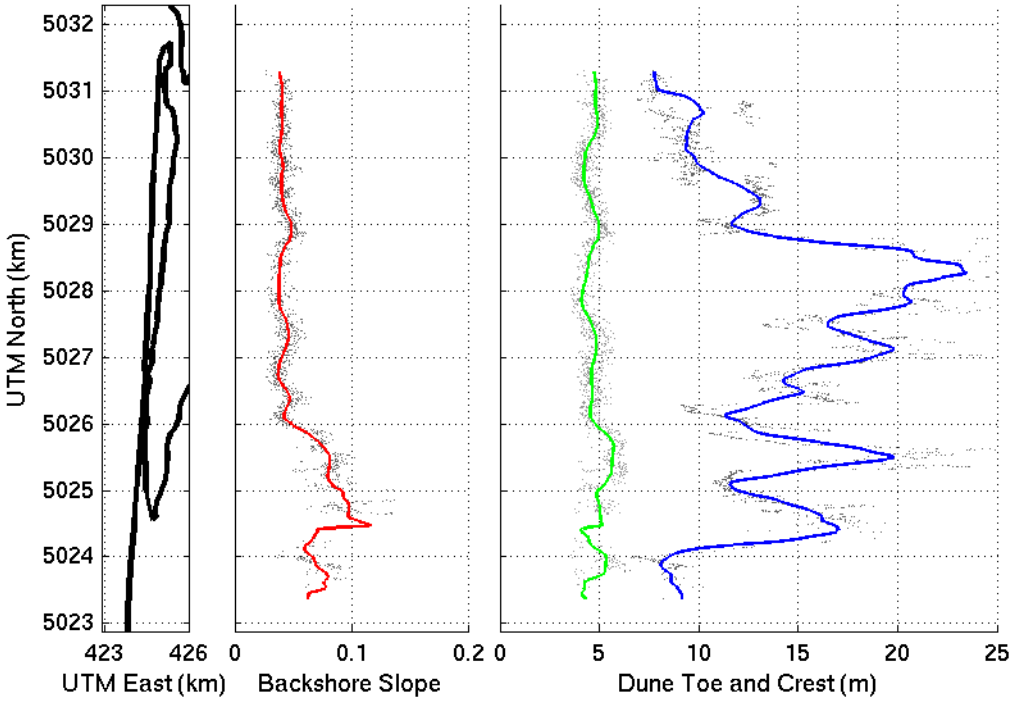

Figure B.3. Foredune parameters for Netarts, OR. The left panel indicates the alongshore position of each profile. The middle panel shows backshore slope values at each profile in grey. The red dots are backshore slope values that have been smoothed in the alongshore direction with a linear loess filter with a window size of 250 m. The right panel shows foredune toe and crest elevations. The toe elevations are shown in light grey and the crest elevations are shown in dark grey. The green dots and blue dots represent smoothed toe and crest elevations, respectively.

Figure B.4 shows relatively tall foredunes in the north of the Sand Lake littoral cell. The foredunes south of the estuary are shorter. The backshore slope and dune toe elevations appear to be correlated with each other.

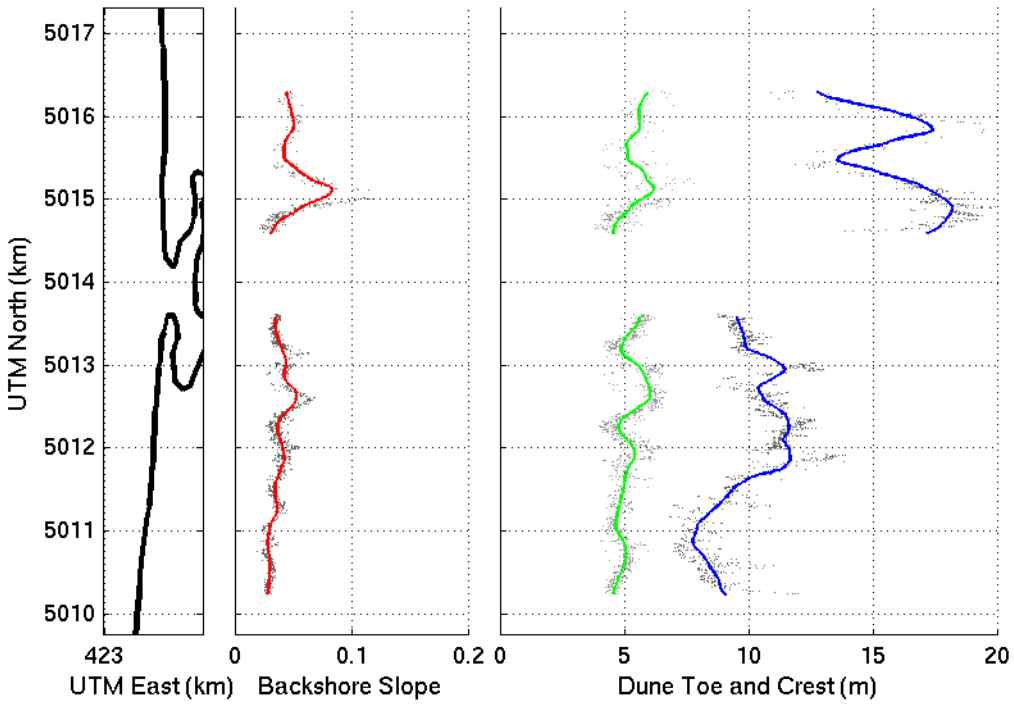

Figure B.4. Foredune parameters for Sand Lake, OR. The left panel indicates the alongshore position of each profile. The middle panel shows backshore slope values at each profile in grey. The red dots are backshore slope values that have been smoothed in the alongshore direction with a linear loess filter with a window size of 250 m. The right panel shows foredune toe and crest elevations. The toe elevations are shown in light grey and the crest elevations are shown in dark grey. The green dots and blue dots represent smoothed toe and crest elevations, respectively.

North-south gradients in slope and dune toe elevations are relatively mild while the gradient in dune crest elevations is strong in the Neskowin Littoral Cell (Figure B.5). This supports models of foredune development that suggest that the upper dune face and crest are formed by a different mechanism than the backshore slope and dune toe. The slope and toe are usually determined by hydrodynamic conditions while the upper dune is formed by aeolian transport (Psuty and Rohr, 2000; Masselink and Hughes, 2002). This is also seen in the different alongshore patterns for the beach and dune. One can see that the backshore slopes and dune toe elevations have rhythmic patterns with wavelengths of

about 1 km. The patterns in these parameters are in phase with one another so that higher dune toes are correlated with greater backshore slopes. The cross-correlation coefficients between the dune toe elevations and the backshore slopes is 0.64 (Table C.8). There is no strong rhythmicity in the dune crest elevations, and the cross-correlation coefficients between these and the other parameters are low. The dunes are much taller in the northern section of the littoral cell. Dune heights decrease near the southern tip of Netsucca Spit, where sediment is rapidly accreting and foredunes are still growing.

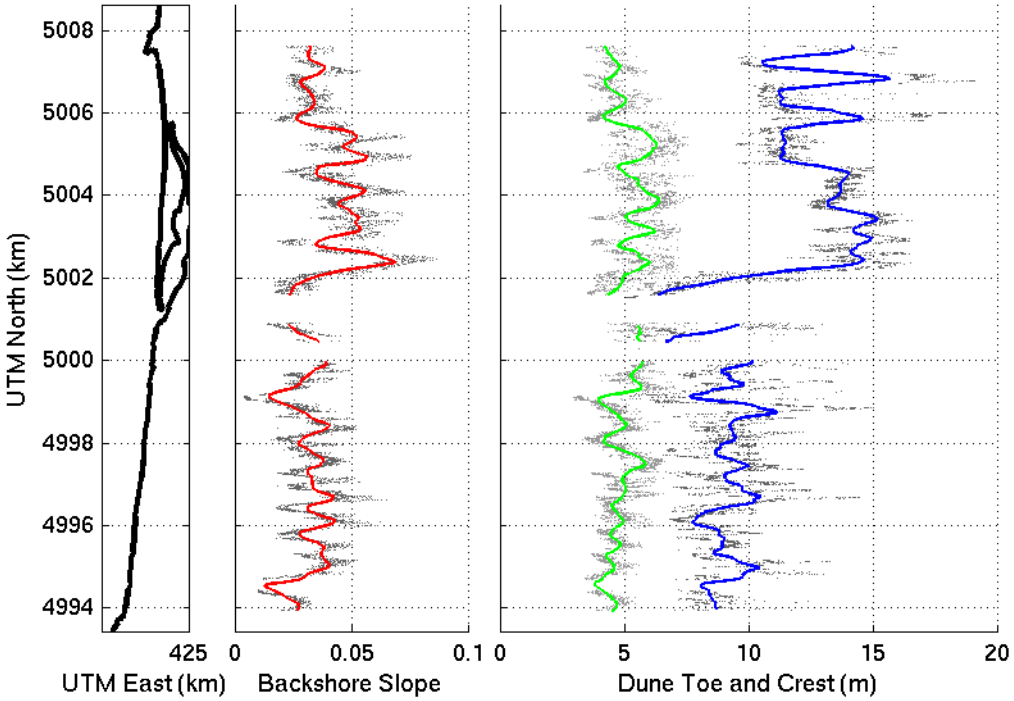

Figure B.5. Foredune parameters for Neskowin, OR. The left panel indicates the alongshore position of each profile. The middle panel shows backshore slope values at each profile in grey. The red dots are backshore slope values that have been smoothed in the alongshore direction with a linear loess filter with a window size of 250 m. The right panel shows foredune toe and crest elevations. The toe elevations are shown in light grey and the crest elevations are shown in dark grey. The green dots and blue dots represent smoothed toe and crest elevations, respectively.

Figure B.6 shows slight north-south gradients in foredune crest elevations and foredune toe elevations along the Siletz Spit in Oregon with lower elevations to the north. The foredune crest elevations and foredune toe elevations appear to be correlated with each other. The northern tip of the spit shifts frequently (Komar, 1998b) which possibly impedes tall foredunes from developing there.

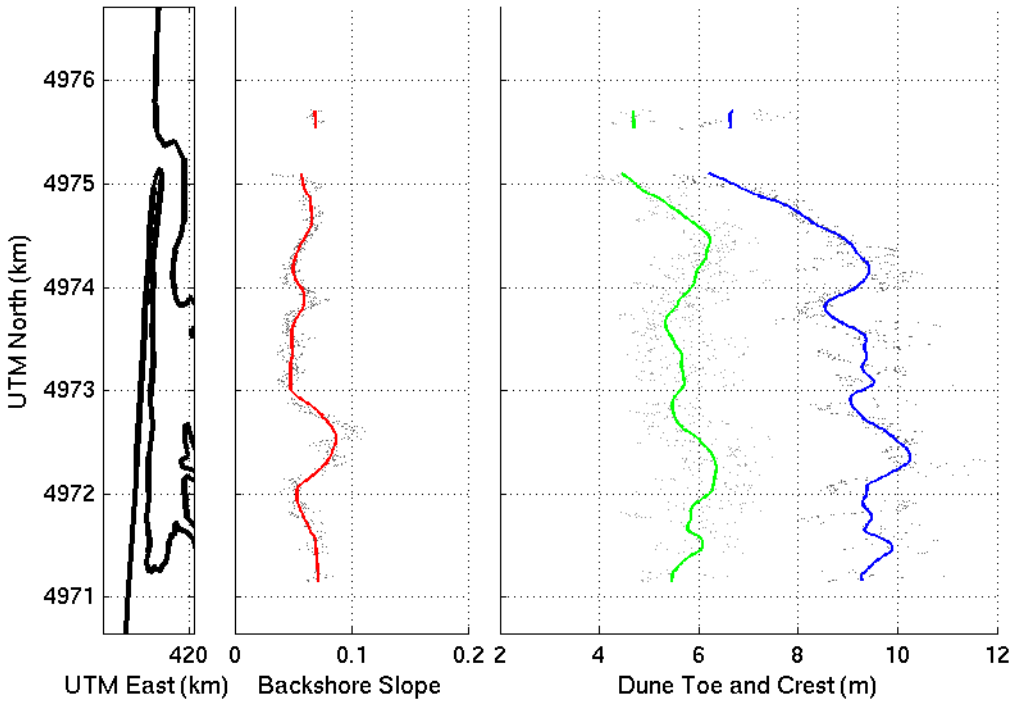

Figure B.6. Foredune parameters for Siletz, OR. The left panel indicates the alongshore position of each profile. The middle panel shows backshore slope values at each profile in grey. The red dots are backshore slope values that have been smoothed in the alongshore direction with a linear loess filter with a window size of 250 m. The right panel shows foredune toe and crest elevations. The toe elevations are shown in light grey and the crest elevations are shown in dark grey. The green dots and blue dots represent smoothed toe and crest elevations, respectively.

Figure B.7 shows variability in backshore slopes and dune crest elevations in Newport, OR. There is relatively low variability in dune crest elevations. South Beach has the highest foredune elevations which could protect development there from flooding.

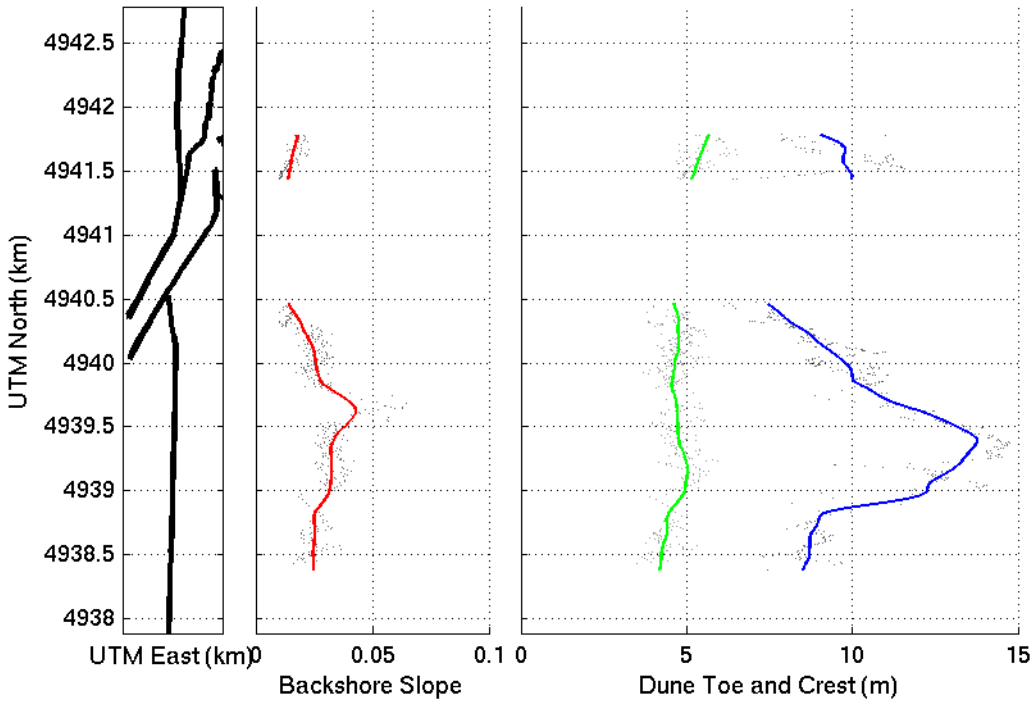

Figure B.7. Foredune parameters for Newport, OR. The left panel indicates the alongshore position of each profile. The middle panel shows backshore slope values at each profile in grey. The red dots are backshore slope values that have been smoothed in the alongshore direction with a linear loess filter with a window size of 250 m. The right panel shows foredune toe and crest elevations. The toe elevations are shown in light grey and the crest elevations are shown in dark grey. The green dots and blue dots represent smoothed toe and crest elevations, respectively.

Figure B.8 shows relatively high variability in the backshore slopes and foredune crest elevations in Bayshore Beach, OR. There are relatively tall foredunes near the Alsea River inlet. This is interesting as spits near inlets can frequently shift with changes in river outflow sediment discharge (Komar, 1998b). One might expect the foredunes to be relatively short in this area as the beach and dune sediment supplies can be variable.

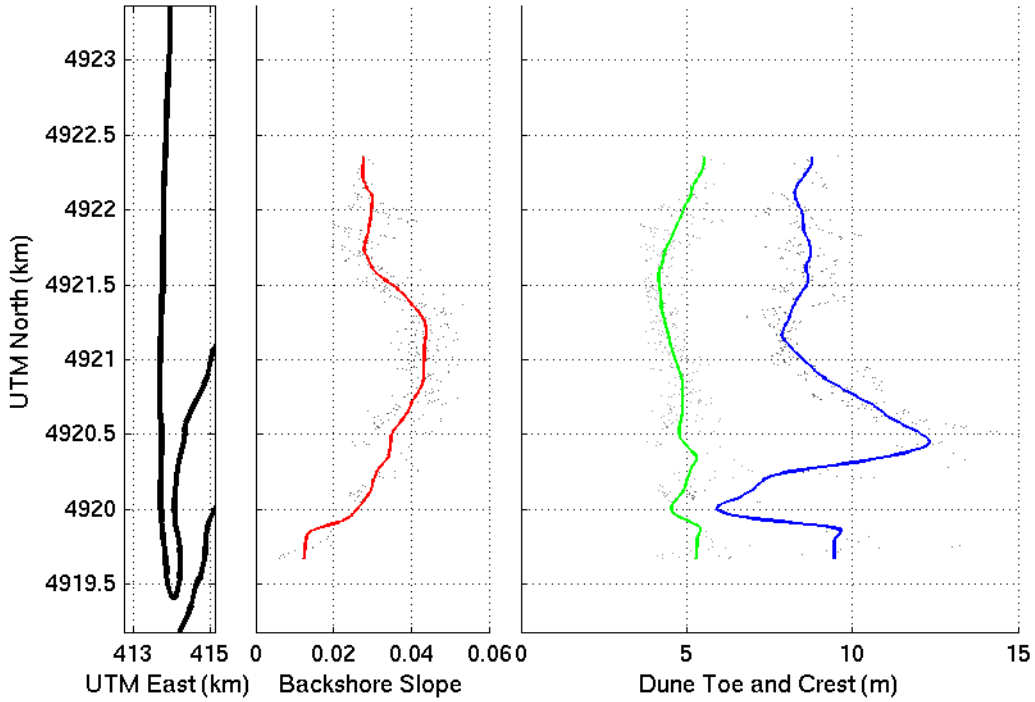

Figure B.8. Foredune parameters for Bayshore Beach, OR. The left panel indicates the alongshore position of each profile. The middle panel shows backshore slope values at each profile in grey. The red dots are backshore slope values that have been smoothed in the alongshore direction with a linear loess filter with a window size of 250 m. The right panel shows foredune toe and crest elevations. The toe elevations are shown in light grey and the crest elevations are shown in dark grey. The green dots and blue dots represent smoothed toe and crest elevations, respectively.

Figure B.9 shows a decrease in backshore slopes, foredune toe elevations, and foredune crest elevations in the middle section of the beach. Coastal bluffs, and not foredunes, can be found in this area.

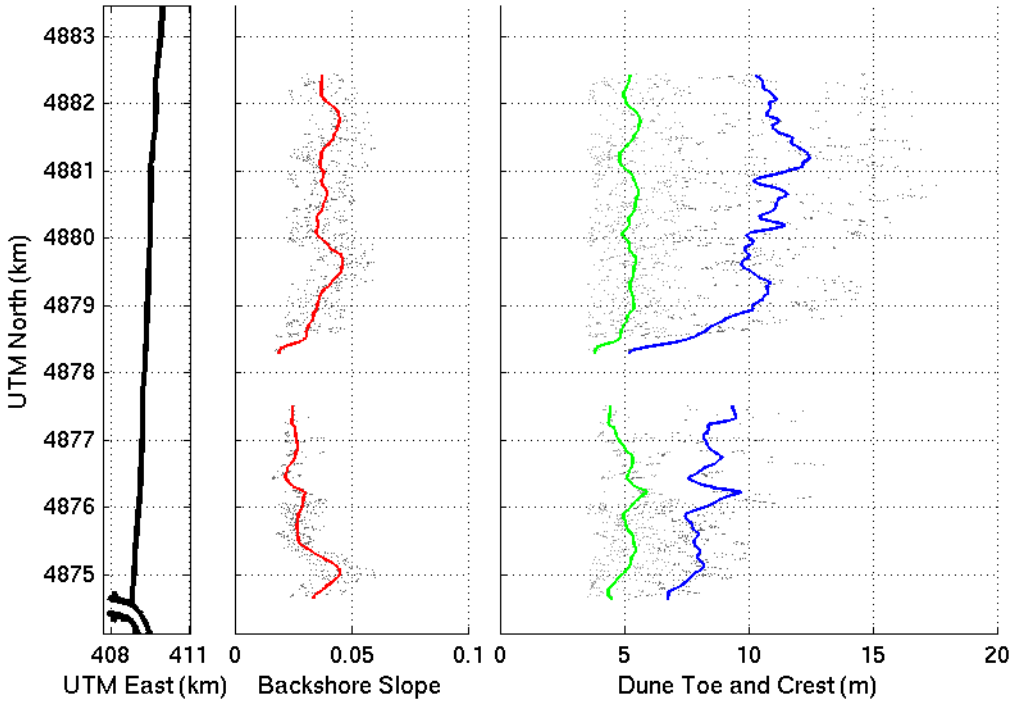

Figure B.9. Foredune parameters for Heceta Beach, OR. The left panel indicates the alongshore position of each profile. The middle panel shows backshore slope values at each profile in grey. The red dots are backshore slope values that have been smoothed in the alongshore direction with a linear loess filter with a window size of 250 m. The right panel shows foredune toe and crest elevations. The toe elevations are shown in light grey and the crest elevations are shown in dark grey. The green dots and blue dots represent smoothed toe and crest elevations, respectively.

Figure B.10 shows relatively high variability in backshore slopes, foredune toe elevations, and foredune crest elevations in Florence, OR. The range of backshore slopes is greater than the range at other beaches and cells. There is a strong north-south gradient in foredune crest elevation with taller foredunes in the north. Foredunes are relatively small near river inlets, where the beach sediment supply is most likely variable and tall foredunes cannot develop.

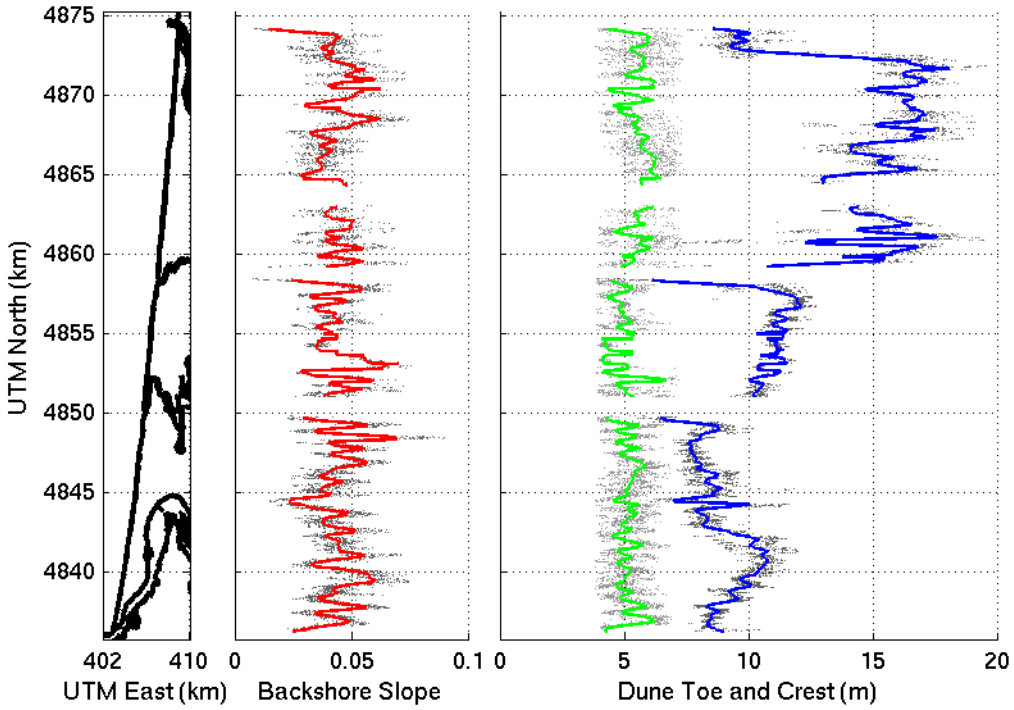

Figure B.10. Foredune parameters for Florence, OR. The left panel indicates the alongshore position of each profile. The middle panel shows backshore slope values at each profile in grey. The red dots are backshore slope values that have been smoothed in the alongshore direction with a linear loess filter with a window size of 250 m. The right panel shows foredune toe and crest elevations. The toe elevations are shown in light grey and the crest elevations are shown in dark grey. The green dots and blue dots represent smoothed toe and crest elevations, respectively.

Figure B.11 shows relatively high variability in backshore slopes and foredune crest elevations in Reedsport, OR. Backshore slopes, toe elevations, and crest elevations all decrease near the stream inlet at 4825 km north (UTM).

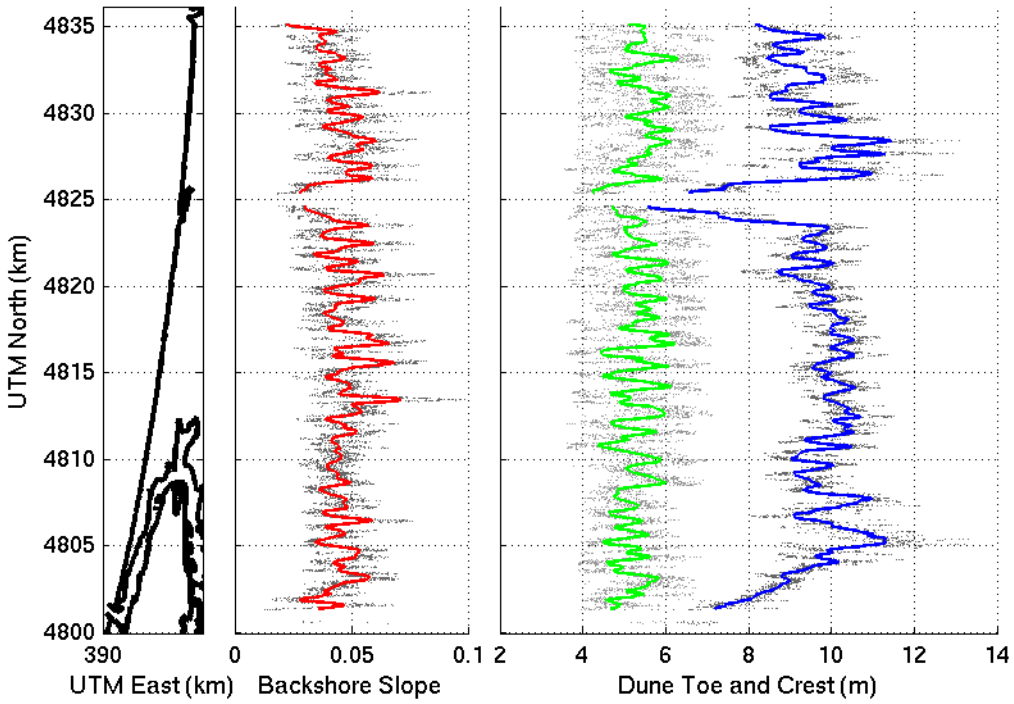

Figure B.11. Foredune parameters for Reedsport, OR. The left panel indicates the alongshore position of each profile. The middle panel shows backshore slope values at each profile in grey. The red dots are backshore slope values that have been smoothed in the alongshore direction with a linear loess filter with a window size of 250 m. The right panel shows foredune toe and crest elevations. The toe elevations are shown in light grey and the crest elevations are shown in dark grey. The green dots and blue dots represent smoothed toe and crest elevations, respectively.

Figure B.12 shows relatively high variability in backshore slopes, foredune toe elevations, and foredune crest elevations in Bandon, OR. There are taller foredunes in the north and south of the littoral cell. Foredunes are interrupted along the coast by sections of bluffs and rocks.

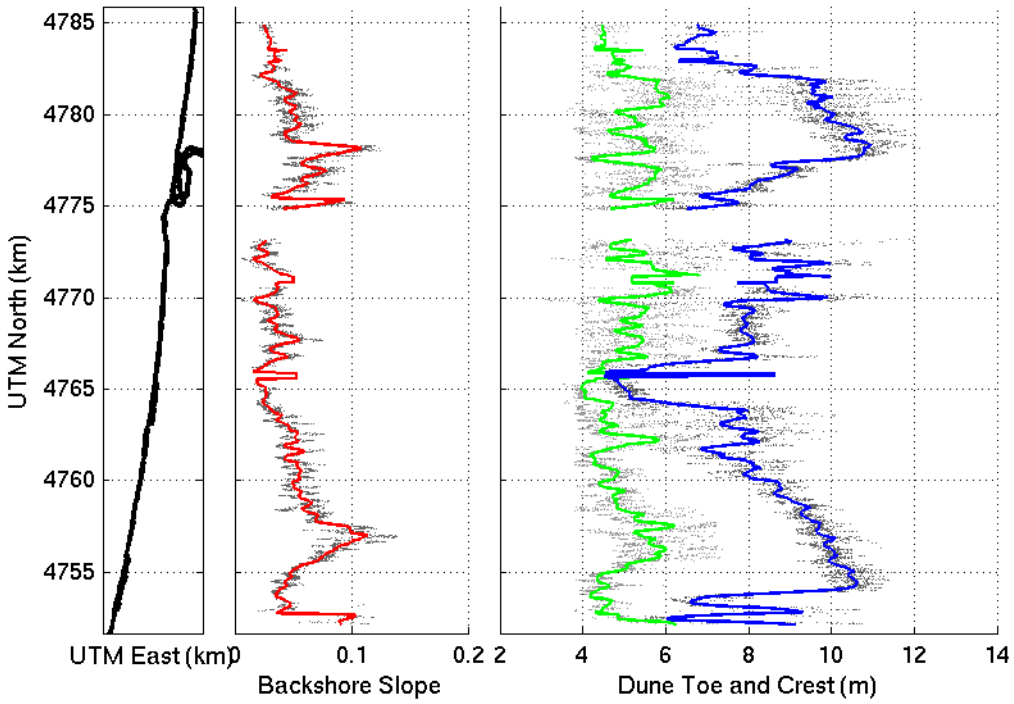

Figure B.12. Foredune parameters for Bandon, OR. The left panel indicates the alongshore position of each profile. The middle panel shows backshore slope values at each profile in grey. The red dots are backshore slope values that have been smoothed in the alongshore direction with a linear loess filter with a window size of 250 m. The right panel shows foredune toe and crest elevations. The toe elevations are shown in light grey and the crest elevations are shown in dark grey. The green dots and blue dots represent smoothed toe and crest elevations, respectively.

APPENDIX C – Cross-correlation coefficients between foredune and beach geomorphological parameters in the PNW.

We examine the correlations between various geomorphological parameters in order to begin to explain which physical mechanisms are important in foredune morphology. Psuty's (1992) model predicts that tall and wide foredunes will develop on stable beaches with neutral sediment supply rates while small foredunes will develop on prograding and eroding beaches. SCR can be used as a proxy for beach sediment supply rate and one might expect to find large foredunes on beaches with SCR of low magnitude. Short foredunes might develop on beaches with SCR of high magnitude.

Beach width could also be an important geomorphological parameters although the relationship between beach widths and foredune heights is not always clear. A relatively wide beach might indicate a prograding beach while a relatively narrow beach might indicate an eroding beach. Small dunes might develop on these beaches. However, a wide beach increases the fetch for wind to transport sand to dunes (Masselink and Hughes, 2002). Larger foredunes can develop on these beaches if the beach sediment supply is neutral.

We calculated the correlation coefficients for several foredune geomorphological parameters, including the foredune volumes, foredune width, beach width, beach slopes, with SCR and each other. The correlation coefficients (R) between alongshore series of the automatically extracted geomorphological parameters and SCR at each beach are presented in Tables C.1 – C.15. All correlations that are significant at the 95% confidence level are indicated by italics. It is important to consider that positive values of SCR indicate progradation and negative values indicate erosion. As both the sign and magnitude of SCR may be important, the absolute values of SCR were also tested.

Foredune crest elevation is moderately inversely correlated with SCR at North Beach, Grayland, Newport, Bayshore Beach, and Heceta Beach. Correlation coefficients range from -0.50 to -0.70. Foredune crest elevation is moderately inversely correlated with the absolute value of SCR at North Beach, Neskowin, and Heceta Beach (*R* ranges from -.50 to -.57). This seems to agree with Psuty's (1992) as it predicts foredune heights to be inversely correlated with the magnitude of SCR. However, foredune crest height is moderately correlated with the absolute value of SCR at Bayshore Beach. The correlations between SCR and foredune crest height are not as strong at other beaches.

V1 and *V2* are moderately correlated with SCR and the absolute value of SCR at Clatsop Plains (*R* = 0.61 to 0.63). *V2* is moderately correlated with SCR at Neskowin (*R* = 0.52) and moderately inversely correlated with SCR at Heceta Beach (*R* = -0.53). Psuty's (1992) model predicts that foredune volume is inversely correlated with the magnitude of SCR, however there is little evidence of this.

Beach width is moderately correlated with SCR and the absolute values of SCR at beaches within the CRLC (*R* ranges from 0.62 to 0.49). This might be due to large beach widths at beaches that are prograding. However, it does not account for beaches that are eroding and have a negative SCR.

Beach width is moderately correlated with SCR and the absolute value of SCR at the Washington Beaches (*R* = 0.52 to 0.60). Beach width is moderately correlated with SCR at Newport Beach (*R* = 0.54). Highly positive SCR indicate progradation and can lead to relatively wide beaches. SCR with low magnitude can create relatively narrow beaches. Beach width is moderately inversely correlated with SCR and the absolute value of SCR at Heceta Beach (*R* = -0.57).

Beach width is moderately correlated with *V1* and *V2* at Florence (R = 0.68 and 0.64). Beach width is moderately inversely correlated with *V2* at Newport (R = -0.57). There is little evidence to suggest that changes in beach width, or the fetch for wind-transported sand, is affecting foredune volume.

Backshore slope is strongly to moderately correlated with foredune crest height at North Beach, Sand Lake, and Newport (R ranges from 0.80 to 0.65) and not correlated at other beaches. Foredune width is moderately correlated with SCR only at Clatsop Plains (R = 0.64).

These results are generally inconclusive. There are no correlations between the geomorphological parameters at the majority of beaches.

Table C.1: Cross-correlation coefficients between foredune and beach geomorphological parameters in North Beach, WA. Statistically significant correlations are italicized and followed by an asterisk.

	SCR	**abs (SCR)**	**dtoe**	**dhigh**	**dheel**	**Fore-shore Slope**	**Back-shore Slope**	**Dune Face Slope**	**V1**	**V2**	**Dune Width**	**Beach Width**
SCR	1.00											
abs(SCR)	*1.00**	1.00										
dtoe	*-0.23**	*-0.23**	1.00									
dhigh	*-0.50**	*-0.50**	*0.73**	1.00								
dheel	*-0.12**	*-0.12**	*0.12**	*0.11**	1.00							
Foreshore Slope	*-0.58**	*-0.58**	*0.44**	*0.56**	0.09	1.00						
Backshore Slope	*-0.58**	*-0.58**	*0.77**	*0.82**	0.10	*0.59**	1.00					
Dune Face Slope	*-0.45**	*-0.45**	*0.69**	*0.73**	*0.12**	*0.48**	*0.68**	1.00				
V1	*-0.40**	*-0.39**	-0.09	*0.38**	0.00	*0.30**	*0.23**	0.06	1.00			
V2	*-0.25**	*-0.23**	*-0.39**	*0.18**	-0.03	*0.12**	-0.02	*-0.29**	*0.67**	1.00		
Dune Width	-0.04	-0.04	*-0.29**	*-0.16**	*-0.14**	0.02	*-0.17**	*-0.27**	*0.63**	*0.29**	1.00	
Beach Width	*0.57**	*0.57**	*-0.11**	*-0.428*	-0.05	*-0.42**	*-0.68**	*-0.27**	*-0.46**	*-0.35**	*-0.12**	1.00

Table C.2: Cross-correlation coefficients between foredune and beach geomorphological parameters in Grayland, WA. Statistically significant correlations are italicized and followed by an asterisk.

	SCR	**abs (SCR)**	**dtoe**	**dhigh**	**dheel**	**Fore-shore Slope**	**Back-shore Slope**	**Dune Face Slope**	**V1**	**V2**	**Dune Width**	**Beach Width**
SCR	*1.00*											
abs(SCR)	*0.61**	*1.00*										
dtoe	*-0.17**	*-0.20**	*1.00*									
dhigh	*-0.50**	*-0.34**	*0.38**	*1.00*								
dheel	*-0.20**	*-0.17**	*0.27**	*0.58**	*1.00*							
Foreshore Slope	0.08	-0.01	*0.21**	*0.16**	-0.05	*1.00*						
Backshore Slope	*-0.25**	*-0.20**	*0.13**	*0.15**	*-0.13**	*0.60**	*1.00*					
Dune Face Slope	*-0.49**	*-0.41**	0.11	*0.17**	-0.06	-0.05	*0.45**	*1.00*				
V1	*-0.17**	0.01	-0.12	*0.62**	*0.39**	*0.20**	0.08	*-0.24**	*1.00*			
V2	*-0.14**	0.04	-0.04	*0.63**	*0.47**	*0.13**	-0.08	*-0.43**	*0.81**	*1.00*		
Dune Width	*0.33**	*0.44**	*-0.24**	0.10	*0.16**	0.12	*-0.15**	*-0.57**	*0.73**	*0.57**	*1.00*	
Beach Width	*0.60**	*0.57**	-0.01	*-0.21**	0.06	*-0.36**	*-0.69**	*-0.41**	-0.10	0.00	*0.19**	*1.00*

Table C.3: Cross-correlation coefficients between foredune and beach geomorphological parameters in Netarts, OR. Statistically significant correlations are italicized and followed by an asterisk.

	SCR	**abs (SCR)**	**dtoe**	**dhigh**	**dheel**	**Fore-shore Slope**	**Back-shore Slope**	**Dune Face Slope**	**V1**	**V2**	**Dune Width**	**Beach Width**
SCR	*1.00*											
abs(SCR)	*-1.00**	*1.00*										
dtoe	0.17	-0.17	*1.00*									
dhigh	*-0.20**	*0.20**	-0.07	*1.00*								
dheel	-0.11	0.11	-0.07	*0.60**	*1.00*							
Foreshore Slope	-0.10	0.10	0.02	*-0.20**	-0.01	*1.00*						
Backshore Slope	*-0.23**	*0.23**	*0.63**	0.02	0.11	*0.31**	*1.00*					
Dune Face Slope	-0.14	0.14	-0.07	*0.49**	*0.24**	*-0.37**	-0.06	*1.00*				
V1	*-0.24**	*0.24**	-0.04	*0.86**	*0.41**	-0.19	0.02	*0.42**	*1.00*			
V2	-0.17	0.17	-0.13	*0.92**	*0.62**	-0.11	-0.01	0.20	*0.81**	*1.00*		
Dune Width	*-0.25**	*0.25**	0.18	*0.36**	0.01	-0.08	*0.20**	*0.20**	*0.71**	*0.27**	*1.00*	
Beach Width	*0.47**	*-0.47**	*-0.34**	*-0.29**	*-0.30**	-0.14	*-0.73**	-0.13	*-0.27**	*-0.21**	*-0.32**	*1.00*

Table C.4: Cross-correlation coefficients between foredune and beach geomorphological parameters in Sand Lake, OR. Statistically significant correlations are italicized and followed by an asterisk.

	SCR	abs (SCR)	dtoe	dhigh	dheel	Fore-shore Slope	Back-shore Slope	Dune Face Slope	V1	V2	Dune Width	Beach Width
SCR	*1.00*											
abs(SCR)	*-1.00**	*1.00*										
dtoe	*0.29**	*-0.29**	*1.00*									
dhigh	*0.39**	*-0.36**	*0.37**	*1.00*								
dheel	-0.07	0.09	0.12	*0.53**	*1.00*							
Foreshore Slope	0.00	-0.01	*0.31**	0.17	0.12	*1.00*						
Backshore Slope	0.15	-0.14	*0.68**	*0.65**	0.22	*0.51**	*1.00*					
Dune Face Slope	-0.18	0.18	0.11	*0.28**	0.17	0.11	0.26	*1.00*				
V1	*0.37**	*-0.37**	0.25	*0.85**	*0.36**	0.21	*0.59**	0.04	*1.00*			
V2	*0.48**	*-0.46**	0.09	*0.83**	*0.47**	0.06	*0.40**	-0.18	*0.83**	*1.00*		
Dune Width	0.23	-0.24	0.22	*0.37**	0.05	0.15	*0.29**	*-0.29**	*0.68**	*0.43**	*1.00*	
Beach Width	0.12	-0.12	0.13	*-0.52**	*-0.29**	*-0.32**	*-0.61**	*-0.28**	*-0.48**	*-0.468*	-0.05*	*1.00*

Table C.5: Cross-correlation coefficients between foredune and beach geomorphological parameters in Neskowin, OR. Statistically significant correlations are italicized and followed by an asterisk.

	SCR	**abs (SCR)**	**dtoe**	**dhigh**	**dheel**	**Fore-shore Slope**	**Back-shore Slope**	**Dune Face Slope**	**V1**	**V2**	**Dune Width**	**Beach Width**
SCR	*1.00*											
abs(SCR)	*-0.86**	*1.00*										
dtoe	*0.18**	*-0.21**	*1.00*									
dhigh	*0.49**	*-0.51**	*0.21**	*1.00*								
dheel	-0.09	0.11	-0.01	0.02	*1.00*							
Foreshore Slope	*-0.25**	*0.22**	-0.04	-0.06	0.14	*1.00*						
Backshore Slope	0.06	-0.13	*0.64**	*0.47**	-0.01	*0.18**	*1.00*					
Dune Face Slope	*-0.23**	*0.15**	-0.08	*0.18**	*0.16**	-0.05	0.07	*1.00*				
V1	*0.41**	*-0.43**	-0.05	*0.83**	0.01	0.00	*0.23**	0.05	*1.00*			
V2	*0.52**	*-0.46**	*-0.19**	*0.74**	-0.03	-0.04	0.08	*-0.24**	*0.81**	*1.00*		
Dune Width	*0.25**	*-0.29**	0.06	*0.58**	-0.12	-0.01	*0.22**	-0.07	*0.84**	*0.53**	*1.00*	
Beach Width	-0.02	0.06	0.11	*-0.42**	0.01	*-0.15**	*-0.60**	-0.05	*-0.36**	*-0.33**	*-0.24**	*1.00*

Table C.6: Cross-correlation coefficients between foredune and beach geomorphological parameters in Siletz, OR. Statistically significant correlations are italicized and followed by an asterisk.

	SCR	**abs (SCR)**	**dtoe**	**dhigh**	**dheel**	**Fore-shore Slope**	**Back-shore Slope**	**Dune Face Slope**	**V1**	**V2**	**Dune Width**	**Beach Width**
SCR	*1.00*											
abs(SCR)	*-0.77**	*1.00*										
dtoe	-0.18	0.36	*1.00*									
dhigh	0.04	0.11	*0.83**	*1.00*								
dheel	-0.29	0.31	0.18	0.29	*1.00*							
Foreshore Slope	-0.35	0.45	-0.29	-0.50	0.26	*1.00*						
Backshore Slope	-0.50	0.33	0.47	0.21	0.14	-0.20	*1.00*					
Dune Face Slope	-0.17	0.04	*0.69**	*0.77**	0.28	*-0.61**	0.58	*1.00*				
V1	0.31	-0.17	-0.18	-0.04	0.09	0.02	-0.19	-0.39	*1.00*			
V2	0.33	0.01	0.16	0.34	0.14	0.13	-0.50	-0.25	*0.71**	*1.00*		
Dune Width	0.08	-0.06	*-0.68**	*-0.73**	-0.15	0.35	-0.21	*-0.79**	*0.60**	0.09	*1.00*	
Beach Width	0.16	-0.40	*-0.82**	*-0.78**	-0.46	0.26	-0.34	*-0.67**	0.13	-0.22	*0.62**	*1.00*

Table C.7: Cross-correlation coefficients between foredune and beach geomorphological parameters in Newport, OR. Statistically significant correlations are italicized and followed by an asterisk.

	SCR	abs (SCR)	dtoe	dhigh	dheel	Fore-shore Slope	Back-shore Slope	Dune Face Slope	V1	V2	Dune Width	Beach Width
SCR	*1.00*											
abs(SCR)	*0.82**	*1.00*										
dtoe	-0.29	-0.33	*1.00*									
dhigh	*-0.70**	-0.38	*-0.15**	*1.00*								
dheel	*-0.49**	-0.24	*-0.04**	*0.45**	*1.00*							
Foreshore Slope	0.44	0.35	*-0.24**	-0.11	-0.23	*1.00*						
Backshore Slope	*-0.54**	-0.26	*0.17**	*0.74**	0.34	0.04	*1.00*					
Dune Face Slope	-0.43	-0.22	*0.16**	*0.67**	0.26	-0.01	*0.68**	*1.00*				
V1	-0.42	-0.21	*-0.41**	*0.72**	0.02	-0.08	0.31	0.12	*1.00*			
V2	-0.42	-0.24	*-0.50**	*0.74**	0.26	0.01	0.36	0.06	*0.90**	*1.00*		
Dune Width	-0.11	0.02	*-0.39**	0.31	-0.24	-0.09	-0.04	-0.24	*0.86**	*0.67**	*1.00*	
Beach Width	*0.54**	0.22	*0.28**	*-0.77**	*-0.58**	0.03	*-0.59**	*-0.50**	*-0.49**	*-0.57**	-0.24*	*1.00*

Table C.8: Cross-correlation coefficients between foredune and beach geomorphological parameters in Bayshore Beach, OR. Statistically significant correlations are italicized and followed by an asterisk.

	SCR	**abs (SCR)**	**dtoe**	**dhigh**	**dheel**	**Fore-shore Slope**	**Back-shore Slope**	**Dune Face Slope**	**V1**	**V2**	**Dune Width**	**Beach Width**
SCR	*1.00*											
abs(SCR)	*-0.57**	*1.00*										
dtoe	-0.05	*0.60**	*1.00*									
dhigh	*-0.59**	*0.68**	0.37*	*1.00*								
dheel	*-0.58**	*0.84**	*0.59**	*0.75**	*1.00*							
Foreshore Slope	-0.09	-0.15	0.18	-0.10	-0.14	*1.00*						
Backshore Slope	*-0.53**	0.01	0.10	-0.13	0.01	*0.40**	*1.00*					
Dune Face Slope	-0.32	0.31	*0.51**	-0.01	0.37	0.02	*0.59**	*1.00*				
V1	-0.36	0.05	*-0.42**	*0.56**	0.04	-0.12	-0.16	*-0.56**	*1.00*			
V2	*-0.41**	0.18	-0.33	*0.67**	0.18	-0.15	-0.23	*-0.58**	*0.96**	*1.00*		
Dune Width	-0.28	-0.04	*-0.53**	*0.43**	-0.07	-0.13	-0.20	*-0.67**	*0.97**	*0.92**	*1.00*	
Beach Width	0.26	0.14	0.07	-0.30	0.02	-0.31	-0.17	-0.01	-0.31	-0.26	-0.30	*1.00*

Table C.9: Cross-correlation coefficients between foredune and beach geomorphological parameters in Heceta, OR. Statistically significant correlations are italicized and followed by an asterisk.

	SCR	abs (SCR)	dtoe	dhigh	dheel	Fore-shore Slope	Back-shore Slope	Dune Face Slope	V1	V2	Dune Width	Beach Width
SCR	*1.00*											
abs(SCR)	*0.96**	*1.00*										
dtoe	*-0.47**	*-0.49**	*1.00*									
dhigh	*-0.63**	*-0.57**	*0.61**	*1.00*								
dheel	0.14	*0.16**	-0.02	0.16	*1.00*							
Foreshore Slope	*0.45**	*0.45**	-0.19	-0.36	-0.03	*1.00*						
Backshore Slope	-0.17	*-0.21**	*0.45**	0.24	-0.25	-0.07	*1.00*					
Dune Face Slope	-0.23	*-0.17**	*0.51**	*0.51**	0.20	-0.04	-0.06	*1.00*				
V1	*-0.47**	*-0.42**	*0.40**	*0.77**	-0.03	-0.28	*0.41**	0.06	*1.00*			
V2	*-0.53**	*-0.49**	0.32	*0.85**	0.08	-0.34	0.28	0.07	*0.93**	*1.00*		
Dune Width	-0.19	-0.14	0.05	0.32	-0.30	-0.13	0.39	-0.27	*0.83**	*0.67**	*1.00*	
Beach Width	*-0.57**	*-0.57**	0.33	*0.54**	-0.11	0.06	0.18	0.21	*0.43**	*0.50**	0.19	*1.00*

Table C.10: Cross-correlation coefficients between foredune and beach geomorphological parameters in Florence, OR. Statistically significant correlations are italicized and followed by an asterisk.

	SCR	abs (SCR)	dtoe	dhigh	dheel	Fore-shore Slope	Back-shore Slope	Dune Face Slope	V1	V2	Dune Width	Beach Width
SCR	*1.00*											
abs(SCR)	*0.68**	*1.00*										
dtoe	*0.14**	*0.19**	*1.00*									
dhigh	-0.04	*-0.12**	*0.27**	*1.00*								
dheel	*0.14**	0.06	*0.16**	*0.24**	*1.00*							
Foreshore Slope	*0.18**	*0.17**	0.08	*0.26**	0.02	*1.00*						
Backshore Slope	*-0.36**	*-0.20**	*0.48**	0.03	-0.08	-0.06	*1.00*					
Dune Face Slope	*-0.13**	*-0.23**	*0.11**	*0.27**	0.04	0.02	*0.12**	*1.00*				
V1	*-0.09**	*-0.18**	0.00	*0.86**	0.05	*0.19**	*-0.10**	0.08	*1.00*			
V2	-0.01	-0.09	-0.05	*0.83**	*0.20**	*0.20**	*-0.16**	*-0.10**	*0.88**	*1.00*		
Dune Width	*-0.17**	*-0.18**	-0.06	*0.65**	*-0.09**	*0.14**	*-0.12**	-0.08	*0.90**	*0.72**	*1.00*	
Beach Width	0.08	0.07	*0.27**	*0.81**	*0.14**	*0.23**	0.00	*0.26**	*0.68**	*0.64**	*0.51**	*1.00*

Table C.11: Cross-correlation coefficients between foredune and beach geomorphological parameters in Reedsport, OR. Statistically significant correlations are italicized and followed by an asterisk.

	SCR	abs (SCR)	dtoe	dhigh	dheel	Fore-shore Slope	Back-shore Slope	Dune Face Slope	V1	V2	Dune Width	Beach Width
SCR	*1.00*											
abs(SCR)	*-0.59**	*1.00*										
dtoe	*0.10**	*-0.13**	*1.00*									
dhigh	*0.17**	*-0.32**	0.04	*1.00*								
dheel	-0.05	0.06	0.06	0.05	*1.00*							
Foreshore Slope	*0.26**	*-0.33**	0.02	*0.20**	0.04	*1.00*						
Backshore Slope	*-0.16**	-0.07	*0.61**	*0.18**	*0.11**	*0.13**	*1.00*					
Dune Face Slope	*-0.14**	0.02	*0.14**	*0.21**	*0.09**	-0.04	0.02	*1.00*				
V1	*0.09**	*-0.18**	*-0.35**	*0.49**	*-0.16**	*0.15**	*-0.11**	*-0.17**	*1.00*			
V2	*0.14**	*-0.15**	*-0.52**	*0.40**	-0.04	*0.15**	*-0.16**	*-0.56**	*0.65**	*1.00*		
Dune Width	0.04	*-0.12**	*-0.24**	*0.35**	*-0.15**	*0.13**	*-0.09**	*-0.17**	*0.88**	*0.50**	*1.00*	
Beach Width	*0.33**	*-0.11**	*0.12**	*-0.10**	0.04	0.06	-0.08	*-0.12**	*-0.26**	*-0.10**	-0.08	*1.00*

Table C.12: Cross-correlation coefficients between foredune and beach geomorphological parameters in Bandon, OR. Statistically significant correlations are italicized and followed by an asterisk.

	SCR	abs (SCR)	dtoe	dhigh	dheel	Fore-shore Slope	Back-shore Slope	Dune Face Slope	V1	V2	Dune Width	Beach Width
SCR	*1.00*											
abs(SCR)	*0.45**	*1.00*										
dtoe	*-0.16**	0.00	*1.00*									
dhigh	*0.06**	0.00	*0.26**	*1.00*								
dheel	0.09	0.00	0.08	0.04	*1.00*							
Foreshore Slope	-0.02	-0.45	*-0.16**	*0.16**	-0.07	*1.00*						
Backshore Slope	-0.50	*-0.38**	*0.48**	*0.41**	-0.04	*0.30**	*1.00*					
Dune Face Slope	*-0.15**	*0.12**	*0.44**	*0.41**	0.05	*-0.26**	*0.16**	*1.00*				
V1	-0.05	*-0.12**	*-0.18**	*0.39**	*-0.21**	*0.31**	*0.31**	*-0.12**	*1.00*			
V2	*0.20**	-0.06	*-0.48**	*0.41**	*-0.03**	*0.35**	0.02	*-0.45**	*0.46**	*1.00*		
Dune Width	*-0.16**	*-0.16**	*-0.21**	*0.20**	-0.25	*0.27**	*0.27**	*-0.16**	*0.91**	*0.36**	*1.00*	
Beach Width	*-0.11**	*0.22**	*0.19**	0.09	*0.11**	*-0.48**	*-0.20**	*0.41**	*-0.45**	*-0.24**	*-0.38**	*1.00*

APPENDIX D – Regional Beach and Foredune Geomorphological Parameters

The means and standard deviations of foredune crest elevations, foredune toe elevations, SCR, dune volumes, beach and dune widths, foreshore slope, and backshore slopes for each beach area show in Figures D.1 – D.4. Figure D.1 shows that SCR are higher and more variable in the north of the PNW. Foredune crest elevations are relatively low and have less variability in this region. There is no regional pattern in foredune toe elevation.

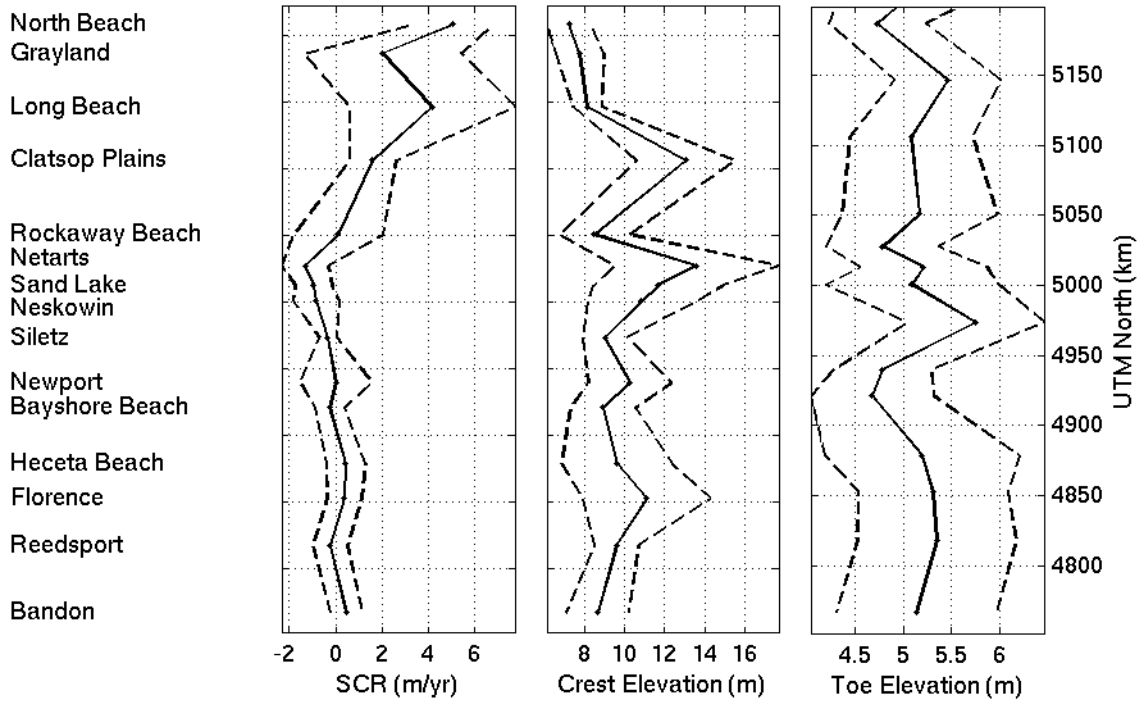

Figure D.1. The means and standard deviations of shoreline change rates, foredune crest elevations, and dune toe elevations for each study beach within the region. The locations of each beach are shown in the left panel. Mean values are indicated by solid black. The mean values with a range of one standard deviation unit are indicated by a dashed red line.

Figure D.2 shows similar patterns in both dune volumes (*V1* and *V2*). Clatsop Plains, OR has relative large foredunes with relatively high variability.

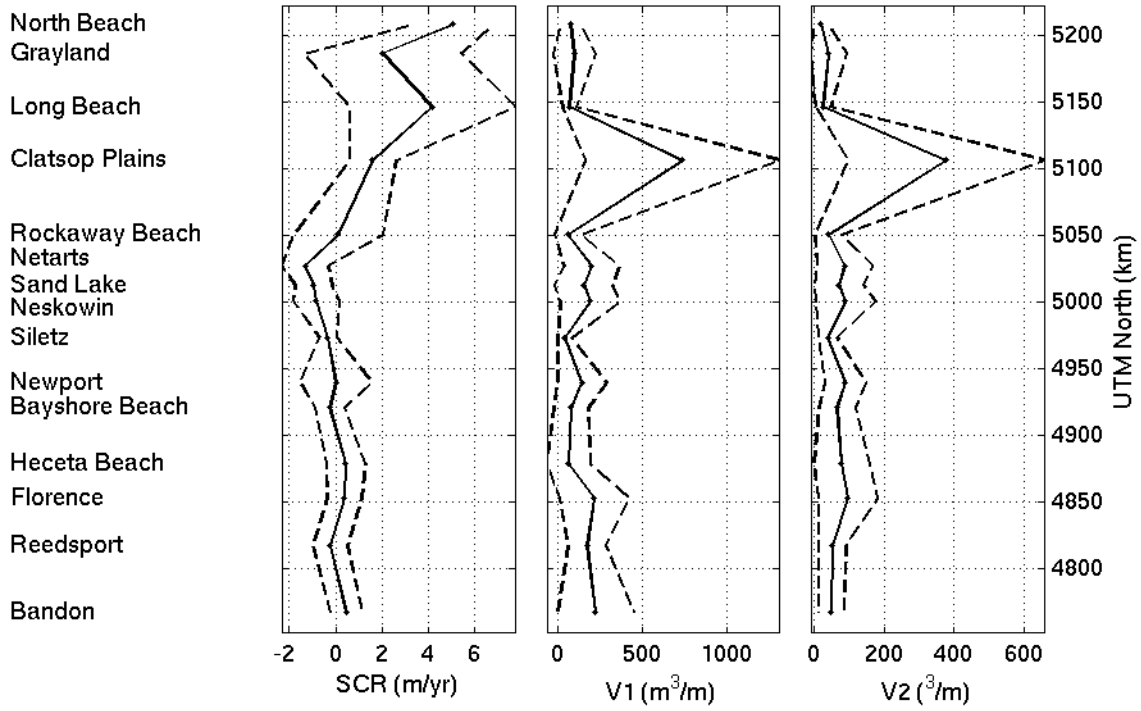

Figure D.2. The means and standard deviations of shoreline change rates, big foredune volume (V1), and small foredune volume (V2) for each study beach within the region. The locations of each beach are shown in the left panel. Mean values are indicated by solid black. The mean values with a range of one standard deviation unit are indicated by a dashed red line.

Figure D.3 shows that the beaches are relatively wide, with high variability, in Washington. Foredunes are relatively wide at Clatsop Plains and southern Oregon. There is a high degree of variability in foredune width at these beaches.

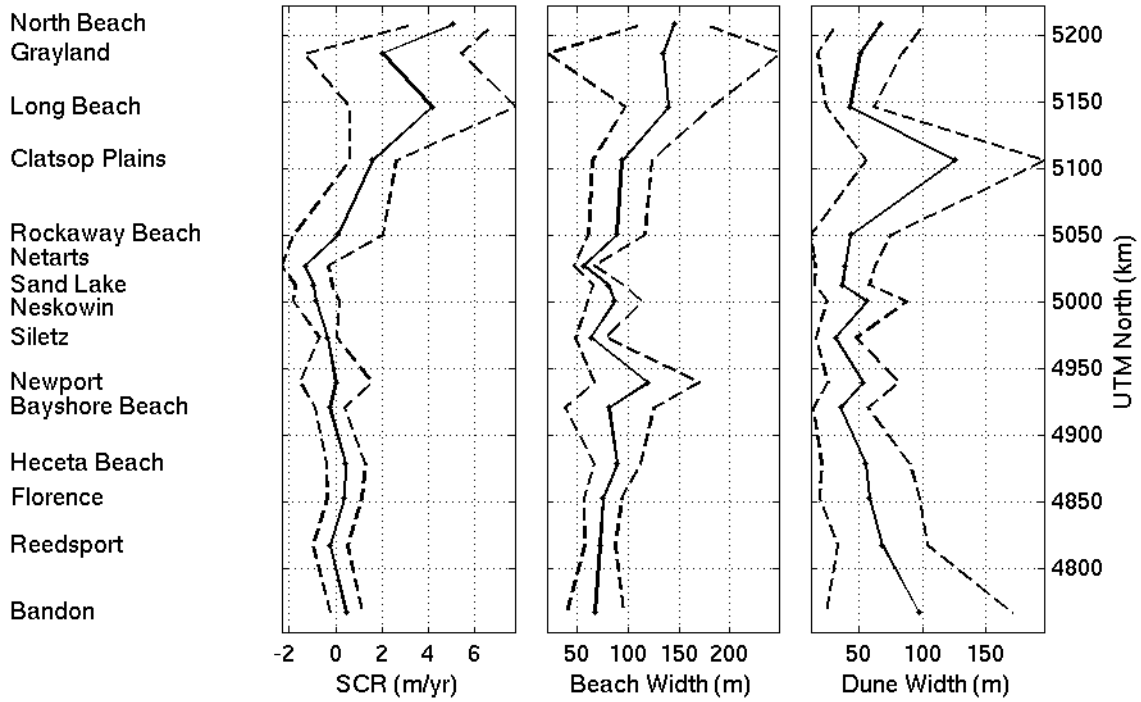

Figure D.3. The means and standard deviations of shoreline change rates, beach widths, and foredune widths for each study beach within the region. The locations of each beach are shown in the left panel. Mean values are indicated by solid black. The mean values with a range of one standard deviation unit are indicated by a dashed red line.

Figure D.4 shows that the foreshore slopes are relatively low in the north. Sand Lake, Neskowin, and Siletz, OR have relatively steep foreshores. Backshore slopes are relatively variable along the coast.

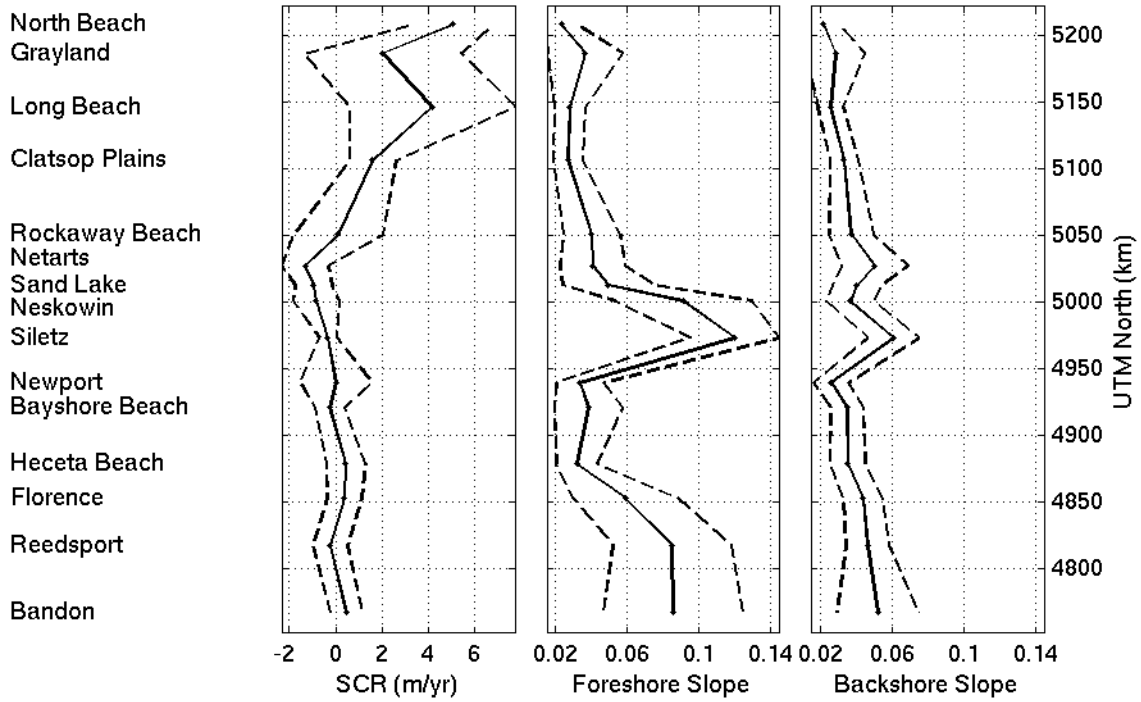

Figure D.4. The means and standard deviations of shoreline change rates, foreshore slopes, and backshore slopes for each study beach within the region. The locations of each beach are shown in the left panel. Mean values are indicated by solid black. The mean values with a range of one standard deviation unit are indicated by a dashed red line.